TECHNICAL UNIVERSITY OF CRETE

DEPARTMENT OF ELECTRICAL AND COMPUTER ENGINEERING

OPTIMAL OPERATION OF INTERCONNECTED MICROGRIDS

By

Konstantinos Moungos

DIPLOMA THESIS

September 2023

EXAMINING COMMITTEE

Professor:	Kanellos D. Fotios (Supervisor)
Professor:	Stavrakakis Georgios
Assistant Professor:	Tsekouras J. Georgios (UNIWA)

Abstract

In response to rising energy consumption and its adverse environmental impact, there is an urgent demand for innovative technologies in intelligent energy management systems. The integration of Renewable Energy Sources into power systems is crucial for achieving short-term reduction in greenhouse gas emissions and long-term elimination. However, this integration presents challenges, particularly with distributed generation, introducing complexities and technical obstacles. This work develops advanced fully parametric systems to optimize energy management within complex Microgrids. It also enables Microgrids to participate in Peer-to-Peer energy markets with their neighbors, enhancing resilience and offering financial benefits by leveraging diverse profiles of non-controllable energy sources based on individual Microgrid locations. The study examines various energy systems, ranging from residential buildings to extensive Plug-In Electric Vehicle parking facilities, and develops models for system components, including thermal and electrical building loads. Critical and non-critical loads are separately addressed in this work. Additionally, a dynamic equivalent aggregate battery model is created for Plug-In Electric Vehicle clusters in Microgrid parking lots. This research presents a comprehensive framework for Energy Management Systems within interconnected Microgrids, reconciling two strategies: Microgrid energy management and participation in the Peer-to-Peer Electricity Market. With this approach, each Microgrid consistently adapts its operations based on market dynamics, aligning actions with financial objectives and operational efficiency. A significant advantage of this thesis is that during participation in the Peer-to-Peer market, each Microgrid shares only information about power quantity and the offered price it is willing to trade, preserving internal information. Furthermore, market participation is achieved through non-cooperative game theory, supporting the idea that each Microgrid can have its distinct objectives. This flexibility is vital in liberalized markets where Microgrids may belong to different companies with unique objectives.

Περίληψη

Εξαιτίας της ολοένα και αυξανόμενης κατανάλωσης ηλεκτρικής ενέργειας και των δυσμενών της περιβαλλοντικών επιπτώσεων, κρίνεται επείγουσα η εύρεση καινοτόμων τεχνολογιών σε έξυπνα συστήματα διαχείρισης ενέργειας. Η ενσωμάτωση των Ανανεώσιμων Πηγών Ενέργειας στο δίκτυο είναι ζωτικής σημασίας για την επίτευξη βραχυπρόθεσμης μείωσης των εκπομπών διοξειδίου του άνθρακα και τη μακροπρόθεσμη εξάλειψή τους. Ωστόσο, η ενσωμάτωση αυτή παρουσιάζει προκλήσεις διότι οι μονάδες διεσπαρμένης παραγωγής εισάγουν αυξανόμενη πολυπλοκότητα και τεχνικές δυσκολίες. Η παρούσα εργασία αναπτύσσει προηγμένα πλήρως παραμετρικά συστήματα για τη βελτιστοποίηση της διαχείρισης ενέργειας σε πολύπλοκα Μικροδίκτυα. Επίσης, δίνει τη δυνατότητα στα Μικροδίκτυα να συμμετέχουν σε ομότιμες (Peer-to-Peer) αγορές ηλεκτρικής ενέργειας με τα συνορεύοντα Μικροδίκτυα, ενισχύοντας την αξιοπιστία του δικτύου και προσφέροντας ταυτόχρονα οικονομικά οφέλη. Η διπλωματική αυτή εξετάζει διάφορα συστήματα ηλεκτρικής ενέργειας από οικιακά κτίρια έως εκτεταμένες εγκαταστάσεις σταθμών φόρτισης ηλεκτρικών οχημάτων, και ταυτόχρονα αναπτύσσει μοντέλα για τα στοιχεία του συστήματος, συμπεριλαμβανομένων των θερμικών και ηλεκτρικών φορτίων των κτηριακών μονάδων του Μικροδικτύου. Κάνει διάκριση μεταξύ κρίσιμων και μη κρίσιμων ηλεκτρικών φορτίων. Επιπλέον, δημιουργείται ένα δυναμικό ισοδύναμο μοντέλο εικονικής μπαταρίας για συστάδες ηλεκτρικών οχημάτων σε χώρους στάθμευσης Μικροδικτύων. Παρουσιάζει ένα ολοκληρωμένο πλαίσιο για συστήματα διαχείρισης ενέργειας σε διασυνδεδεμένα Μικροδίκτυα, συνδυάζοντας δύο στρατηγικές: Διαχείριση της ενέργειας του Μικροδικτύου και συμμετοχή στην ομότιμη αγορά ηλεκτρικής ενέργειας. Με την προσέγγιση αυτή, κάθε Μικροδίκτυο προσαρμόζει με συνέπεια τις λειτουργίες του με βάση τη δυναμική της αγοράς, ευθυγραμμίζοντας τις δράσεις του με τους οικονομικούς του στόχους. Ένα σημαντικό πλεονέκτημα αυτής της εργασίας είναι ότι κατά τη συμμετοχή στην αγορά, κάθε Μικροδίκτυο μοιράζεται μόνο πληροφορίες σχετικά με την ποσότητα ισχύος και την προσφερόμενη τιμή που είναι διατεθειμένο να ανταλλάξει, διατηρώντας κρυφές εσωτερικές του πληροφορίες καθώς και σημαντικά δεδομένα. Επιπλέον, η συμμετοχή στην αγορά επιτυγχάνεται μέσω της θεωρίας μη συνεργατικών (ανταγωνιστικών) παιγνίων, υποστηρίζοντας την ιδέα ότι κάθε Μικροδίκτυο μπορεί να έχει τους δικούς του ξεχωριστούς στόχους. Αυτή η ευελιξία είναι ζωτικής σημασίας καθώς στην απελευθέρωση της αγοράς ηλεκτρικής ενέργειας, τα Μικροδίκτυα μπορεί να ανήκουν σε διαφορετικές εταιρείες με διαφορετικούς στόχους.

Acknowledgements

First and foremost, I would like to extend my heartfelt gratitude to my supervisor, professor Kanellos Fotios. I owe him a debt of gratitude that goes beyond words, for he not only introduced me to a multitude of captivating concepts and research domains but also treated my endeavors with utmost humanity and professionalism. His unwavering support and guidance during the journey of my diploma's thesis have been invaluable. His extensive research expertise and active engagement in the field, coupled with his profound knowledge, served as a constant source of inspiration and motivation throughout my academic pursuit. Additionally, he patiently explained to me a wide range of different topics, further enriching my educational experience.

I would also like to thank my friends that have helped me along the way through their selfless interest and support both inside and outside the classes.

Last but not least, I owe my family the warmest hug for their unconditional love and support on every step of the way.

Contents

List of Figures

1 Introduction

In response to the mounting concerns regarding the escalating consumption of energy and its resulting adverse environmental impacts, the development of innovative technologies for intelligent energy management systems has become an urgent necessity. These systems are designed not only to conserve energy but also to align with the forthcoming changes in electric power systems driven by the growing adoption of renewable energy sources (RES). However, the widespread integration of RES presents challenges in the operation of power systems. Distributed generation facilitates this transition but also introduces intricacies and technical hurdles. Microgrids were initially introduced to tackle the integration challenges posed by dynamic distributed resources. They accomplish this by aggregating these resources alongside local loads within specific geographic areas. In the current context, advancements in technology, such as smart meters, communication systems, and management protocols, empower individuals to engage in peer-to-peer (P2P) resource trading among microgrids located in close proximity. Geographically adjacent microgrids can collaborate to form a cyber-physical interconnected multi-microgrid system. This collective system manages various aspects, including energy flow, information exchange, and financial transactions among stakeholders. This convergence of technologies and concepts represents significant progress towards sustainable and efficient energy management within an evolving power framework. Consequently, the establishment of Interconnected Microgrids (IMGs) has gained particular relevance. These IMGs leverage a diverse mix of complementary power sources and facilitate efficient energy sharing and trading both within microgrids and with the main grid. By doing so, IMGs enable localized coordination that capitalizes on nearby production and demand diversity. This optimization enhances capacity utilization and diminishes reliance on the central grid. The concept of IMGs aligns seamlessly with emerging smart grid trends. As the utilization of renewable energy resources continues to soar, interconnected microgrids play a pivotal role in enhancing efficiency, alleviating strain on the main grid, alleviating distribution line congestion, and bolstering overall system reliability and energy efficiency through optimized energy distribution. Nonetheless, challenges arise due to the inherent volatility of renewable resources, coupled with fluctuating microgrid loads, interconnected power generation, and the complexities of energy trading. Addressing these challenges systematically is imperative to ensure stable operations and optimal scheduling. This study presents a comprehensive framework for EMS within IMGs.

2 Background

2.1 Microgrid Operational Configurations

2.1.1 Conceptual Structure of Distribution Systems

Electrical utility distribution systems can be classified into three primary types: centralized, decentralized, and distributed. The fundamental characteristic of a centralized system involves a straightforward connection of nodes to a central electricity production source. In a centralized distribution system, electricity is generated at large power plants, often located far away from the end-users. The generated electricity is transmitted over long distances through high-voltage transmission lines to substations, where it is stepped down to lower voltages for distribution to homes, businesses, and industries. This model is the traditional approach for delivering electricity. The presence of multiple generator units within central power plants ensures a consistent power supply, enhancing system reliability. However, it's important to note that if the configuration at the central station experiences a failure, the entire system could collapse.

In contrast, in a decentralized configuration, electricity generation is positioned closer to end-users. Small to medium-sized power generation sources, including combined heat and power (CHP) plants, solar installations, wind turbines, and small natural gas generators, are strategically scattered throughout the distribution network. These sources are connected to their corresponding loads via various remote stations. This approach not only enhances energy security and minimizes transmission losses but, more importantly, demonstrates a higher level of resilience when contrasted with centralized setups.

Distributed configurations, resembling a web-like structure, feature nodes that incorporate both generation and loads, interconnected with all other generation and load points. This could include rooftop solar panels, small wind turbines, microturbines, and fuel cells installed in homes, businesses, or industrial sites. These distributed networks exhibit remarkable robustness due to their ability to reroute transmission in the event of a station or link failure, ensuring system reliability. Such distributed or decentralized network architectures are commonly found in microgrids. They excel in scenarios where a single transmission pathway or specific nodes are compromised.

2.1.2 Distributed Generation

Distributed generation (DG) refers to a modern approach to electricity production where smaller power generation sources are strategically placed near the point of consumption, offering numerous benefits for energy systems. Common sources of distributed generation include combined heat and power (CHP) units, microturbines, fuel cells, Internal Combustion Engines (ICE), and renewable energy sources (RES). Renewable energy encompasses power derived from natural resources like sunlight, wind, waves, tides, geothermal heat, and biomass. This enhances energy resilience, reduces transmission losses, enhances power quality, provides better voltage support, and minimizes the environmental impact by utilizing renewable resources. DG systems can operate independently or in coordination with the main grid, providing uninterrupted power during grid outages. These generation units are generally linked to the power grid at the lower voltage distribution level.

Distributed generation exhibits distinct attributes that are absent in centralized systems. The generated power is relatively moderate and subject to fluctuations based on the availability and variability of the primary energy source. Power flow in distributed generation is bidirectional, in contrast to the unidirectional flow typical of central generation systems. The effectiveness and output of distributed generation are intrinsically linked to the proximity of the primary energy source in the region.

The main challenge in distributed generation pertains to efficiently coordinating an array of widely dispersed energy sources and loads. This complexity magnifies significantly with the increasing number of distributed generators, resulting in progressively demanding computational requirements. To address this challenge, microgrids emerge as a strategic solution. They leverage advanced control techniques and supervisory systems to

seamlessly integrate diverse elements, thus harnessing the full spectrum of benefits inherent in this decentralized approach.

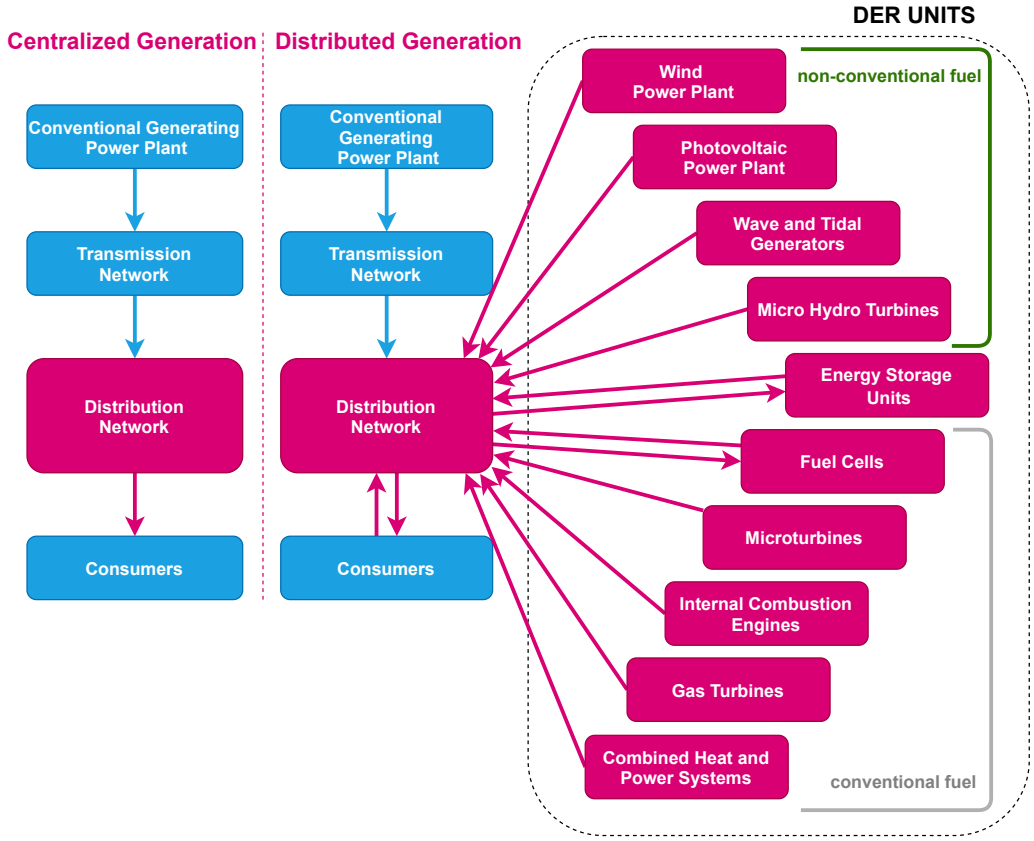

Figure 1: (a): centralized unidirectional system and (b): bidirectional distributed generation system

2.2 Advantages of Microgrids

Microgrids are an expanding segment of the energy sector that signifies a fundamental change from distant centralized power plants to a more localized and dispersed generation approach, particularly in urban areas, communities, and campuses. Their capability to isolate from the main grid in a process called islanding during emergencies ensures ongoing power supply to their loads and offers critical support to surrounding communities. This offers resiliency and reliable operation across various activities and services. Microgrids yield several advantages for the environment, utility operators, and consumers [4]:

Microgrids offer a compelling solution for reducing greenhouse gas emissions. By incorporating renewable sources such as solar, wind, and biomass, microgrids can substantially diminish reliance on fossil fuels, thus effectively mitigating greenhouse gas emissions. Employing sophisticated control technologies, such as local energy management systems, enables the effective balance of generation from unpredictable renewable sources with controlled distributed generation, like combustion turbines powered by natural gas. Moreover, energy storage systems and electric vehicle batteries can be used to stabilize power production and consumption within the microgrid. Ultimately, the adoption of microgrids has the potential to foster a cleaner and more sustainable energy landscape, thereby aligning with global endeavors to combat climate change and curtail the carbon footprint.

Microgrids present an effective solution to mitigate electricity line and heat transmission losses within energy distribution systems. They capture on-site energy that would otherwise dissipate during transmission and harness heat typically lost in pipelines. With their localized and compact design, microgrids minimize the

distance electricity travels, reducing resistive losses encountered in long-distance transmission. This enhances energy efficiency and minimizes wastage, as lengthy electrical line transmission results in losses and necessitates additional generation to meet distant demand. Furthermore, centralized power sources, like fossil fuels and nuclear power, produce considerable heat energy often released into the atmosphere without use. By generating power closer to end-users, this heat energy can be productively employed, such as for water or space heating in nearby establishments, thus once again curbing greenhouse gas emissions.

Microgrids offer distinct advantages in enhancing the local management of power supply and demand. By virtue of their decentralized nature, microgrids allow communities, industries, and even individual buildings to exercise greater control over their energy resources. This localized management enables efficient matching of energy generation with local demand, reducing the strain on larger grid systems during peak periods. Through real-time monitoring and intelligent load management, microgrids can dynamically balance supply and demand, optimizing energy use and minimizing waste, which in turn helps alleviate grid congestion. As a result, microgrids can improve system reliability, efficiency, and potentially reduce the necessity for new power capacity investments like peaker plants, substations, transmission lines, energy storage, or other infrastructure. When linked to the local distribution network or transmission system, microgrids can also export surplus electricity or address imbalances from the surrounding system through a single connection point.

Microgrids offer significant advantages in bolstering grid resilience against extreme weather events and cyber-attacks. Their decentralized structure enables microgrids to function autonomously, ensuring continued power supply even if the larger grid experiences disruptions. In the face of severe weather, such as storms or natural disasters, microgrids can seamlessly isolate affected areas and sustain critical operations, minimizing downtime. Additionally, microgrids can enhance cybersecurity by isolating themselves from the broader network, mitigating the potential impact of cyber-attacks on the entire grid. With their ability to operate independently, self-heal, and quickly restore power, microgrids provide a crucial layer of protection against unforeseen disruptions, contributing to the overall resilience and reliability of our energy infrastructure. Microgrids also aid the macrogrid's recovery from system failures, either indirectly by maintaining essential services needed by restoration crews or directly by contributing to grid re-energization.

Briefly Described Benefits of Microgrids Include:[4]

- Provide efficient, low-cost, clean energy
- Improve the operation and stability of the regional electric grid
- Critical infrastructure that increases reliability and resilience
- Reduce grid "congestion" and peak loads
- Enable highly-efficient CHP, reducing fuel use, line losses, and carbon footprint
- Integrate CHP, renewables, thermal and electric storage, and advanced system and building controls
- Make RTO markets more competitive
- Offer grid services including: energy, capacity, and ancillary services
- Support places of refuge in regional crises and first responders
- Use local energy resources and jobs
- Diversified risk rather than concentrated risk
- Using electric and thermal storage capabilities, a microgrid can provide local management of variable renewable generation, particularly on-site solar
- When properly designed, a regional power grid that combines both large central plants and distributed microgrids can be built with: less total capital cost, less installed generation, higher capacity factor on all assets, and higher reliability.

2.3 Challenges of Microgrids

Despite their numerous benefits, the implementation of microgrids encounters significant technological challenges in operational and deplayments level. These chalenges include:

- Balancing Generation and Load: Maintaining equilibrium between power generation and load in island mode stands as a frequent microgrid challenge. The continuous upkeep of this balance is crucial. Abrupt or substantial load changes can introduce instability into the islanded system. This requires sophisticated energy management systems that can predict and manage generation and load fluctuations.
- Energy storage: Microgrids often rely on energy storage systems to provide backup power and balance energy supply and demand. Nonetheless, effectively overseeing energy storage systems presents difficulties, demanding meticulous supervision and upkeep to guarantee their optimal performance.
- Energy dispatch: Microgrids frequently depend on diverse energy sources, encompassing renewables like solar and wind energy, alongside conventional options like diesel generators. Coordinating the distribution of these energy sources to fulfill system requirements can present intricate challenges.
- Grid connection: Microgrids must be able to connect to the main power grid and manage the flow of energy between the microgrid and the grid. This requires careful coordination to ensure the safety and stability of the system.
- Managing Fault Current: Microgrids can experience higher fault currents than those seen in distributed systems. This disparity can adversely impact protection mechanisms. Particularly concerning during island operation, hasty microgrid integration without meticulous protective measure analysis can lead to substantial grid harm.
- Initiating Island Mode: The initial phases of transitioning to island mode can trigger sudden current surges, influencing system frequency and voltage. This abrupt change may lead to generator tripping and downtime during this phase. Overcoming this requires an evaluation of energy generation control techniques specific to island mode and the development of specialized controls.

The Figure [2] underscores the primary challenges at operational level that need to be resolved, allowing microgrids to become more prominent in our lives.

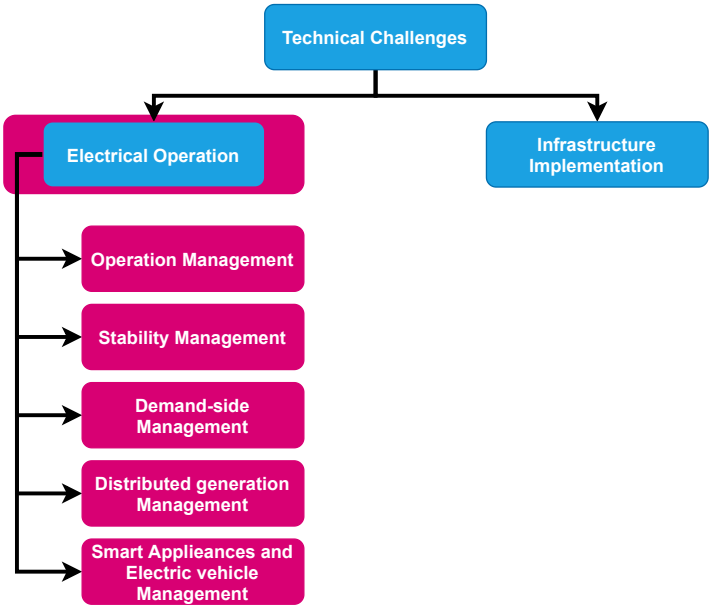

Figure 2: Key technical challenges in Operational level.

2.4 Microgrid Energy Production

Microgrids harness electricity by utilizing distributed energy resources (DERs), where electrical generation and storage systems collaborate within numerous units. These DERs encompass diverse components, including distributed fossil-fuel generators, batteries, and renewable sources like solar panels and wind turbines. Several components have been summarized in [5]. It is worth mentioning that batteries, when discharging, are perceived as power generation sources. The microgrid architecture offers the advantage of selecting from a variety of generation sources, often combined to optimize output based on available resources, efficiency, and cost-effectiveness.

In microgrids, maintaining a balance between power supply and demand is crucial, given the intermittent nature of sources like photovoltaic panels and wind turbines, which are subject to fluctuations due to varying primary resources. This challenge becomes more pronounced when the microgrid operates in isolation, relying on a limited supply to meet demand [6]. The main objectives of controlling DERs in microgrids are outlined in [5] as follows:

- Synchronizing DERs with the utility grid.
- Maintaining a power balance between generation and load, particularly in the islanded mode of operation.
- Ensuring stable voltage and frequency.
- Maintaining the quality of power injected into the utility grid.
- Enabling smooth power transfer between the microgrid and the utility grid to ensure stable system operations under various conditions.
- Extracting the maximum power from DER units based on various renewable energy sources.

2.5 Microgrid Energy Storage

Energy storage systems play a crucial role in microgrids, particularly during their autonomous operations, due to their ability to ensure reliability and balance energy supply and demand. By storing excess energy generated during periods of high production, these systems enable consistent power availability during times of low generation. This process not only enhances the microgrid's resilience but also facilitates the efficient utilization of renewable sources, reducing reliance on conventional power. Various technologies are used for energy storage, as depicted in Figure [3]. Among the energy storage technologies suitable for microgrids, batteries, flywheels, and hydrogen storage units stand out. The choice of suitable energy storage technology hinges on key parameters: unit size, storage capacity, available capacity, self-discharge time, efficiency, durability, autonomy, mass and volume densities, cost, feasibility, and reliability [7]. These factors collectively determine the technology's applicability, performance, and value within a given context. Parameters such as unit size and storage capacity influence the technology's scale and potential applications, while efficiency and durability impact its energy conversion and lifespan. Autonomy and available capacity highlight the system's ability to sustain energy release, and mass and volume densities play a role in efficient space utilization. The technology's cost and feasibility, along with reliability assurances, further guide its selection for optimal integration into various energy storage applications including microgrids.

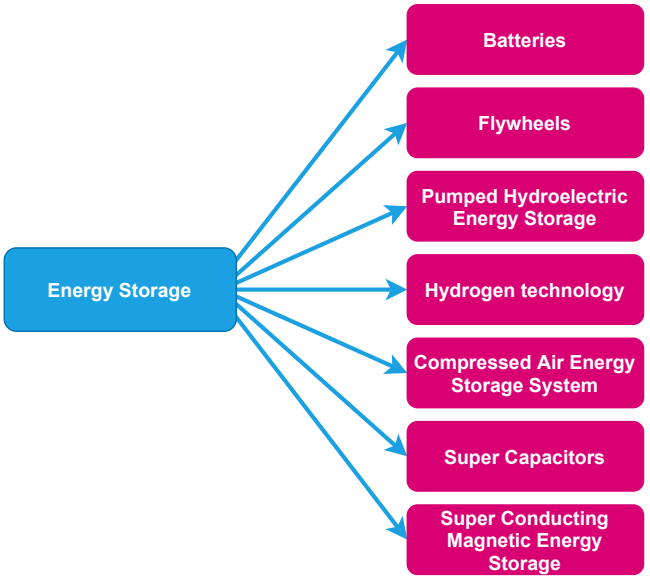

Figure 3: Storage Technologies

2.5.1 Batteries

Batteries serve as fundamental devices that store electricity in electrochemical form. In today's market, a diverse range of rechargeable batteries is available, with several types standing out for their distinct characteristics. One such example is the Lithium-Ion battery, known for its high energy density and lack of memory effects, which makes it well-suited for applications like smartphones and laptops [8]. Despite occupying less space than lead-acid batteries, their cost makes Lithium-Ion batteries impractical for large-scale applications [7].

In contrast, Lead-Acid batteries, while exhibiting moderate efficiency, are extensively employed in scenarios like vehicle engine startups due to their durability and cost-effectiveness [9]. Flow Batteries share similarities with lead-acid batteries, differing in their approach to storing electrolytes externally, which then circulate through the battery cell stack. These batteries offer scalable energy storage capacity, limited only by the size of the electrolyte storage reservoir [7]. They present a reliable, affordable, and environmentally friendly solution for electrical energy storage across various applications [10]. Nevertheless, they are subject to a limited number of usage cycles, requiring replacement within three to five years [7].

2.5.2 Flywheels

Flywheels are being increasingly employed as innovative solutions for energy storage. These mechanisms consist of rapidly rotating disks or cylinders intentionally designed to retain kinetic energy, which can be effortlessly converted into electrical energy by simply connecting them to generators. This technology offers numerous advantages [7]. These include rapid charge and discharge times, resilience to temperature fluctuations, relatively modest spatial requirement, a long lifespan, tolerance to abuse, and reduced maintenance costs when compared to conventional battery setups. However, flywheel systems exhibit a higher rate of power dissipation compared to batteries and have a higher initial cost.

2.5.3 Pumped Hydroelectric Energy Storage

Pumped hydro storage systems are prominent methods of energy storage. These systems involve two reservoirs positioned at different elevations. This method is widely adopted for storing substantial amounts of energy on a large scale. It comprises two sizable reservoirs located at locations with notable differences in elevation. Alongside these reservoirs, there are mechanisms such as pumps and hydro turbines. During periods of excess energy in the grid, water is pumped from the lower reservoir to the upper one, thereby storing potential

energy. When demand increases, the stored water is released, flowing downhill and turning turbines to generate electricity. This technology offers numerous advantages, as outlined in [7], including availability, high power capabilities, lower cost of power, and grid-balancing features like frequency regulation and reserve capacity. However, a major disadvantage is its reliance on geographical features, limiting implementation to areas with hills.

2.5.4 Fuel Cells – Hydrogen Energy Storage

A fuel cell employs the chemical potential of hydrogen to generate electricity in a clean and highly efficient manner. These devices hold the potential to revolutionize various sectors, from transportation to residential and industrial power generation, by emitting only water vapor as a byproduct. Additionally, they contribute to long-term grid energy storage through reversible systems. In comparison to conventional combustion-based technologies prevalent in power plants and vehicles, fuel cells offer numerous advantages. They can achieve superior efficiencies to combustion engines and directly convert chemical fuel energy into electrical power, reaching efficiencies that may surpass 60% [11]. Hydrogen storage is a critical component of fuel cell utilization, involving methods like compression, liquefaction, and solid-state storage to safely contain and deliver hydrogen gas to fuel cells when needed.

2.5.5 Compressed Air Energy Storage Systems

Compressed Air Energy Storage (CAES) systems capitalize on surplus electricity generated during off-peak periods, channeling it to compress air and store it within subterranean caverns. This stored air is subsequently released, expanding to drive combustion turbines that, in turn, power electric generators to produce electricity. The approach boasts notable advantages: it conserves natural gas resources by utilizing economically viable, heated compressed air to fuel turbines, generating electricity during periods of lower demand. Nevertheless, CAES does present certain drawbacks. Its efficiency is somewhat diminished due to the additional energy required for reheating to activate the turbines. This results in an energy output that is less than the input – for every kilowatt-hour of energy input, only 0.5 kilowatt-hours can be extracted [7].

2.5.6 Supercapacitors

Supercapacitors, also known as ultracapacitors, are electronic devices that represent an energy storage technology offering high power density, nearly instant charging and discharging, exceptional reliability, straightforward charging methods, and virtually limitless life cycles. These ultracapacitors currently confer significant economic advantages across diverse markets, including automotive, grid and renewables, transportation, and industrial applications [12]. They combine the characteristics of capacitors and electrochemical batteries, except that there is no chemical reaction. On the downside, the linear discharge voltage restricts the utilization of the complete energy spectrum, they exhibit low energy density, the cells operate at low voltages, and they also experience high self-discharge rates [7].

2.5.7 Super Conducting Magnetic Energy Storage

In these devices, energy is stored within the magnetic field generated by the flow of direct current through a coil of superconducting material, which has been cryogenically cooled. This signifies a cutting-edge approach to energy storage. This method presents notable advantages, such as nearly instantaneous power availability, enabling high-power output for short bursts. The absence of moving parts ensures minimal power loss and heightened reliability. However, this approach does come with limitations. The energy capacity of the magnetic field is relatively modest and has a brief lifespan. Furthermore, the use of cryogenic technology and the necessity for cold temperature maintenance can present technical challenges. As research advances to refine these systems, addressing these drawbacks will be crucial for fully realizing the potential of this innovative energy storage method [7].

2.6 Electric Vehicles

In the near future, there will be a rapid rise in the number of electric vehicles plugging into the electricity grid, mostly because of their significant environmental benefits. This leads to new possibilities and challenges for how electric power systems work. Electric vehicles rely on electric motor to propel the vehicle, either entirely or in combination with conventional mechanical drive systems, to generate a portion of the mechanical driving force.

2.6.1 Types of Electric Vehicles

There are four types of electric vehicles:

- Battery Electric Vehicles BEVs
- Hybrid Electric Vehicles HEVs
- Plug-In Hybrid Electric Vehicles PHEVs
- Fuel Cell Electric Vehicles FCEVs

Battery Electric Vehicles
BEVs rely exclusively on the electrochemical energy stored within their batteries. While various battery technologies exist, recent advancements in lithium-ion (Li-ion) batteries have positioned them as the probable dominant choice [13] [14]. Vehicles equipped with a battery pack are seamlessly linked to the grid for charging, resulting in minimal added expense for incorporating Vehicle-to-Grid technology [14].

Hybrid Electric Vehicles
HEVs ingeniously combine an internal combustion engine (ICE) with an electric motor, although other hybrid configurations exist with varying degrees of efficiency. These vehicles implement battery recharging through regenerative braking to enhance their range. Regenerative braking is an innovative mechanism that converts kinetic energy into a storable form of energy, thereby recovering energy that would otherwise be lost as heat in brake discs. This technique, where the electric motor functions as a generator, harnesses the vehicle's momentum, potentially extending driving autonomy by 20% to 25% [15].

The generator and battery power one or more electric motors. Hybrid vehicles fall under three structural classifications, briefly elucidated below: (a) Series hybrid: the internal combustion engine propels an electric generator that charges the battery, providing energy for the electric motor to propel the vehicle. The electric motor serves as the sole power source for the vehicle. (b) Parallel hybrid: Both the internal combustion engine and electric motor contribute to mechanical transmission. Typically, the internal combustion engine takes the lead, while the electric motor acts as a supplementary power source. (c) Combined hybrid: This configuration amalgamates features from both series and parallel hybrid systems [13] [14]. Regrettably, hybrid vehicles are incapable of establishing electrical connections to the grid, as depicted in Figure [4], and thus cannot fulfill Vehicle-to-Grid functions.

Plug-In Hybrid Electric Vehicles
PHEVs encompass all the attributes of conventional hybrid vehicles, distinguished by the incorporation of a larger battery capacity and a port for an electrical connection to the grid, facilitating battery charging [13]. This enhanced capability enables them to engage in energy interchange with the grid, both for gaining energy (Grid-to-Vehicle) and returning energy (Vehicle-to-Grid). Like Hybrids, PHEVs offer greater range than fully electric vehicles.

Fuel Cell Electric Vehicles
FCEVs utilize an integrated fuel cell that directly transforms hydrogen fuel into electricity, subsequently storing it in the vehicle's battery. The battery then supplies the necessary energy to the electric motor. Nevertheless, the widespread production of such vehicles remains unrealized, primarily due to limitations imposed by hydrogen production prerequisites and the elevated expenses associated with fuel cell arrays [1].

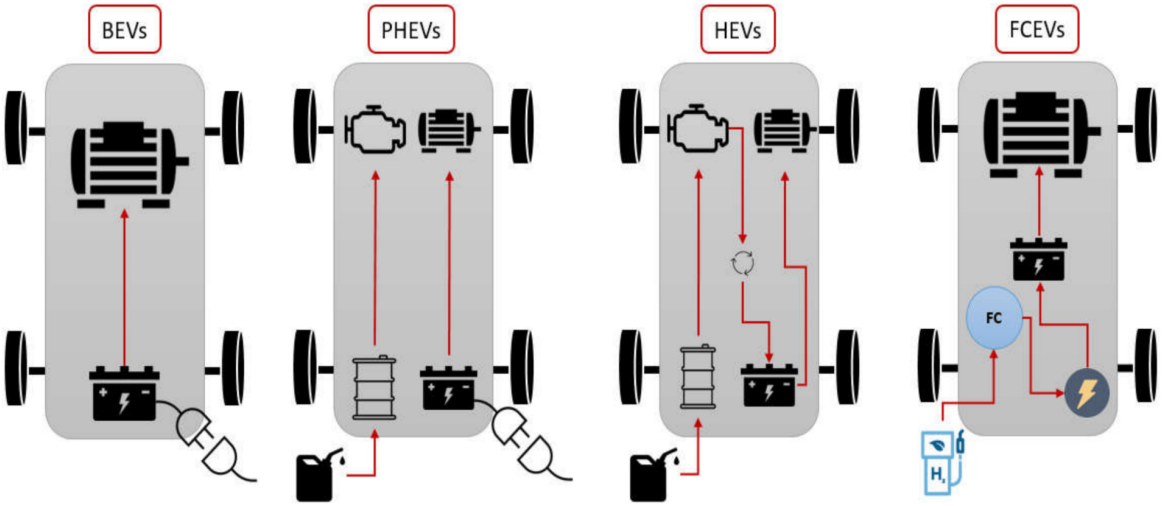

Figure 4: Types of electric vehicles and configuration of the drivetrain [1].

2.6.2 Advantages of Electric Vehicles

Electric vehicles offer a range of compelling advantages [16], [17]. These advantages collectively underscore the transformative potential of electric vehicles, not only in curbing emissions and environmental impact but also in terms of economic feasibility and improved driving dynamics.

- Emission Reduction for Environmental Benefit: Traditional vehicles emit carbon dioxide, contributing to the greenhouse effect and climate change. Unlike their gasoline counterparts, all-electric vehicles produce zero carbon dioxide emissions. Additionally, hybrid electric cars employ their batteries to enhance their range alongside a gasoline engine, leading to improved efficiency and reduced emissions compared to conventional vehicles. EVs can also be powered by renewable sources like wind, solar, and hydropower, bolstering their environmental friendliness. Their design prioritizes sustainability, including the recyclability of the sizeable battery housed within the EV.
- Economical Operation and Maintenance: The operational disparity between fully electric vehicles and gasoline-powered cars is pronounced in terms of cost. Electric energy, being both cheaper and more stable in price than gasoline, delivers considerable savings. This financial advantage is further heightened by the reduced need for frequent maintenance, in stark contrast to the ongoing expenses associated with maintaining traditional combustion engines.
- Enhanced Efficiency and Responsiveness: Electric motors outshine their conventional counterparts in terms of efficiency and responsiveness. Their design and inherent characteristics contribute to better overall performance.
- Quieter Roads and Reduced Noise Pollution: Electric vehicles possess a distinct advantage in noise reduction. The absence of exhaust systems and the inherent quietness of electric motors translate into significantly reduced traffic-related noise. This contributes to quieter roadways, offering more quiet urban environments.

Expected to experience rapid growth in the upcoming years, the electric vehicle market is projected to expand substantially. Coupled with the advancement of suitable control systems, these vehicles are poised to gain new capacities. Mobile storage systems, such as electric vehicle batteries, are anticipated to partially replace stationary storage units designed for storing energy. These systems are capable of operational cycles spanning from one second to an entire day [18].

The batteries within electric vehicles will have the ability to function as dispersed energy storage units for grid-related services. In this manner, electric vehicles will have the capability to balance loads, provide direct

support for renewable energy sources, and hasten the integration of renewables into the grid. The ultimate goal is a complete transition to 100% renewable energy production [19]. Moreover, they will enhance efficiency and grid reliability [20], ensuring the equilibrium of demand and generation. They will offer ancillary services such as frequency and voltage stabilization, as well as flattened load profiles [21], [22].

It's important to note that plug-in electric vehicles boast an impressive power/energy ratio. This quality makes them particularly suitable for grid regulation services, as they can deliver substantial power within a short period of time compared to conventional energy storage devices. To put this ratio into perspective, [23] reports a ratio of 0.44 for electric vehicles, while pumped storage stations have a much lower ratio of 0.035 (an order of magnitude lower).

2.6.3 Operation Mode of Electric Vehicles

The charging stations within the parking area possess the capability for bidirectional power exchange, encompassing two distinct operational modes:

- Grid to Vehicle (G2V) Mode:
  In this mode, plug-in electric vehicles (PEVs) draw power from the electricity grid to charge their battery packs. The amount of power taken from the grid can be flexibly adjusted based on factors such as electricity pricing and network load.
- Vehicle to Grid (V2G) Mode:
  During this mode, PEVs have the ability to inject power back into the grid. Consequently, electricity stored within PEV batteries can be redirected back to the grid during periods of grid congestion or high electricity prices.

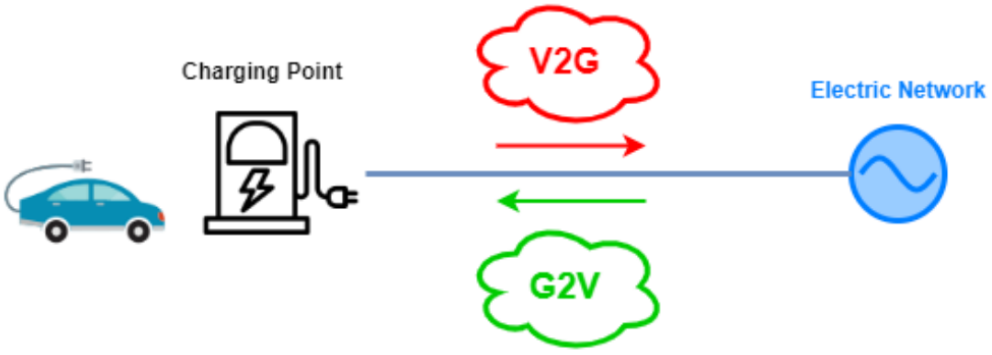

Figure 5: V2G and G2V Operation mode of Electric vehicle.

2.6.4 Challenge Of V2G and G2V

An essential requirement for achieving widespread adoption of Vehicle-to-Grid technology is the capacity to fulfill the needs of both the network operator and the vehicle owner. To align these different interests, the term "dispatch" refers to the strategic planning and control of electric vehicle activity. This involves the planned start and stop of V2G operations, harmonizing the requirements of both the power system and the vehicle owner [24].

The power grid operator needs to manage when electricity is produced and consumed, especially during critical times. On the other hand, the driver of the vehicle requires enough energy stored in the vehicle to meet their transportation needs. To strike a harmonious balance between these potentially opposing demands, effective control becomes paramount. Microgrids emerge as the vital link, skillfully harmonizing these conflicting requirements through an integrated, comprehensive, and refined solution.

2.7 Load Management

Effective load modeling necessitates the incorporation of flexibility, which stems from the involvement of end-users in Demand Response (DR) programs. The concept of modeling flexibility involves depicting how energy consumption alters concerning a reference load profile in response to price signals or incentives. Flexibility can be attributed to various household appliances through reduction and/or shifting. Accordingly, loads are categorized as shiftable, curtailable, and inflexible [2]

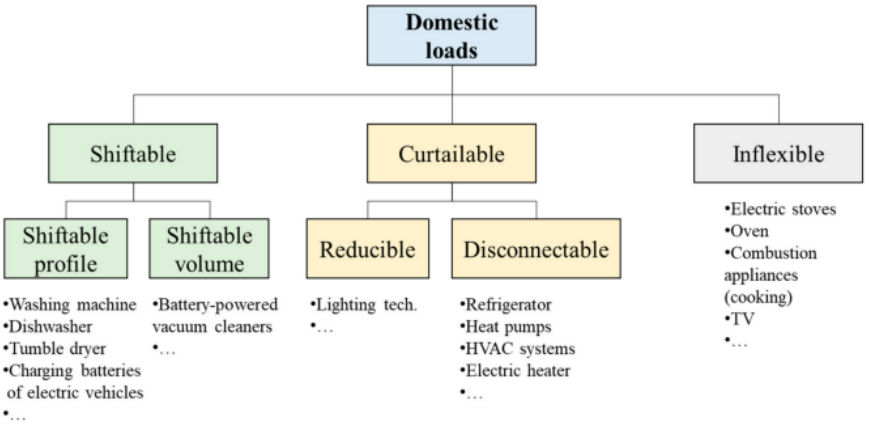

Figure 6: Loads classification [2].

- Shiftable / Shedable loads denote appliances whose total load must always be met but can be relocated within a specified time frame, typically a day. Within this category, a further division is possible between shiftable profile loads, whose profile can be shifted but not altered, and shiftable volume loads, where the total volume must be met across specific time intervals, though the profile can be adjusted within limits. For instance, electrical appliances like washing machines, dishwashers, tumble dryers, and uncontrolled electric vehicle battery charging exemplify shiftable profile loads, while a battery-powered vacuum cleaner serves as a clear instance of a shiftable volume load.
- Curtailable / Adjustable loads encompass those that can be reduced, with or without a potential inconvenience for users. Among curtailable loads, reducible and disconnectable loads can be differentiated; the former can only be decreased up to a certain level, such as dimming lights, while the latter can be either on or completely off. This category includes thermal and electro-thermal loads, along with refrigerators, collectively referred to as "thermostatically controllable loads". Typically, disconnectable loads leverage the inertia of thermodynamic systems when adapting to shifts in energy supply. As a result, their connection/disconnection does not immediately lead to service interruption, thereby offering flexibility both upward and downward. For example, considering thermal and electro-thermal loads for space cooling, thermal energy can be stored or curtailed within the building's thermal mass by adjusting the set-point temperature (respectively upward/downward flexibility). However, this necessitates suitable design of buildings with appropriate thermo-physical attributes.
- Inflexible / Sensitive loads encompass all appliances that require uninterrupted and reliable operation, necessitating a constant assurance of their nominal power. Such loads could encompass elevators, emergency lighting, computers, and televisions. It is assumed that these loads remain beyond the scope of control by demand response programs.

Numerous applications of Demand Response involving electrical appliances have been proposed in the existing literature, while the maturation of Demand Response for district heating-connected buildings is still in progress, and limited studies have explored its potential. This is likely due to the constrained adoption of district heating in various regions.

2.8 Microgrid Control

Efficient energy management within Microgrid systems is essential for enhancing the system's overall effectiveness, cutting down electricity expenses, and extending the lifespan of its components such as converters, batteries, and fuel cells. The utilized control strategies fall into three primary categories: centralized, decentralized, and hierarchical control [25].

2.8.1 Centralized Control

Centralized control methods utilize a single central controller to manage various components within the system. This central controller is equipped with a high-performance processing unit and a secure communication architecture. Each individual component requires a local controller to establish direct communication and interaction with the central controller. Modern communication and computing technologies facilitate real-time data monitoring, collection, and analysis by the central control. This collaborative setup empowers all components to engage with the central controller, ensuring operational flexibility for the microgrid, both in grid-connected and island modes. The central controller compiles data encompassing factors like renewable energy system (RES) production, energy consumption patterns, energy prices set by market operators, and weather conditions. Subsequently, it employs these insights to implement the most optimal and efficient system control strategy.

2.8.2 Decentralized / Distributed Control

In contrast to centralized methods, decentralized control revolves around the concept of individual entities operating autonomously via their dedicated local controllers. This means that distinct leadership roles are designated for various clusters of entities. The terms "decentralized" and "distributed control" are often employed interchangeably in the literature. Essentially, distributed control can be regarded as a type of decentralized control, where local controllers make use of local measurements like frequency and voltage values. Furthermore, they possess the capability to exchange information with adjacent controllers. Within the context of distributed control, local controllers not only depend on localized measurements but also have the ability to share essential information with other controllers. The decentralized control model hinges on constrained local connections, with control decisions being exclusively formulated based on local measurements.

2.8.3 Hierarchical Control

A middle ground between fully centralized and decentralized control frameworks is achieved by introducing hierarchical control structures, comprising three levels of control: Primary, secondary, and tertiary.

- Primary Control: The primary control level focuses on stabilizing the voltage and frequency produced by each source, ensuring they adhere to the required standards. Furthermore, it allocates both active and reactive power. Additionally, this primary control level identifies the operational mode of the microgrid, granting the capability to function in both grid-connected and island modes.
- Secondary Control: At the secondary control level, corrective measures are implemented to reestablish microgrid voltage and frequency following load variations and changes introduced by renewable energy sources. The aim is to guarantee and improve power quality, aligning with the standards, and enabling synchronization between microgrid systems and the main electrical grid.
- Tertiary Control: Tertiary control involves the optimization of the microgrid's operational schedule over a defined timeframe. This encompasses the minimization of operational costs, factoring in load forecasts, renewable energy production, and electricity prices.

2.9 Interconnected Microgrids Control

The control and energy management of interconnected microgrids can utilize various architectures to ensure the best possible and synchronized performance of each system in both grid-connected and islanded modes, while

also reducing operational costs. These architectural options encompass centralized, decentralized, distributed, or hierarchical structures, similar to the MG control approach mentioned above. Additionally, alternative configurations for control and energy management architecture involve the application of multi-agent technology or system-of-systems frameworks [26].

- Centralized Control: subsection: 2.8.1
- Decentralized / Distributed Control: subsection: 2.8.2
- Hierarchical Control: subsection: 2.8.3
- Multi-Agent Control: Distributed control, employing multi-agent technology, involves several self-governing and smart agents spread throughout the system. Unlike the typical agents in traditional distributed control methods, these advanced agents can tackle much more intricate coordination issues, aiming to achieve shared or individual goals. This approach also offers the advantage of high network scalability and the ability to seamlessly add new components. However, all control agents in this setup are connected, needing communication links to interact with each other effectively.
- System of Systems Control: Control rooted in a system-of-systems framework integrates and harmonizes multiple independent systems to create a larger and more intricate system, capable of accomplishing objectives or tasks that a solitary system or a collection of uncoordinated systems couldn't achieve. All these systems are interconnected and collaboratively share their resources to enhance the overall operation of the entire cluster and achieve the overarching goal.

Typically, control strategies for clusters of MGs are structured into multiple layers or arranged in a hybrid hierarchical manner, often with specific control tiers implemented either in a centralized or decentralized approach [26].

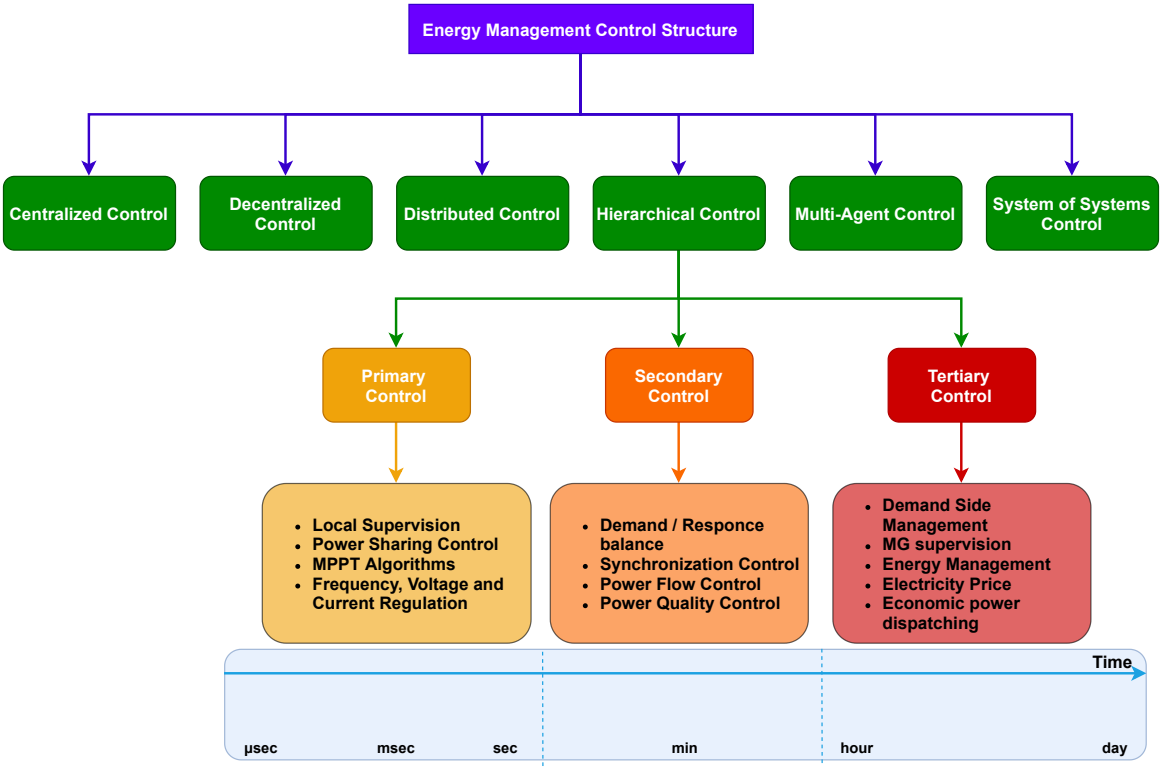

Figure 7: Control Structure for Energy Management in Cluster of Microgrids

2.10 Electricity Markets

In the context of electricity markets, vertical integration involves one company owning the generation, transmission, and distribution sectors. This structure is common in unregulated markets and vertically integrated utilities not only produce energy but also provide fixed-rate electricity to consumers. They can purchase power from independent suppliers and seek approval from state commissions for energy investments, with these commissions overseeing rates and returns. Due to concerns, especially in western countries, about the implications of vertical integration, there has been a substantial ongoing effort to restructure electricity markets. In restructured setups, Independent System Operators (ISOs) and Regional Transmission Organizations (RTOs) manage markets to ensure equitable access to transmission. While state commissions still set customer rates, restructured areas offer consumers the choice of their electricity supplier, encouraging competition and lowering costs.

Electricity exhibits unique characteristics that set it apart from conventional commodities [27]:

- Time: Economically storing substantial amounts of electricity remains a challenge. Consequently, the value of electricity changes over time.
- Location: Controlling electricity flows efficiently is complex, with transmission components requiring adherence to safe flow limits. Deviating from these limits risks cascading failures and blackouts, resulting in electricity's differing spatial value.
- Flexibility: Synchronization between demand and generation is crucial to avoid blackouts. However, demand and the availability of renewable energy resources can fluctuate considerably over time. Some power stations adjust output slowly and have extended start-up times, while sudden power station failures can occur. Thus, the ability to swiftly modify electricity generation/consumption holds significant value.

2.10.1 Types of Wholesale and Electricity Markets

Day-Ahead Market
The Day-Ahead Energy Market allows market participants to make advance commitments for purchasing or selling wholesale electricity a day prior to the actual operating day, aiming to mitigate price fluctuations. This market results in a single financial settlement. Day-Ahead Markets typically employ hourly clearance, where market participants present bids for buying and selling to the auction-administering operator responsible for overseeing the process.

Intra-Day Market
The Intra-Day Market, playing a pivotal role in the electricity trading landscape, allows market participants to engage in wholesale electricity transactions within the operating day, ensuring a dynamic balance between supply and demand. These markets hold a crucial responsibility in maintaining grid stability, enabling participants to manage unforeseen changes in electricity consumption or generation. Furthermore, they determine the real-time locational marginal price (LMP), which compensates participants in the Day-Ahead Energy Market for deviations from their initial commitments. This intricate mechanism ensures the equilibrium of electricity supply and demand while governing the financial dynamics of energy transactions. The Intraday markets operate through continuous trading, where member orders are perpetually entered into the order book. As soon as two orders match, the trade is executed. Contracts for hourly, half-hourly, and quarter-hourly power quantities can be traded up to 5 minutes before delivery [28].

Ancillaty Services Markets
Ancillary Service Markets serve as a financial tool designed to streamline the operation of the electrical power system. Within RTOs, these markets categorize into two segments: regulation services and operating reserves services, both accessible through bid-based auction setups [29]. These services play a crucial role in ensuring the security and stability of the power system, encompassing tasks like frequency regulation, voltage regulation, load shedding, automatic islanding, and additional functions such as black start and power quality services.

Ballancing Markets

The final phase of electric energy trading is the balancing market, a pivotal component where maintaining a balance between production and consumption in electric power systems is imperative. This aspect is particularly crucial due to the current economic impracticality of storing large amounts of electric energy. Balancing markets typically function as single-period markets, featuring distinct sessions for each trading interval. These markets enable not only the trading of electric energy but also ancillary services, such as voltage control, essential for upholding electric system stability. Conventional producers are regular participants in the balancing market, primarily engaging to supply regulating power. This involvement spans both the upward direction (increasing production) and the downward direction (reducing production) [30].

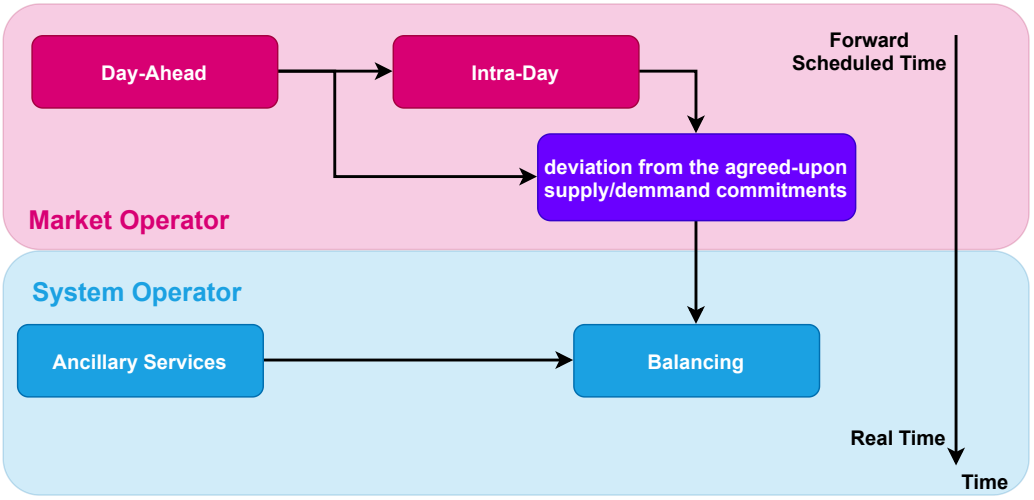

Figure 8: Electricity Market Timeline

2.10.2 Peer to Peer Electricity Trading

Peer-to-Peer Electricity Trading denotes the direct exchange of electricity between grid users without intermediaries. This approach brings substantial benefits, including higher renewable power deployment, increased flexibility, efficient balancing, congestion management, and contributing ancillary services to the grid. This concept transforms energy consumers into prosumers, allowing them not only to consume energy but also to generate and share it within their local network.

The P2P model can find application both within local communities, connecting neighbors, and on a larger scale, linking different Microgrids. Transactions facilitated under P2P protocols rely on the distribution and transmission systems to manage the power flow. This necessitates either integration with ISOs and RTOs or maintaining close communication with them. This is due to factors such as the impact of power flow on local networks, the operational and remunerative needs of the distribution network, and the requirement for upstream trading of excess load/generation [31].

Considering these factors, the growing adoption of renewable energy sources and distributed energy systems has led to the emergence of peer-to-peer (P2P) electricity markets. These markets play a crucial role in dealing with the uncertainty of renewable energy generation, aiding in managing power demand, and improving grid stability. P2P energy trading also offers an opportunity to reduce dependence on traditional grids, promote sustainability, and even generate extra income for households.

2.10.3 Non-Cooperative Games in Electricity Markets

Non-cooperative games find particular utility in peer-to-peer (P2P) electricity markets due to their ability to model the decentralized and self-interested nature of interactions between individual participants. In a P2P

electricity market, where individuals or small entities can directly trade energy with one another, participants act autonomously to make decisions that align with their preferences and constraints. Non-cooperative game theory allows for the analysis of how these independent agents strategize to optimize their outcomes within this context. By modeling these interactions as non-cooperative games, the dynamics of supply, demand, pricing, and energy sharing can be better understood. Moreover, the equilibrium points in such games offer insights into potential stable outcomes, helping to predict market behaviors and facilitating the design of mechanisms that incentivize efficient energy trading and resource allocation among peers. Therefore, non-cooperative game theory provides a valuable framework for studying and designing effective strategies in peer-to-peer electricity markets, ultimately enabling more resilient and adaptive decentralized energy systems.

3 Microgrid Components Modelling

3.1 Model of Building Thermal Load

The room's air capacity serves as a storage medium, incorporating a built-in delay function. This inherent delay stems from the time required for the heating or cooling system to effectively adjust the air temperature. By capitalizing on this innate phenomenon, each thermal zone of house can essentially function as a miniature virtual battery. Through energy management, these zones offer economic advantages while seamlessly fulfilling the preferences and needs of the room's occupants. This approach not only meets the residents' demands but also optimizes energy consumption for cost-efficient operation.

In this work each building is divided into thermal zones. To study the behavior of each thermal zone, a mathematical relationship between the internal temperature, thermal gains, thermal loads, and ambient temperature can be created using the thermal equilibrium equation shown below [32],[33],[34].

$$\begin{aligned} &p_z \cdot C_z \cdot V_z \cdot \frac{dT_{in,z}}{dt} = \\ &\dot{Q}_{ex,wall,z} + \dot{Q}_{in,wall,z} + \dot{Q}_{win,z} + \dot{Q}_{in,z} + \dot{Q}_{sw,z} + \dot{Q}_{sg,z} - Q_{HVAC,z} \end{aligned} \tag{3.1}$$

Equations (3.2) through (3.5) use the thermal zones' parameters, ambient temperature and ambient irradiation, to describe the heat exchange between a thermal zone and its surrounding environment, while Equation (3.6) calculates the heat exchange between a thermal zone and its neighboring zones.

$$\dot{Q}_{ex,wall,z} = \sum_{y \in \varepsilon} \left(U_{wall,y} \cdot F_{wall,y} \cdot (T_{out} - T_{in,z}) \right) \tag{3.2}$$

$$\dot{Q}_{win,z} = \sum_{y \in \varepsilon} \left(U_{win,y} \cdot F_{win,y} \cdot (T_{out} - T_{in,z}) \right) \tag{3.3}$$

$$\dot{Q}_{sw,z} = \sum_{y \in \varepsilon} \left(\alpha_w \cdot R_{se} \cdot U_{wall,y} \cdot F_{wall,y} \cdot I_{T,z} \right) \tag{3.4}$$

$$\dot{Q}_{sg,z} = \sum_{y \in \varepsilon} \left(\tau_{win} \cdot SC \cdot F_{win,y} \cdot I_{T,z} \right) \tag{3.5}$$

$$\dot{Q}_{in,wall,z} = \sum_{y \in \varepsilon} \left(U_{wall,y} \cdot F_{wall,y} \cdot (T_{in,nz} - T_{in,z}) \right) \tag{3.6}$$

with:

$$I_{T,z} = I_b \cdot R_b + I_d \cdot \left(\frac{1 + \cos \beta_z}{2} \right) + I \cdot p_g \cdot \left(\frac{1 - \cos \beta_z}{2} \right) \tag{3.7}$$

$$R_b = \frac{\cos \theta}{\cos \theta_z} \tag{3.8}$$

The state-space representation for each building is generated by appropriately changing equations (3.1) through (3.6), succinctly encapsulating the system's dynamic behavior.

$$\frac{d\mathbf{T_{in}}(t)}{dt} = \mathbf{A_b} \cdot \mathbf{T_{in}}(t) + \mathbf{B_b} \cdot \mathbf{U} \tag{3.9}$$

$$\frac{d\mathbf{Y}(t)}{dt} = \mathbf{C_b} \cdot \mathbf{T_{in}}(t) + \mathbf{D_b} \cdot \mathbf{U} \tag{3.10}$$

with input vector U with dimension ($2N_z+2$) $\times$ 1 given in (3.11):

$$\mathbf{U} = \begin{bmatrix} Q_{HVAC,1}(t) \\ \vdots \\ Q_{HVAC,N_z}(t) \\ Q_{in,1}(t) \\ \vdots \\ Q_{in,N_z}(t) \\ T_{out}(t) \\ I_T(t) \end{bmatrix}_{(2N_z+2)\times 1} \tag{3.11}$$

The elements of matrix $\mathbf{A_b}$ with dimensions $N_Z \times N_Z$ are computed using equations (3.12) and (3.13).

$$\begin{aligned} A_{j,j} = &- \sum_{y\in\varepsilon} \left(U_{wall,y} \cdot F_{wall,y} \right) - \sum_{x\in\jmath} \left(U_{wall,x} \cdot F_{wall,x} \right) \\ &- \frac{1}{p_z \cdot C_z \cdot V_z} \sum_{y\in\varepsilon} \left(U_{win,y} \cdot F_{win,y} \right) \end{aligned} \tag{3.12}$$

$$A_{j,i} = \begin{cases} \dfrac{1}{p_z \cdot C_z \cdot V_z} \cdot U_{\text{wall},x} \cdot F_{\text{wall},x}, & j,i \in N \\ 0, & j,i \notin N \end{cases} \tag{3.13}$$

The matrix $\mathbf{B_b}$ with dimensions $N_Z \times (2N_Z+2)$ is computed using the following equation.

$$\mathbf{B_b} = \frac{1}{p_z \cdot C_z \cdot V_z} \cdot \begin{bmatrix} -\mathbf{I}_{N_z\times N_z} & \mathbf{I}_{N_z\times N_z} & \mathbf{B}_{ex,w_{N_z\times 1}} & \mathbf{B}_{rad_{N_z\times 1}} \end{bmatrix}_{N_z\times(2N_z+2)} \tag{3.14}$$

with:

$$\mathbf{B_{ex,w}} = \begin{bmatrix} B_{ex,w,1} \\ \vdots \\ B_{ex,w,N_z} \end{bmatrix}_{N_z\times 1} \tag{3.15}$$

$$\mathbf{B_{rad}} = \begin{bmatrix} B_{rad,1} \\ \vdots \\ B_{rad,N_z} \end{bmatrix}_{N_z\times 1} \tag{3.16}$$

Each element inside the submatrices $\mathbf{B_{ex,w}}$ and $\mathbf{B_{rad}}$ is calculated using respectively the equations (3.17) and (3.18).

$$B_{ex,w,z} = \sum_{y\in\varepsilon} \left(U_{wall,y} \cdot F_{wall,y} \right) - \sum_{y\in\varepsilon} \left(U_{win,y} \cdot F_{win,y} \right) \tag{3.17}$$

$$B_{rad,z} = \sum_{y \in \varepsilon} \left(\alpha_w \cdot R_{se} \cdot U_{wall,y} \cdot F_{wall,y}\right) + \sum_{y \in \varepsilon} \left(\tau_{win} \cdot SC \cdot F_{win,y}\right) \tag{3.18}$$

Given the internal temperature of the thermal zones as the output, the matrices $\mathbf{C_b}$ and $\mathbf{D_b}$ are defined as follows,

$$\mathbf{C_b} = \mathbf{I}_{N_z \times N_z} \tag{3.19}$$

$$\mathbf{D_b} = \mathbf{0}_{N_z \times (2N_z+2)} \tag{3.20}$$

From the system of continuous time equations (3.9), (3.10) the system of discrete time equations (3.21), (3.22) is created.

$$\mathbf{T_{in}}(k+1) = \mathbf{A_{b,d}} \cdot \mathbf{T_{in}}(k) + \mathbf{B_{b,d}} \cdot \mathbf{U} \tag{3.21}$$

$$\mathbf{Y}(k) = \mathbf{B_{b,d}} \cdot \mathbf{T_{in}}(k) + \mathbf{D_{b,d}} \cdot \mathbf{U} \tag{3.22}$$

3.2 Model of Building Electrical Load

Each thermal zone of the building has various types of electrical loads that can be characterized as either critical or non-critical. Examples of critical loads include televisions, lighting, personal computers, security systems, medical equipment, and other systems whose power consumption cannot be altered. Non-critical loads involve devices such as washing machines, dryers, dishwashers, smart refrigerators, and smart heating and cooling systems, which possess some degree of flexibility in adjusting their electricity usage across different time periods of the day.

The power consumption of zth thermal zone of building, denoted as $P_{el\_load,z}$ is determined by considering the forecasted number of occupants that are active (not sleeping) and their respective appliance utilization [35]. The cumulative electrical power consumption of the entire building is calculated using the formula below:

$$P_{el,b} = \sum_{z} P_{el_{load},z} \tag{3.23}$$

Wherein $P_{el\_load,z}$ symbolizes the power consumption attributed to the electrical loads within the zth thermal zone. In this work, we assume that the power consumption of non-critical loads represents a proportion denoted as n_{non_cr} of the overall power consumed by the building's electrical loads.

$$P_{non_{cr}}(t) = \sum_{b} \left(n_{non_{cr}} \cdot P_{el_{load},z}\right) \tag{3.24}$$

The controllable loads can be scheduled in a specific time zone and not in the whole 24-hour period, and thus $[T_{shift,0}\ T_{shift,f}]$ defines the starting and stopping points of the optimization horizon for the controllable (schedulable) loads. The load shifting algorithm is designed to move a certain portion of the non-critical load power consumption from one timeslot to another. However, there are physical limitations in the maximum and minimum power transfers. This limitation is represented in $[\eta_{shift,min}\ \eta_{shift,max}]$. The transfer is done under the condition that the total energy consumption before and after the load adjustment remains unchanged.

$$P^*_{non_{cr}}(t) = \begin{cases} \eta_{shift}(t) \cdot P_{non_{cr}}(t), & \forall t \in [T_{shift,0} T_{shift,f}] \\ P_{non_{cr}}(t), & \text{otherwise} \end{cases} \tag{3.25}$$

$$\eta_{shift,min} \leq \eta_{shift}(t) \leq \eta_{shift,max} \tag{3.26}$$

3.3 Analysis of Electrical and Thermal Load Origins in Residential Buildings

The number of permanent occupants, their distribution across the house, and whether they are asleep or active constitute crucial information. As mentioned, this data shapes the electrical and thermal load profiles of each household.

Referring to the chart provided by the European Health Information Gateway of the World Health Organization, it can be inferred that assuming one permanent occupant per room of the house is a reasonable premise [36]. The probability distribution used to determine the count of permanent occupants is illustrated in detail in the case study shown in Figure [21].

To efficiently extract occupancy data regarding indoor occupants, we utilized information from the American Time of Use Survey, which is available on the official website of the United States Government, U.S. BUREAU OF LABOR STATISTICS. This survey examines the percentage of the population participating in various activities throughout the day, spanning from 12 AM to 11 PM [37]. The data represents averages for the combined years 2013-2017, offering insights into individual activities at different times of the day. This dataset serves as the foundation for constructing realistic occupancy profiles.

To quantify the likelihood of individuals being indoors and their corresponding states (such as being active or asleep), relevant activity weights were incorporated. These weights were derived to quantify how likely these activities take place indoors. The methodology involved referring to the survey's analytical guide and relevant examples to ensure accurate calibration of the weights given in the activities [38].

(a) ante meridiem

Table A-3A. Percent of the population engaging in selected activities by time of day, 12 AM to 11 AM, average for the combined years 2013-17

Activity	12 AM	1 AM	2 AM	3 AM	4 AM	5 AM	6 AM	7 AM	8 AM	9 AM	10 AM	11 AM
Total, all activities[1]	100.0	100.0	100.0	100.0	100.0	100.0	100.0	100.0	100.0	100.0	100.0	100.0
Personal care activities	86.2	92.3	94.9	95.9	93.6	88.7	75.4	52.7	32.7	20.0	12.3	8.5
Sleeping[2]	84.8	91.6	94.2	95.2	91.3	84.6	65.3	42.2	24.8	13.8	7.5	4.9
Eating and drinking	0.6	0.3	0.3	0.3	0.5	1.1	3.1	5.9	7.2	6.4	5.2	6.1
Household activities	0.7	0.3	0.3	0.3	0.9	1.8	4.5	8.0	10.5	13.2	14.1	13.8
Housework	0.2	0.1	0.1	–[3]	0.1	0.3	0.7	1.8	3.6	5.3	6.0	5.7
Food preparation and cleanup	0.2	0.1	0.1	0.1	0.5	0.9	2.4	3.7	3.7	3.4	2.9	2.9
Lawn and garden care	–[3]	–[3]	–[3]	–[3]	–[3]	–[3]	0.2	0.4	0.9	1.4	1.9	1.9
Household management	0.1	0.1	–[3]	–[3]	0.1	0.1	0.2	0.5	0.6	0.8	1.0	0.9
Purchasing goods and services	0.2	0.1	0.1	0.1	0.1	0.2	0.4	1.0	2.0	3.9	5.8	7.2
Consumer goods purchases	0.1	–[3]	–[3]	–[3]	–[3]	–[3]	0.1	0.2	0.6	1.1	2.3	3.2
Professional and personal care services	–[3]	–[3]	–[3]	–[3]	–[3]	–[3]	–[3]	0.1	0.3	0.8	0.9	1.1
Caring for and helping household members	0.3	0.3	0.2	0.2	0.4	0.5	1.6	3.9	3.6	2.6	2.4	2.3
Caring for and helping household children	0.2	0.2	0.2	0.2	0.3	0.3	1.3	2.7	2.2	1.8	1.7	1.7
Caring for and helping nonhousehold members	0.1	0.1	0.1	–[3]	–[3]	0.1	0.2	0.4	0.8	1.0	1.1	1.3
Caring for and helping nonhousehold adults	–[3]	–[3]	–[3]	–[3]	–[3]	–[3]	–[3]	0.1	0.2	0.4	0.5	0.6
Working and work-related activities	2.2	1.7	1.5	1.5	2.3	3.9	7.9	16.0	25.1	29.0	30.4	30.8
Working	1.9	1.5	1.4	1.3	1.9	2.8	5.7	11.8	21.5	27.0	29.0	29.6
Educational activities	0.3	0.2	0.1	–[3]	–[3]	0.1	0.3	1.4	3.2	4.2	4.5	4.5
Attending class	–[3]	–[3]	–[3]	–[3]	–[3]	–[3]	0.1	0.5	2.5	3.3	3.5	3.3
Homework and research	0.3	0.2	0.1	–[3]	–[3]	0.1	0.1	0.2	0.4	0.6	0.7	0.9
Organizational, civic, and religious activities	0.2	0.1	0.1	0.1	0.1	0.4	0.6	0.9	1.5	2.6	3.6	3.8
Religious and spiritual activities	0.1	–[3]	–[3]	–[3]	0.1	0.3	0.5	0.5	0.7	1.0	1.8	2.1
Volunteering (organizational and civic activities)	0.1	–[3]	–[3]	–[3]	–[3]	–[3]	0.1	0.2	0.5	1.0	1.3	1.3
Leisure and sports	8.7	4.4	2.3	1.5	1.7	2.9	5.3	8.4	11.5	15.1	18.3	19.5
Socializing and communicating	1.0	0.5	0.2	0.1	0.1	0.1	0.2	0.6	0.9	1.5	2.2	2.7
Watching television	4.6	2.2	1.1	0.7	0.9	1.3	2.1	3.4	4.7	6.0	7.2	8.1
Participating in sports, exercise, and recreation	0.2	0.1	0.1	0.1	0.1	0.4	0.9	1.2	1.6	2.0	2.0	1.9
Telephone calls, mail, and e-mail	0.3	0.2	0.1	0.1	0.1	0.1	0.2	0.3	0.6	0.7	0.8	0.8
Other activities, not elsewhere classified	0.2	0.1	0.1	0.1	0.2	0.3	0.5	1.1	1.2	1.3	1.4	1.4

[1] All major activity categories (the activity names that are not indented) include related travel time.
[2] Includes naps and spells of sleeplessness.
[3] Estimate is approximately zero.
NOTE: These data are a snapshot of the main activities people were doing at the time indicated. At each time of day, the major activity categories sum to 100 percent, although sums may not be exact due to rounding. Data refer to persons 15 years and over. For technical information about the American Time Use Survey, see the ATUS User's Guide at https://www.bls.gov/tus/atususersguide.pdf.
Source: American Time Use Survey, Bureau of Labor Statistics

(b) post meridiem

Table A-3B. Percent of the population engaging in selected activities by time of day, 12 PM to 11 PM, average for the combined years 2013-17

Activity	12 PM	1 PM	2 PM	3 PM	4 PM	5 PM	6 PM	7 PM	8 PM	9 PM	10 PM	11 PM
Total, all activities[1]	100.0	100.0	100.0	100.0	100.0	100.0	100.0	100.0	100.0	100.0	100.0	100.0
Personal care activities	6.4	6.4	6.7	6.7	6.3	6.0	5.5	6.2	9.8	22.0	46.2	71.4
Sleeping[2]	3.6	4.1	4.5	4.4	3.8	3.0	2.5	3.0	5.8	16.6	40.7	68.2
Eating and drinking	16.0	10.8	5.9	4.2	4.8	9.0	15.4	13.7	8.5	4.4	2.1	0.9
Household activities	13.2	12.4	11.8	11.8	13.1	15.2	14.5	11.3	8.0	5.1	3.0	1.4
Housework	4.6	4.4	4.1	3.7	3.4	2.6	2.2	2.1	1.9	1.6	0.9	0.4
Food preparation and cleanup	3.6	2.8	2.5	3.0	4.6	7.9	8.5	6.0	3.5	1.8	0.8	0.3
Lawn and garden care	1.6	1.7	1.7	1.6	1.4	1.2	1.0	0.8	0.4	0.1	–[3]	–[3]
Household management	0.9	0.9	1.0	0.9	1.0	0.8	0.7	0.7	0.6	0.6	0.4	0.3
Purchasing goods and services	7.9	7.7	7.4	7.3	6.9	6.4	5.3	3.8	2.5	1.5	0.8	0.4
Consumer goods purchases	3.5	3.7	3.6	3.4	3.0	2.8	2.3	1.8	1.3	0.7	0.3	0.1
Professional and personal care services	0.8	0.7	0.7	0.8	0.7	0.5	0.3	0.1	0.1	–[3]	–[3]	–[3]
Caring for and helping household members	2.1	2.1	2.6	3.8	4.2	4.3	4.0	4.5	4.8	3.3	1.5	0.6
Caring for and helping household children	1.5	1.5	1.8	2.5	2.8	2.8	3.0	3.9	4.3	2.9	1.2	0.4
Caring for and helping nonhousehold members	1.4	1.5	1.5	1.7	1.9	1.7	1.4	1.1	0.9	0.9	0.5	0.3
Caring for and helping nonhousehold adults	0.6	0.6	0.6	0.6	0.6	0.5	0.4	0.3	0.2	0.2	0.1	0.1
Working and work-related activities	24.0	28.0	30.0	29.2	25.9	19.3	12.0	8.4	6.6	5.7	4.6	3.4
Working	22.3	26.3	28.3	26.9	22.4	14.6	8.9	6.9	5.7	4.9	3.9	2.9
Educational activities	3.9	4.0	4.1	3.1	2.2	2.0	1.7	1.7	1.7	1.5	1.0	0.5
Attending class	2.7	2.8	2.9	1.4	0.5	0.3	0.3	0.4	0.3	0.1	–[3]	–[3]
Homework and research	0.9	0.9	1.0	1.1	1.4	1.3	1.2	1.2	1.3	1.1	0.9	0.5
Organizational, civic, and religious activities	2.8	1.9	1.7	1.5	1.4	1.6	1.9	2.3	2.1	1.4	0.7	0.3
Religious and spiritual activities	1.3	0.7	0.5	0.4	0.4	0.5	0.6	0.9	0.9	0.6	0.4	0.2
Volunteering (organizational and civic activities)	1.0	0.9	1.0	0.8	0.8	0.8	0.9	1.1	1.0	0.5	0.2	0.1
Leisure and sports	20.0	22.9	26.0	28.2	30.9	32.3	36.1	44.7	52.5	52.0	37.7	19.8
Socializing and communicating	2.9	3.3	4.1	4.5	5.1	5.6	6.0	6.4	6.1	5.0	3.4	2.0
Watching television	8.2	9.5	10.6	11.6	13.4	14.9	18.4	25.7	33.5	34.8	24.6	11.5
Participating in sports, exercise, and recreation	1.8	1.9	1.9	2.1	2.2	2.1	2.2	2.1	1.5	0.9	0.4	0.2
Telephone calls, mail, and e-mail	0.8	0.8	0.9	1.0	1.1	1.1	1.2	1.2	1.2	1.2	1.1	0.6
Other activities, not elsewhere classified	1.4	1.4	1.5	1.5	1.4	1.3	1.2	1.1	1.2	1.1	0.8	0.4

[1] All major activity categories (the activity names that are not indented) include related travel time.
[2] Includes naps and spells of sleeplessness.
[3] Estimate is approximately zero.
NOTE: These data are a snapshot of the main activities people were doing at the time indicated. At each time of day, the major activity categories sum to 100 percent, although sums may not be exact due to rounding. Data refer to persons 15 years and over. For technical information about the American Time Use Survey, see the ATUS User's Guide at https://www.bls.gov/tus/atususersguide.pdf.
Source: American Time Use Survey, Bureau of Labor Statistics

Table 1: Percent of the population engaging in selected activities by time of day, 12 AM to 11 AM, average for the combined years 2013-17 [37]

Utilizing these percentages, we can generate a profile for each permanent occupant of the house, indicating whether the occupant is indoors or outdoors. Additionally, since we possess data regarding sleeping habits and assume that sleep occurs entirely indoors (as occupants sleep within their houses), we can distinguish two further states for indoor occupants: being actively awake or asleep. The profiles of sleeping and active occupants contribute to occupancy-dependent internal thermal loads within the household. Conversely, for electrical loads that are occupancy-dependent, only the active profile influences them.

To visually illustrate the relationship between these percentages and the loads, we present Figure [9]. This figure depicts probability diagrams and demonstrates the correlation between each probability, along with indicating which percentages influence the various load types (thermal or electrical).

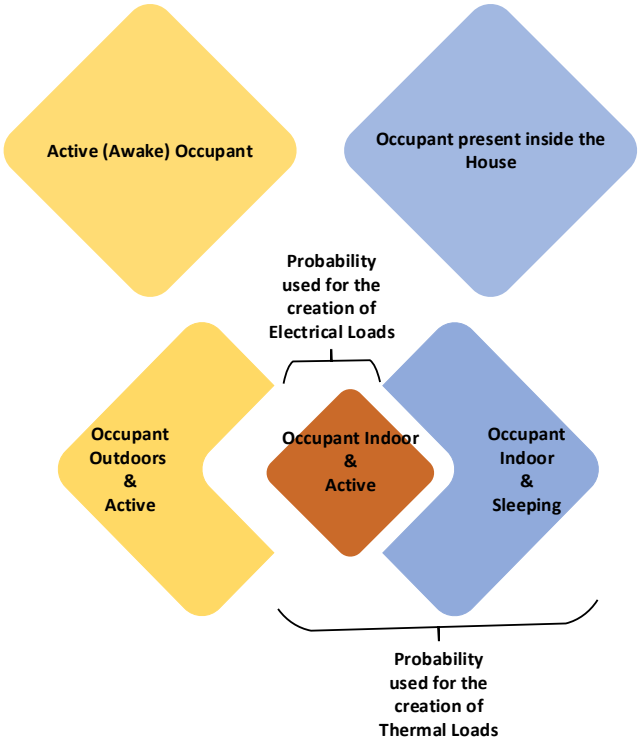

Figure 9: Venn Diagrams illustrating the relation between each state (Indoor, Sleep, Active)

The functions of individual rooms vary across houses, influenced by factors such as the house's size (number of rooms) and the count of permanent residents. To assign distinct roles to each room within a house, the allocation of room roles was approached with an element of randomness, yet firmly anchored in a logical framework, as depicted in details in the case study in Figure [22]. This figure outlines the potential room roles within a household, contingent on the household's characteristics and the count of permanent residents.

The way the occupants are distributed within the rooms of a house follows a specific logic that takes into account whether they are sleeping or active. By following this approach, we generate a profile for each room in the house over a 24-hour period. This profile includes the count of sleeping and active occupants in each room, allowing us to understand the indoor occupancy at different times of the day. When occupants are sleeping (as indicated by their sleeping profile), they are assigned to rooms with a "bedroom" role, ensuring they have a designated place to sleep. Meanwhile, the distribution of active occupants operates differently. At every hour, each occupant is placed in the room with the fewest fellow occupants. To encourage active occupants to be in separate rooms from sleepers, an artificial weight is introduced, steering the algorithm towards dispersing active individuals away from the same rooms as those who are sleeping. By summing up the profile of both active and sleeping occupants, we obtain a comprehensive overview of individuals present indoors during each time interval of the day. This method provides valuable insights into the household's electrical and thermal activity patterns throughout the day.

In order to accurately model the electrical loads of the house, we must consider two distinct load categories. Firstly, there are loads that remain consistent regardless of whether people are present in the house. These loads, such as the refrigerator and freezer, are represented as constant time series over the 24-hour period. Together, they constitute the foundational power consumption of the house, known as the baseload power. The second category encompasses loads that vary based on the presence of occupants in the house's rooms. These loads are simulated by multiplying the number of active occupants in a given thermal zone with an assigned artificial weight. It's worth noting that both categories are also influenced by the overall area of the house in order to make the load fully parametric and adjustable with the change of house dimensions.

In the category of loads that are independent of the presence of people (non-occupancy dependent loads), we have the refrigerator, freezer, and an unknown factor (used to represent an increase in baseload consumption with an increase in the house's area). On the other hand, the loads dependent on the presence of people—specifically active occupants—(occupancy dependent loads) are calculated as a product of the number of active occupants and the house's area. By summing up these contributions, the total house load profile is computed, encompassing non-occupancy dependent load, occupancy-dependent load, and light load.

We construct the profile for the lighting in each room of the house according to the time of day. The logic underlying this lighting profile is straightforward: if there is at least one active person in a room, the lights are turned on. In this regard, the count of active occupants is not the focus; rather, the presence of an active individual within a room during a specific hour determines the lighting status. For an accurate representation of the lighting profile, we also account for the natural outdoor illumination that lights up the house. Specifically, using data from Australia as a reference (given the similarity between an Australian January day and a Greek July day, which is pivotal for this simulation centered around a Greek summer day), we find that from 9:00 AM to 10:00 AM until 6:00 PM to 7:00 PM, the natural outdoor light is sufficient to meet the lighting needs. In order to assess the electrical power consumption required to meet the lighting demands of the house, we combine the unitary lighting necessity profile (which hinges on the presence of an active person) with the installed capacity. This merging allows us to accurately measure both the electrical and thermal load generated by addressing the house's lighting needs. The calculation of the installed light capacity, tailored to the distinct roles of each room, is explained in detail within Flowchart [10].

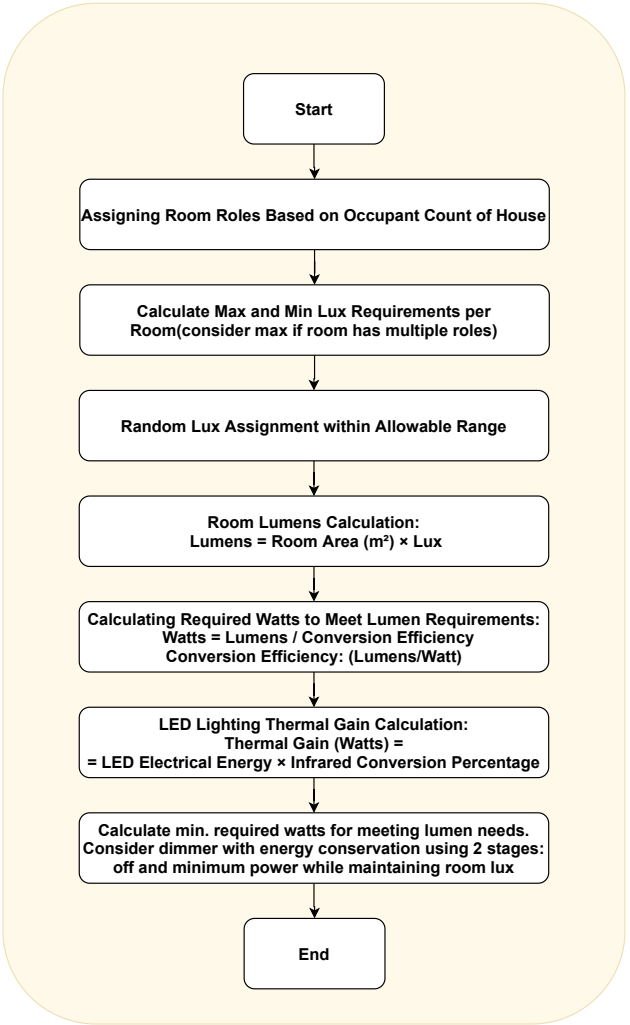

Figure 10: Installed Electrical and Thermal Load from House Lighting

For designing the lighting layout of houses (installed capacity), it's essential to recognize that each room's lighting requirements can differ due to the varied activities undertaken. For instance, the kitchen, being a space for cooking and other tasks, demands higher lighting levels compared to bedrooms, primarily used for relaxation.

When addressing thermal loads, the process begins by considering the established thermal loads for a single occupant, measured in watts. These values are multiplied by the profile of indoor occupants, regardless of whether they are sleeping or active. Additionally, we possess information regarding the thermal loads of appliances per person, where "person" in this context pertains to active occupants. These appliance-related thermal loads per person can be approximated as a fraction of the total electrical power output generated by these appliances. It is reasonable to assume that a portion of residential electricity consumption is converted into thermal load through household appliances. With this understanding, we proceed to calculate the internal heat gains or thermal loads for all the thermal zones within the building. These thermal loads emanate from three sources: people, appliances, and lighting.

3.4 Parking Lot Dynamic Aggregate Battery

A novel dynamic equivalence battery model is formulated for PEVs within MG parking lots. This innovative model relies on forecasts of PEVs' plug-in time, dwell time duration, initial SoC, and battery specifications. The primary objective of this framework is to aggregate multiple PEVs (concentrated in parking lots or dispersed) together and represent them as a virtual equivalent battery, with the total SoC of the equivalent battery comprising the summation of the SoC of individual PEVs. The total power capacity available for interactions with the MG is determined in the same way as with the SoC. Thus, the Capacity of the virtual battery can be exploited to implement energy management techniques to provide services to the MG.

The concept of a virtual aggregator is very important because, in this way, the system operator disengages from the complexity of taking into account all technical constraints of individual PEVs because this task is assigned to the Aggregator. The graphical representation of an individual PEV's viable operational range is depicted in Figure [11].

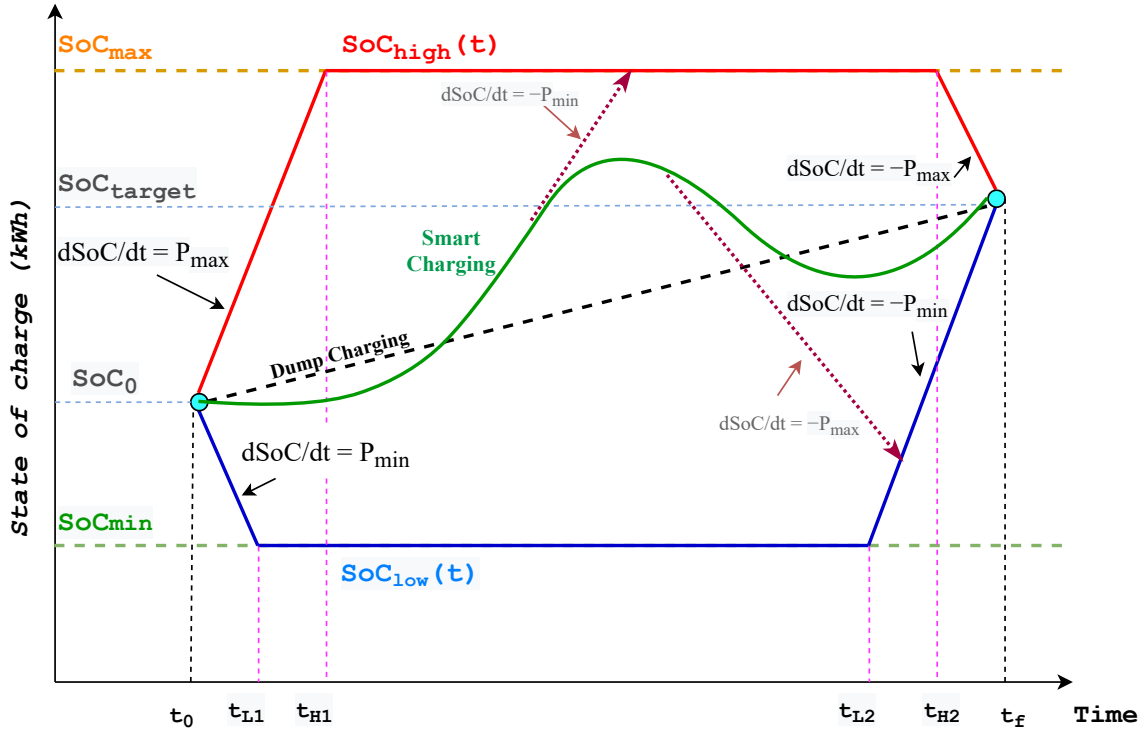

Figure 11: Bounds of PEV's Stored Energy

In the above figure, the time points at which the EV is connected (plugged) to and disconnected (unplugged) from the network are designated as t_0 and t_f, correspondingly. Most of the time, the vehicle's battery operates not at extreme values but within a range of values around an optimal level in order to mitigate degradation. Consequently, it is necessary to establish the minimum and maximum allowable limits for the charge level. The upper and lower bounds of the PEV's battery SoC are denoted as SoC_{max} and SoC_{min} (measured in kWh), respectively. SoC_0 is the initial SoC (measured in kWh) of each PEV. SoC_{target} is the predetermined energy storage objective that the driver sets for the PEV to have at the end of the dwell time. P_{max} and P_{min} signify the highest and lowest power levels at which the PEV's battery can exchange energy with the network, respectively, and they are defined by the technical characteristics of the vehicle.

It is also necessary to define the dynamic lower and upper SoC thresholds (SoC_{high}, SoC_{low}) which depend on the time t. They are defined by four points where they start to increase or decrease with a constant rate of charge, P_{min} or P_{max}. These points are (t_0, SoC_0), (t_{L1}, SoC_{min}), (t_{L2}, SoC_{min}), (t_f, SoC_{target}) for SoC_{low} and (t_0, SoC_0), (t_{H1}, SoC_{max}), (t_{H2}, SoC_{max}), (t_f, SoC_{target}) for SoC_{high}.

At time points close to plug-in and plug-out times, the flexibility decreases due to constraints set by the need for the SoC to have a specific value. Intuitively, the allowable states of the SOC are located inside the area of Figure [11]. If the SoC is outside this range, then the only way for the vehicle to achieve the required SoC at the end of the charge will be to increase the power exchanged with the electricity network beyond the allowed limits P_{max} or P_{min}. This is unacceptable, as compliance with the maximum and minimum power constraints is essential.

t_{L1}, t_{L2}, t_{H1} and t_{H2} are estimated by the equations (3.27)-(3.30), [39] [40] .

$$t_{L_1}(i) = t_0(i) + \frac{SoC_{min}(i) - SoC_0(i)}{P_{min}(i)} \tag{3.27}$$

$$t_{H_1}(i) = t_0(i) + \frac{SoC_{max}(i) - SoC_0(i)}{P_{max}(i)} \tag{3.28}$$

$$t_{L_2}(i) = t_f(i) + \frac{SoC_{target}(i) - SoC_{min}(i)}{P_{min}(i)} \tag{3.29}$$

$$t_{H_2}(i) = t_f(i) + \frac{SoC_{target}(i) - SoC_{max}(i)}{P_{max}(i)} \tag{3.30}$$

The dynamic upper and lower bounds SoC_{high} and SoC_{low} of the ith PEV are estimated at time t as:

$$SoC_{high}(i,t) = \begin{cases} SoC_{max}(i), & t_{H_1}(i) \le t \le t_{H_2}(i) \\ SoC_{max}(i) - P_{max}(t - t_{H_2}(i)), & t_{H_2}(i) \le t \le t_f(i) \\ SoC_0(i) + P_{max}(t - t_0(i)), & t_0(i) \le t \le t_{H_1}(i) \end{cases} \tag{3.31}$$

$$SoC_{low}(i,t) = \begin{cases} SoC_{min}(i), & t_{L_1}(i) \le t \le t_{L_2}(i) \\ SoC_{min}(i) + P_{max}(t - t_{L_2}(i)), & t_{L_2}(i) \le t \le t_f(i) \\ SoC_0(i) - P_{max}(t - t_0(i)), & t_0(i) \le t \le t_{L_1}(i) \end{cases} \tag{3.32}$$

The nature of the aggregator is dual because it works simultaneously both as a load and as a battery. SoC changes constantly due to both the charging and discharging of PEV batteries and the continuous connection or disconnection of EVs. The change in SoC due to the first reason can be optimally controlled in order to

optimize the SoC trajectory for the whole cluster of PEVs and also to provide services to the MG. This part of the controllable SoC is responsible for the battery equivalent role of the aggregator.

The time-dependent technical boundaries of the aggregate equivalent battery (denoted with subscript: PB) are determined using the equations (3.33)-(3.39).

$$P_{PB,max}(t) = \sum_i P_{max}(i,t) \tag{3.33}$$

$$P_{PB,min}(t) = \sum_i P_{min}(i,t) \tag{3.34}$$

$$SoC_{PB,max}(t) = \sum_i \big(SoC_{high}(i,t) - SoC_{diff}(t)\big) \tag{3.35}$$

$$SoC_{PB,min}(t) = \sum_i \big(SoC_{low}(i,t) - SoC_{diff}(t)\big) \tag{3.36}$$

$$SoC_{PB,0}(t) = \sum_{\substack{\forall \text{ ith EV} \\ \text{plugged at t}}} SoC_0(i) \tag{3.37}$$

$$SoC_{PB,target}(t) = \sum_{\substack{\forall \text{ ith EV} \\ \text{unplugged at t}}} SoC_{target}(i) \tag{3.38}$$

On the other hand, the second reason introduces an unpredictable element to SoC changes. This is because when an EV connects, the aggregator gains a certain amount of initial SoC, and when a PEV disconnects, the Aggregator loses a proportion of the SoC that corresponds to the targeted SoC of the departing EV. This part of the uncontrollable SoC is responsible for the behavior of the aggregator as a load. It is denoted by $\mathrm{SoC_{diff}}$ and contains the energy needs of the aggregator.

$$SoC_{diff}(t) = \sum_{T_0:\Delta t:t} \big(SoC_{PB,0}(t) - SoC_{PB,target}(t)\big) \tag{3.39}$$

By denoting as $\mathrm{P_{opt}(t)}$ the optimal active power exchange between the aggregated equivalent battery and the electricity grid and by adopting generator convention, the resulting SoC (measured in kWatts) is calculated at each interval as:

$$SoC_{PB}(t+\Delta t) = \begin{cases} SoC_{PB}(t) - P_{opt}(t)\cdot\eta_{ch}\cdot\Delta t, & P_{opt}(t) < 0 \\ SoC_{PB}(t) - \dfrac{P_{opt}(t)}{\eta_{disch}}\cdot\Delta t, & P_{opt}(t) \geq 0 \end{cases} \tag{3.40}$$

4 Optimal Operation Scheduling of Microgrid

In this work, particle swarm optimization (PSO) has been used in order to optimally schedule the operation of the examined system. PSO is one of the most highly efficient heuristic methods and its implementation is remarkably simple. PSO has proved very robust and efficient for application to complex optimization problems as it does not depend on the selected initial point and leads to a global optimum with a high rate of success. It is difficult to find the global optimum for large-dimension optimization problems and formulate extremely complex objective functions using classical methods. In the examined problem, the building thermal model's differential equations and PEVs aggregated model should be solved within the optimization procedure, making its implementation difficult if classical optimization techniques are applied. However, using PSO algorithm, this problem is overcome since the objective function can be arbitrarily complex and of any form. It can also be easily adjusted in case that new components need to be included.

At this stage, the MGs operate islanded (autonomously) from the peer-to-peer electricity market. Particle Swarm Optimization (PSO) is applied at the MG scale to facilitate the optimization process. Each MG tries to achieve an optimal overall electrical power demand for HVAC systems, strategically rescheduling non-critical electrical loads within the houses and coordinating the charging of hosted PEVs while also optimizing the power exchange between the MG and the main electrical grid. The objective at this stage is to minimize the total daily energy demand and the associated cost of the MG.

It is crucial to comprehend that each MG functions as an independent entity. The optimization objective, which encompasses all the parameters for optimization, is addressed separately by the energy management system (EMS) of each individual MG. In this thesis, optimization within a specific MG is executed through hierarchical control. However, when considering multiple MGs, the EMS of each MG operates autonomously in a decentralized manner. This approach is logical because, within the framework of market liberalization, distinct MGs may come under the jurisdiction of different companies, each with its unique objectives.

The structure of each particle of the swarm, with its different parts comprising the respective decision variables associated with the optimization of the aforementioned MG subsystems are given in Figure (12).

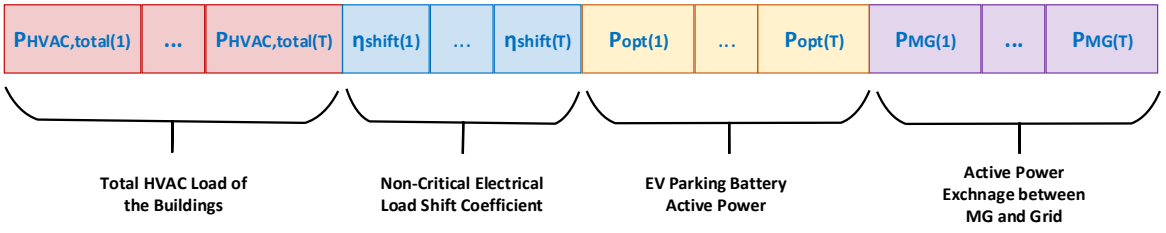

Figure 12: PSO Particle Structure used for Operation Scheduling of MG

The augmented cost function used by the PSO including the applied constraints, are given in (4.1). In this stage of optimization, the algorithm aims to minimize the total operational cost of the microgrid while satisfying all of the associated technical and operation constraints integrated in term (Penalty) of the objective function (4.2)-(4.12).

$$TC_{MG} = \min_{\substack{\mathrm{P_{opt}},\mathrm{P_{MG}},\\ \mathrm{P_{HVAC}},\eta_{\mathrm{shift}}}} \left\{ \left(\sum_{t} P_{MG}(t) \cdot EP(t) \right) \cdot \Delta t \right\} \tag{4.1}$$

s.t.

• Power Balance Constraint(4.2)

$$\sum_{b\in\mathcal{B}}\left(P_{HVAC,total,b}(t)+P_{el,b}(t)\right)=P_{MG}(t)+P_{opt}(t)+P_{PV}(t)+P_{WT}(t) \tag{4.2}$$

• Building Thermal Load Constraints (4.3) - (4.7)

$$T_{min,z}\leq T_{in,z}(t)\leq T_{max,z},\quad \forall z\in b \tag{4.3}$$

$$P_{HVAC,total,min,b}\leq P_{HVAC,total,b}(t)\leq P_{HVAC,total,max,b},\quad \forall b\in\mathcal{B} \tag{4.4}$$

$$P_{HVAC,z}=\frac{Q_{HVAC,z}}{COP},\quad P_{HVAC,total,b}=\frac{Q_{HVAC,total,b}}{COP} \tag{4.5}$$

Smart power dispatch technique is developed for the optimal dispatch of the electric power consumed by building thermal loads to its thermal zones. As a result, the required computation time is kept very low, since the total required electric power of the building is optimized and then dispatched to the thermal zones. The electric power that is required to be provided to each thermal zone, $P_{HVAC,z}$ is a function of the total power that is required by the building, its thermal zone volume, and its estimated internal temperature together with its upper and lower limits.

The thermal model dispatch is implemented as formulated in (4.6)-(4.7).

$$P_{HVAC,z}(t)=\frac{FL_z(t)\cdot V_z}{\sum_z\left\{FL_z(t)\cdot V_z\right\}}\cdot P_{HVAC,total,b}(t) \tag{4.6}$$

with:

$$FL_z(t)=\frac{T_{in,z}(t)-T_{min,z}}{T_{max,z}(t)-T_{min,z}} \tag{4.7}$$

• Building Electrical Load Constraints (4.8)-(4.9)

$$\eta_{shift,min}\leq\eta_{shift}(t)\leq\eta_{shift,max} \tag{4.8}$$

$$\sum_{t=T_{shift,0}}^{T_{shift,f}}P_{non_{cr}}(t)\cdot\Delta t=\sum_{t=T_{shift,0}}^{T_{shift,f}}P^{*}_{non_{cr}}(t)\cdot\Delta t \tag{4.9}$$

• Dynamic Equivalent Battery Constraints (4.10)-(4.12)

$$SoC_{PB}(T_0)=SoC_{PB}(T_f) \tag{4.10}$$

$$SoC_{PB,min}(t)\leq SoC_{PB}(t)\leq SoC_{PB,max}(t),\quad \forall t\in[T_0\ T_f] \tag{4.11}$$

$$P_{PB,min}(t) \leq P_{opt}(t) \leq P_{PB,max}(t), \quad \forall t \in [T_0 \; T_f] \tag{4.12}$$

5 Participation Framework of Microgrid in Peer to Peer Energy Market

5.1 Overview and Key Concepts

The MG engages in the Peer-to-Peer Electricity Market to optimize its profit potential. Due to its unique ability to act as a prosumer (both a producer and a consumer simultaneously), the MG assumes a dual role. The engagement within the P2P market not only aids the MG in reducing energy expenses but also provides stability and resilience to both the other MGs and the main Grid.

At this stage, the MG has optimized its Operation Scheduling for the next 24-hour period (at Section [4]). However, the strategy used for Optimal Operation Scheduling of the MG is interconnected with the strategy used for participation in the P2P energy market. Flowchart [13] provides a concise overview of the subsequent simple yet effective method. Its purpose is to demonstrate the overarching perspective and facilitate the separation of the two coupled strategies. Following the flowchart, the method is further elaborated.

Figure 13: Framework for Decoupling the Coupled Strategies

This Method of MG participation in the market unfolds in a sequence of well-defined steps. Initially, the maximum and minimum power deviations from the established optimal operational point of the MG are calculated, considering the specific time interval that the market's participation will take place. Concurrently, the associated cost increase is evaluated at both of these deviation points. These derived deviation points, accompanied by their respective costs, are used to formulate a comprehensive cost function curve for the MG. This curve cost function captures the relationship between power deviations and the corresponding cost variations, thereby offering a holistic representation of the MG's cost dynamics. Therefore, the cost function curve is established, coupled with the operational boundaries of the MG. This composite information is then forwarded to the MG's market participation agent. Armed with this knowledge, the agent is well-equipped to engage in market negotiations, leverage the cost curve to make informed decisions and optimize MG's position within the market landscape. As the market negotiation concludes, if the MG has secured a profitable deal, the resulting new optimal set point, which originated from the deal, is communicated back to the MG. With this new set point, the MG embarks on a renewed round of Operation Scheduling for the forthcoming 24-hour span. This iterative cycle ensures that the MG consistently adapts its operations based on market dynamics, pursuing optimal outcomes, and effectively aligning its actions with both its financial objectives and operational efficiency. The interplay between the EMS Strategy and the P2P Market Approach, illustrating their dynamic relationship graphically, is depicted in Figure [14].

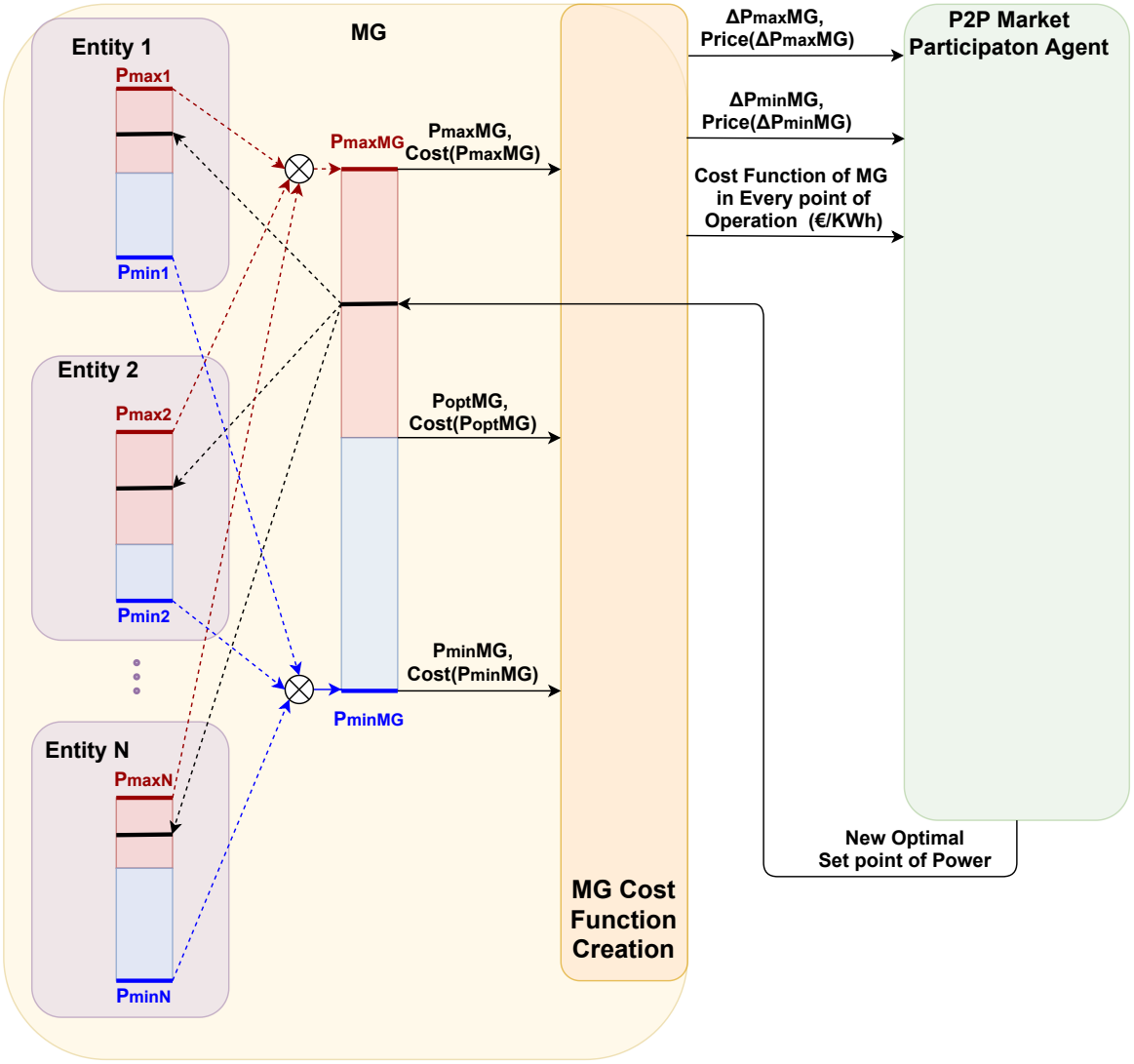

Figure 14: Interplay: EMS Strategy & P2P Market Approach

5.2 Discovering Maximum and Minimum Deviation Points in MG

In the course of the above method, it is essential to consider specific challenges that arise. In establishing the maximum and minimum deviation points that satisfy MG's technical constraints, a structured approach is followed. The maximum and minimum deviations from the optimal point are expressed as percentages, presented in descending order for the maximum deviation search and ascending order for the minimum deviation search. The design characteristics, including the maximum percentage deviation ($P_{perc,max}$), minimum percentage deviation ($P_{perc,min}$), and the step size ($Step_{perc}$), can vary based on the complexity and flexibility of the MG entity. For instance, in the case of MG buildings, which exhibit lower flexibility, the maximum and minimum percentage deviations are comparatively smaller in absolute values than those associated with aggregators. This distinction is illustrated in Figure [23] presented in the case study.

Then the optimal point for the first interval that the bargain will take place increases (decreases) by the percentage, and the optimal operation scheduling is executed for the next 24-hour span. With the additional constraint, that the values of power for the first time interval of the bargaining will remain fixed and equal to the amount that is indicated by the increased (decreased) percentage. If technical constraints are met, the maximum (minimum) deviation point is confirmed; otherwise, the process iterates, progressively reducing (increasing) the deviation percentage. In cases where constraints aren't met after all iterations, MG's participation in the market is prohibited due to physical limitations (non-participation occurs because of zero $P_{max}(P_{min})$). Nonetheless, implementing PSO possibly multiple times for the objective:(4.1) introduces computational challenges. To mitigate the issues stemming from a serial search, a variable-step search function is introduced—a variant of binary search but adapted, as depicted in the Flowchart[15]. It is important to note that the variable step search function is the same for maximum and minimum percentages, with the only difference being that depending on the search for maximum or minimum point of deviation, the percentages must be given in the format shown in Figure[23].

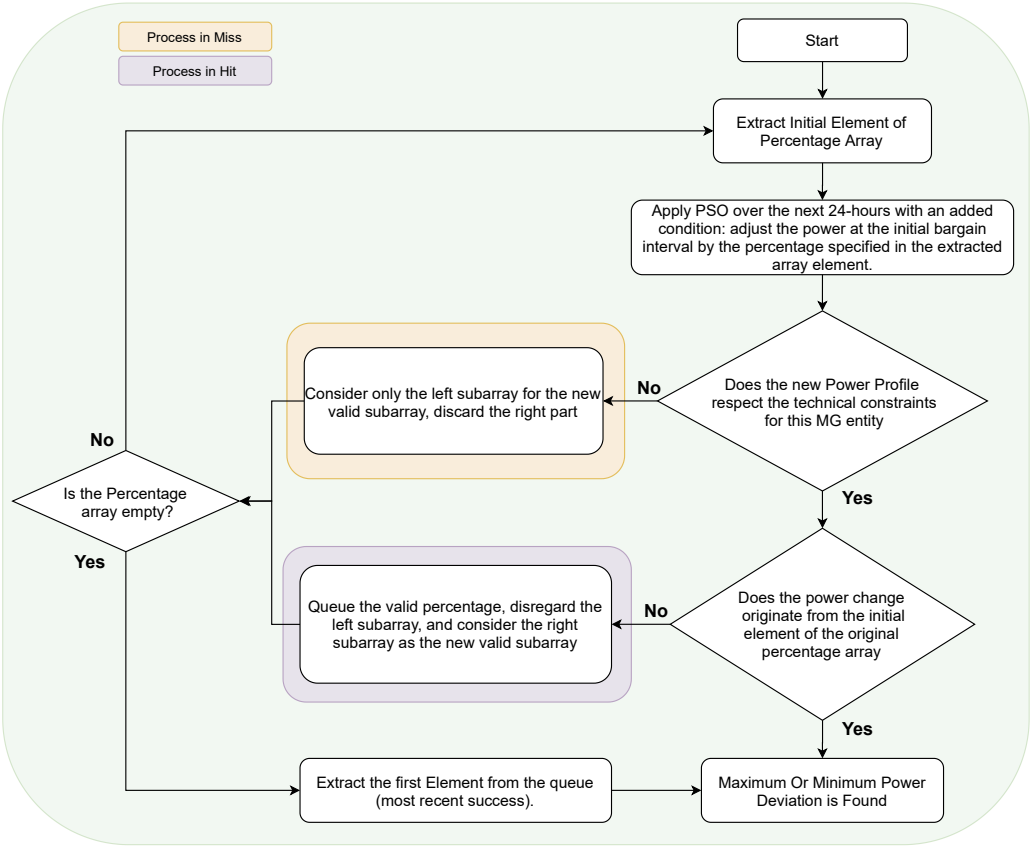

Figure 15: Flowchart of Variable step Search for maximum-minimum deviation

In order for the MG to identify the highest and lowest deviations from optimal operation during its current participation interval in the peer-to-peer market, it leverages the active involvement of distributed residential houses and the PEV-Aggregator. These entities, possessing varying degrees of flexibility in power consumption and energy storage. Regarding the residential houses utilized in this thesis, as will be elaborated further upon the case study, it is important to recognize that due to confined storage capacity within each thermal zone—driven by its compact design—the system's available degrees of freedom are notably restricted, representing an inherent constraint. Consequently, the potential for flexible adjustment in the power consumption profile is considerably limited

To address this issue and introduce greater flexibility to the MG derived from the collective contribution of the individual houses, we implement a temperature adjustment of one degree. This adjustment relates to the upper and lower temperature bounds, involving a modification of the current range to a new range that is expanded by one degree Celsius. These adjusted bounds are exclusively applicable when the MG engages in the participation for regulation (ancillary)services or takes part in peer-to-peer (P2P) market activities.

This arbitrary assumption is grounded in the logical perspective that an increase in the MG's profitability justifies a minor level of occupant dissatisfaction. This trade-off is deemed acceptable since any inconvenience experienced by occupants can be compensated through the gains achieved by the MG. However, it is crucial that any discomfort remains within a minor threshold, which is why the relaxation of temperature bounds is limited to a single Celsius degree, as illustrated in Table [2] in the case study. Consequently, as the technical limitations are relaxed, each individual house can exhibit more significant deviations from the optimal setpoints. This, in turn, results in an augmented power capacity that the MG can harness to participate in the P2P market with larger power quantities and consequently, greater gains.

On the contrary, the virtual equivalent battery stands as an entity with significant flexibility in altering power consumption. Additionally, the constraints in place do not originate from occupants' preferences, but rather from technical limitations that, if breached, would result in damage to the individual EVs. Given this context, the initial constraints cannot be relaxed.

5.3 Formulation of Comprehensive Cost Function of MG

Currently, we have successfully identified both the maximum and minimum deviation points, along with calculating the associated operational costs for these operational states. It is important to note that greater operational costs are anticipated at the deviation points due to their deviation from the original optimal point. The term "cost" pertains to covering MG's energy requirements for the entire 24-hour duration. There is a need to formulate a comprehensive cost function for MG, for every point in power between [P_{min}, P_{max}]. This involves the implementation of a best-fitting strategy and approximating the cost function using a polynomial function. So far the notion of "Cost" specifically refers to daily expenditures. To convert this into €/kWh units, the following equations come into play:

$$Cost_{seller} = \frac{\Delta_{cost}}{|\Delta P| \cdot \Delta t} + EP_{sell} \tag{5.1}$$

$$Cost_{buyer} = \frac{\Delta_{cost}}{|\Delta P| \cdot \Delta t} + EP_{buy} \tag{5.2}$$

It's important to note that the Grid sells power to MGs at different prices than it buys. MGs will sell power back to the grid at a lower price compared to their buying rate. This market design serves to encourage the adoption of clean energy and motivate MGs to employ energy management techniques. The goal is to offset the surplus power that can be sold back to the grid. Consequently, this strategy promotes the utilization of clean energy and facilitates peer-to-peer trading among participants.

It is necessary to reflect the Buyer's Cost function across the x-axis at x = EP_{buy}. The Buyer's objective is to buy power at the lowest possible price, with the intention of reserving it for consumption rather than purchasing

it from the grid during later periods. The mirroring action symbolizes that, for the Buyer to operate at a point deviating from the optimum, the price at which power is bought must decrease. This adjustment allows the Buyer to consider operating at a suboptimal point by accepting a lower price for the purchased power. The process described above can be visually comprehended through the aid of a diagram, which presents the sequence in a more illustrative manner: Figure [16].

One crucial aspect of formulating the cost function is worth highlighting: the recognition that within a MG, deviations from the optimal point of operation lead to an expected increase in associated costs. As a result, buyers strive to secure power at more economical prices, while sellers aim to vend power at higher rates. When the minimum electricity price allowed by the market operator surpasses the buyer's cost, this point of operation establishes the new minimum allowable deviation point (P_{min}) for the MG. Beyond this point, the MG operates at a loss instead of a profit, since the MG operator lacks the ability to demand a price sufficient to cover their cost beyond that specific operational point. Similarly, in the context of the seller role, if the maximum electricity price permitted by the market operator is lower than the cost at a specific operational point, this specific point becomes the new maximum allowable deviation point (P_{max}). Operating the MG beyond this threshold results in a financial loss, as the operator cannot request a price adequate to offset their cost beyond that specific operational point.

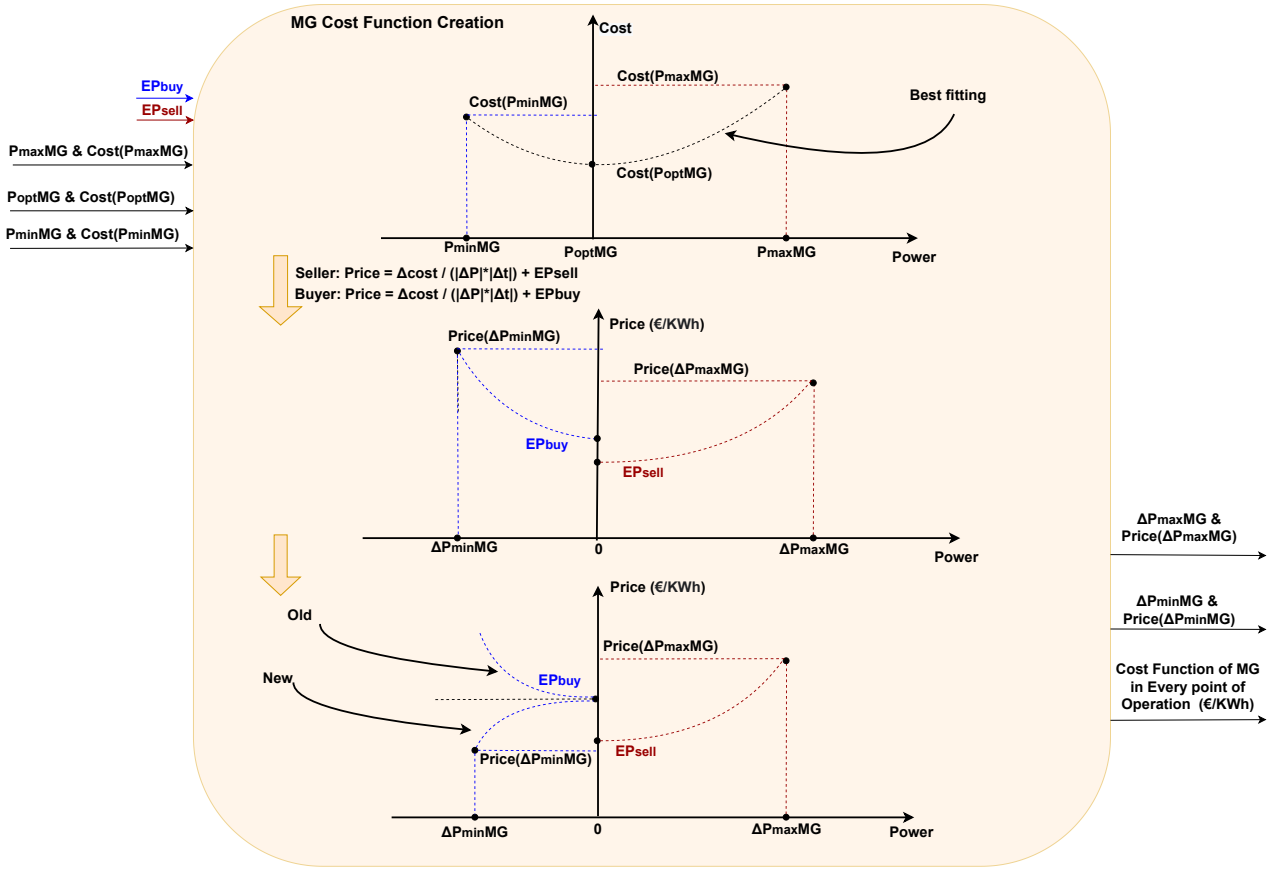

Figure 16: MG Comprehensive Cost Function Creation

Every participant in the electricity market operates with individual rationality, engaging in transactions with competitors solely when it leads to financial benefit. Figure [17] illustrates MG's cost function alongside its maximum and minimum power capacity. The shaded area defines the region within which MG can secure gains and achieve convergence. This convergence will occur if an opponent expresses a desire for MG to operate at

any point within this region.

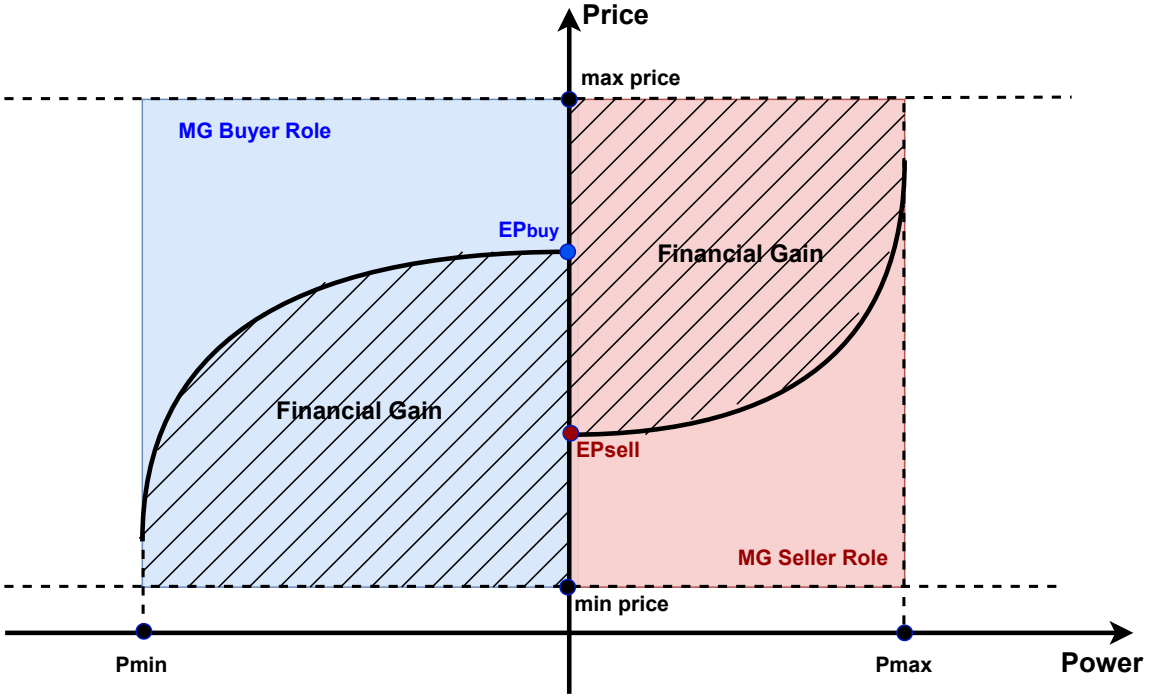

Figure 17: Cost Function of MG

5.4 Peer-to-Peer Market Participation Agent of MG

In the P2P framework, the MG receives offers from its opponents and evaluates each one individually. The producer role engages in negotiation with its rival's consumer role, and the consumer role bargains with its rival's producer role.

The MG aims to maximize its profit, and by adopting generator convention, the objective for profit maximization is formulated in equations (5.3) - (5.5) for the producer role and in equations (5.6) - (5.8) for the consumer role.

$$\text{SellOffer}(P_{(i,t)}, \lambda_{(i,t)}) = \max_{P_{(i,t)}, \lambda_{(i,t)}} \left\{ P_{(i,t)} \cdot \left(\lambda_{(i,t)} - \lambda_{\text{cost}(P_{(i,t)})} \right) \right\} \tag{5.3}$$

s.t.

$$0 \leq P_{(i,t)} \leq P_{max(i,t)} \tag{5.4}$$

$$\lambda_{\text{cost}(P_{(i,t)})} \leq \lambda_{(i,t)} \leq \overline{\lambda}_{(i,t)} \tag{5.5}$$

$$\text{BuyOffer}(P_{(i,t)}, \lambda_{(i,t)}) = \min_{P_{(i,t)}, \lambda_{(i,t)}} \left\{ P_{(i,t)} \cdot \left(\lambda_{(i,t)} - \lambda_{\text{cost}(P_{(i,t)})} \right) \right\} \tag{5.6}$$

s.t.

$$P_{min(i,t)} \leq P_{(i,t)} \leq 0 \tag{5.7}$$

$$\underline{\lambda}_{(i,t)} \leq \lambda_{(i,t)} \leq \lambda_{\text{cost}(P_{(i,t)})} \tag{5.8}$$

At the beginning of the negotiation for a specific time-instant$_\text{t}$, each MG$_\text{i}$ solves an optimization problem formulated in (5.3) - (5.5) for the producer role and (5.6) - (5.8) for the consumer role. The initial power limits

(P_{min}, P_{max}) originate from the maximum and minimum power that the MG can deviate from the optimal point of the current time interval: subsection [5.2]. This optimal point, originated from the optimal operation scheduling of the preceding time instance as discussed in section [4]. The cost of MG for each feasible operational point $\lambda_{cost(P_{(i,t)})}$ has been ascertained, as detailed in subsection [5.3]. The market operator establishes the initial price bounds ($\underline{\lambda}_{(i,t)}$, $\overline{\lambda}_{(i,t)}$).

Each MG operates within a non-cooperative framework. Thus, the primary goal is to strike a beneficial agreement. This approach stems from a logical premise: within a competitive arena, the pursuit of maximum profit can sometimes lead to risky negotiations. In this pursuit, there is a chance that a rival strikes a deal with another entity, leaving the MG with no profit at all. As a result, the market's "invisible hand" comes into play, aligning the transaction price with the genuine needs of both producers and consumers. Consequently, MG's strategy is to accept the first offer that guarantees a profit. After the deal has closed between the two MGs, in the second stage, they will try to optimize their combined position. To summarize, each MG follows a risk-averse strategy. It should be emphasized that the assumption is made that each individual MG is sincere in its intentions and, although operating in a competitive context, does not seek to manipulate its opponent (Truthful Bidding).

In this second stage, the price will remain fixed where the MGs converged in the first stage. This is due to the fact that it is a competitive variable; the producer wants to increase it while the consumer wants to decrease it, and thus any attempt by the MG to alter it will result in conflict. The MG engages in an optimization process, keeping the electricity price constant while varying the offered power. Its objective is to maximize its profit using equations (5.3) - (5.5) if it's the seller or (5.6) - (5.8) if it's the buyer, with the only difference now being that the price is fixed and equal to the agreed upon value. If the MG can optimize its position by deviating from the agreed-upon quantity of exchanged power, a counteroffer is extended to the adversary from the new optimal power point of the MG. The acceptance criterion of its rival is a potential increase in profit; if unmet, the counteroffer is rejected. Ultimately, during the first rejection of the offer, the clarity of the negotiation relies on the most recently accepted offer, if available; otherwise, the bargaining continues.

As the algorithm progresses, a potential convergence point begins to emerge. Over successive iterations, the participants initiate from a standpoint where each aims for maximum financial gain, and then progressively make concessions until an agreement is reached. In a subsequent phase, as a design mechanism with perfect information, the convergence point can be verified by evaluating whether it falls within the Nash equilibrium region between the producer and the consumer involved in the transaction. This will serve as an additional measure to validate the algorithm's accuracy (considered for future work).

Within the assessment of the rival's offer, the player engages in a process termed "benefit relaxation". Should the player's maximum absolute power surpass the opposing bid, a reduction strategy is employed. This strategic reduction seeks to align both parties on a power balance, an essential precondition for a successful deal. The same strategic approach is applied when there's a difference in price with the opponent. By making a small compromise in price, the player takes steps closer to reaching equilibrium.

To gain a comprehensive understanding of the agents' interactions during their involvement in the non-cooperative game, an interactive flowchart [18] is presented, depicting the interaction between an MG assuming a seller role and another MG taking on a buyer role. Upon initialization and after both parties have identified their optimal bids, one of them will randomly initiate the process by offering the startup (first bid) price and power. From that point onward, the sequence is iterated until a deal reached between the two competitors, or until a predetermined number of iterations (which is a design consideration) is achieved.

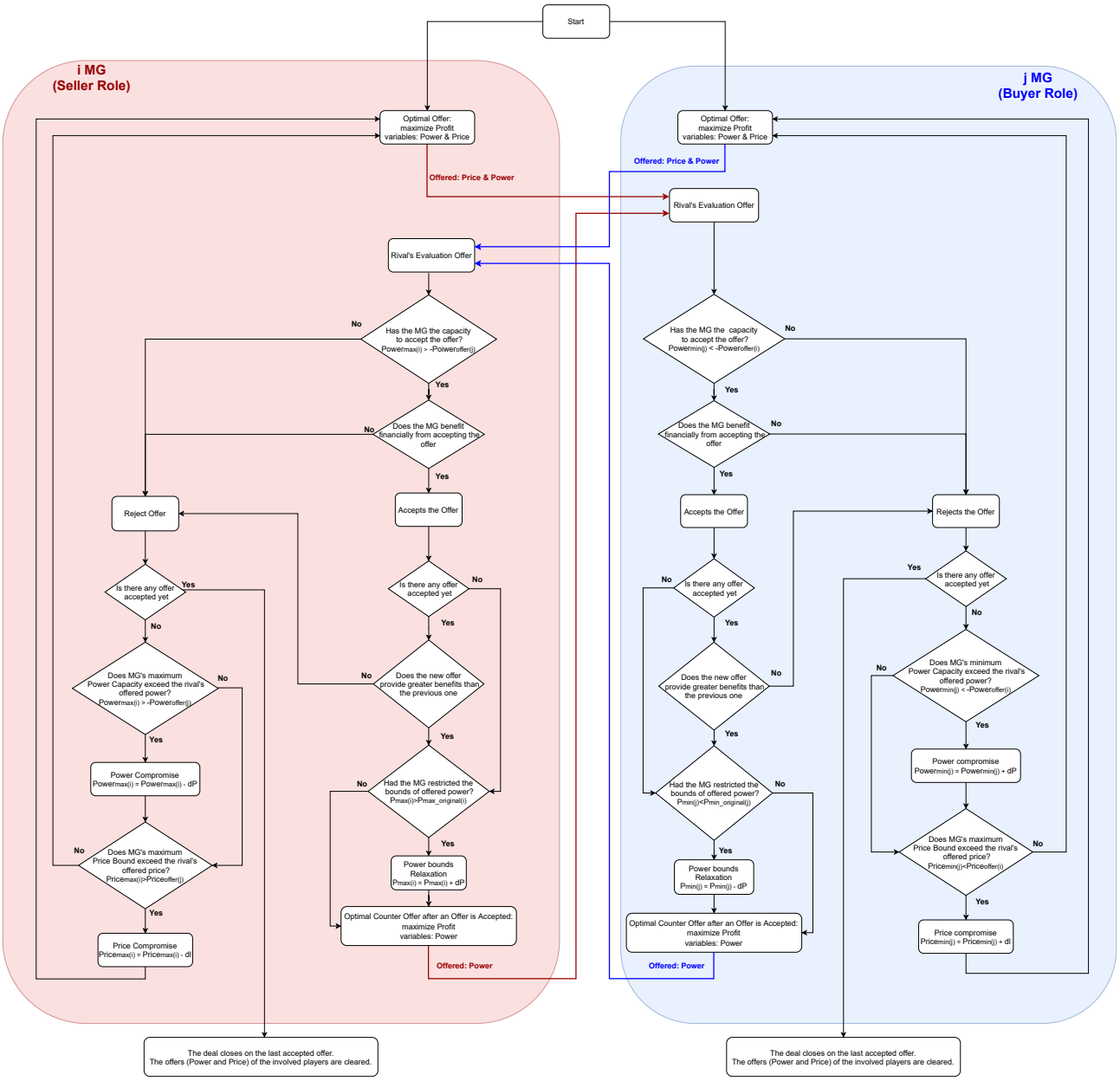

Figure 18: P2P Participation FrameWork

5.5 Aftermath of Deal in P2P Market

At this stage, a mutually advantageous agreement has been reached between the two MGs, leading to the establishment of a new operational point – a new setpoint for each MG. This information is communicated back to the Energy Management Systems (EMS) of each individual MG, as depicted in Figure [14].

Subsequent to this, any surplus or deficit power is distributed among the entities within the MG, including the virtual skyscrapers (clusters of residential buildings that share an identical geometry, as will be showcased in the case study), and the aggregator. This distribution is done in proportion to their respective offered maximum deviation points (if the concluded deal results in the MG having a deficit due to selling power, following the generator convention) or minimum deviation points (if the concluded deal leads to the MG having a surplus due to purchasing power, following the generator convention). With the power values for the current time interval fixed for all "balancing entities," as dictated by the bidding obligation of the MG, a new optimal operational schedule is formulated for the upcoming 24 hours.

It's important to highlight that within the aggregator, the optimization process closely mirrors that of the initial scheduling. However, an additional constraint becomes relevant. This constraint is formulated to uphold power consumption at a steady level during the obligation time period, which coincides with the peer-to-peer market activity. This level is established based on the original value and is modified through incremental or decremental adjustments proportional to the power equivalent received by the aggregator from the distribution of "Balancing Needs" across all entities. This adjustment factor takes into consideration whether the MG acted as a seller or a buyer.

Conversely, in the Virtual Skyscrapers, alongside this additional constraint, which mirrors that of the aggregator, an additional consideration comes into play. This stems from the relaxation of temperature boundaries, allowing each virtual skyscraper to provide a more effective and wider range of deviation from the optimal point of operation. The algorithm is now tasked with effectively managing indoor temperatures, encompassing a broader spectrum of temperature limits compared to the initially ideal settings. With the negotiation phase concluded, it becomes imperative for the algorithm to harmonize the newly relaxed temperature constraints with the original ones. This alignment of different temperature bounds is achieved gradually. At the outset of the 24-hour period of peer-to-peer market participation, the temperature boundaries are set to the relaxed values, as temperatures might be in close proximity to them and could potentially violate original limits. Over time, within a brief timeframe, temperatures should progressively decrease to reach the optimal allowable limits. To meet these criteria, the temperature boundaries are initialized based on regulatory limits and are incrementally adjusted towards the ideal values before the relaxation takes place. To ensure a seamless transition, it was determined that this reduction in limits would follow a linear pattern. This transition process is designed to be completed within a span of three hours, specifically three hours after the MG's commencement of participation in the market.

6 Case Study – Optimal Operation of Interconnected MGs

The models and algorithms created in this study have been tested using simulations replicating realistic scenarios of clusters of MGs operation. An important aspect of this thesis is that the methods developed are fully parametric and easily adjustable, allowing them to be used for energy systems of different sizes and complexities. The suggested energy system can include various types and sizes of residential buildings that are found in each individual microgrid. This flexibility is achieved by appropriately adjusting various parameters of the models, such as the dimensions, and construction details. Similarly, the profiles of thermal and electrical loads for each thermal zone within a building can be customized.

In this study, we have opted to analyze spatially distributed simple residential buildings across each MG, a choice that poses challenges due to the increasing complexity as the number of houses rises. We have selected three types of residential house geometries within the current thesis, chosen to showcase and compare the thermal behaviors of houses with distinct characteristics and complexities Figure[19].

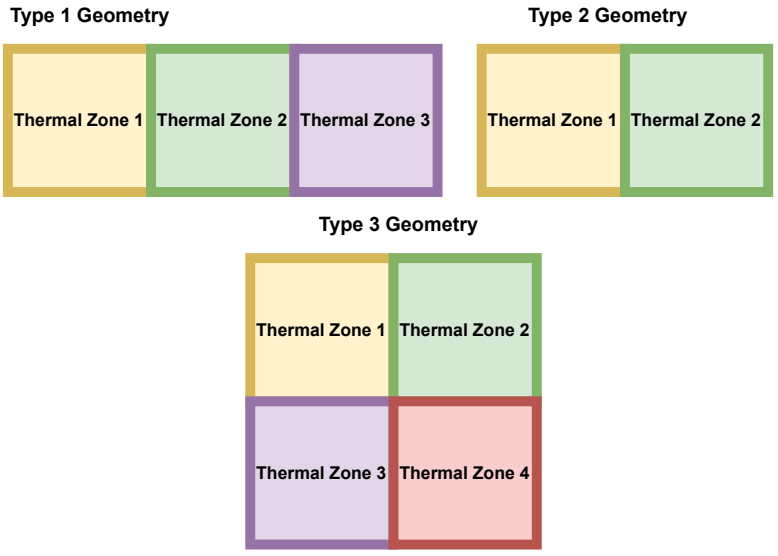

Figure 19: Houses of MGs

Given the substantial quantity of houses involved, the computational challenges escalate swiftly for cities or even small villages. To overcome this, we propose aggregating multiple buildings into a virtual skyscraper model, where each floor of the skyscraper corresponds to an individual building (with consideration of thermal insulation between each floor). This approach is particularly applicable as each house in this study, consists of just one floor. By implementing this strategy, we can efficiently aggregate the total electrical and thermal power requirements of each building into the virtual skyscraper. Following this, with the aid of PSO, we can allocate the overall required thermal power for covering the virtual skyscraper's collective needs and then distribute the thermal power fairly to each individual real building. This approach significantly reduces computational time. It's important to note that for buildings to be aggregated into a virtual skyscraper, they must share identical geometries. Figure [20] illustrates the aggregation of real buildings into virtual skyscrapers.

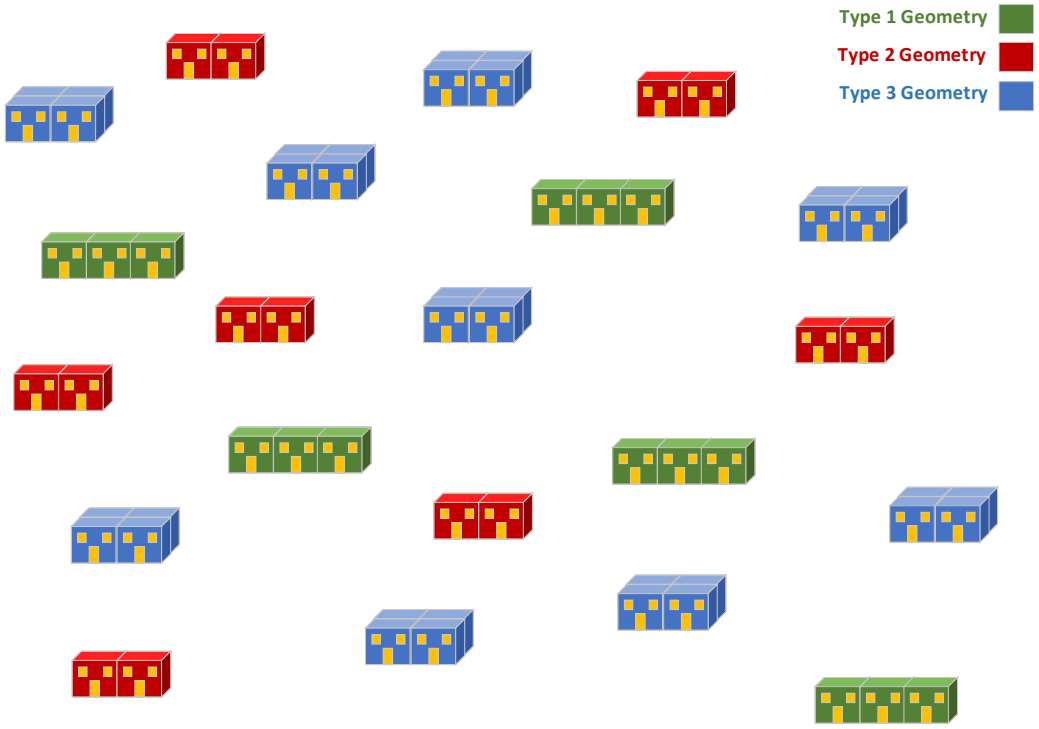

(a) Real Residential Buildings

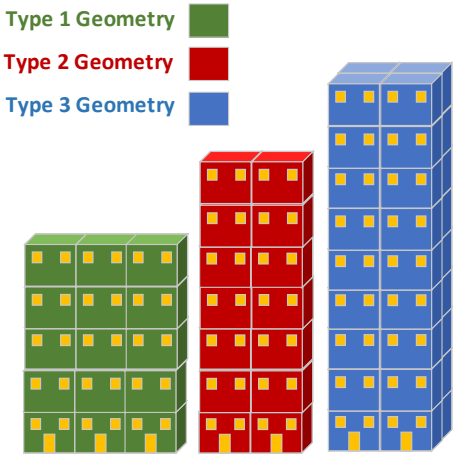

(b) Virtual Skyscrapers

Figure 20: Proposed Aggregation Framework of Residential Buildings

Each MG under examination consists of residential houses, an EV Parking-Lot, a PV Park, and a WT Park. Comprehensive details pertaining to the model parameters of the MG's residential buildings are delineated in Tables (2) - (5) . The forecasted count of connected EVs is presented in Table [6], setting the stage for the subsequent analysis. The thesis further delves into an examination of four distinct types of PEV batteries, each defined by its technical specifications. These specifications are detailed in Table [7], contributing to a comprehensive understanding of the research landscape.

THERMAL ZONES MODELLING DATA									
	Thermal zones			All thermal zones					
	B1	B2	B3						
Side_1 (m)	[5, 6]	[5, 6]	[5, 6]	$p_z(kg/m^3)$	1.2	$\tau_{win,z}$	$1.1 \cdot 10^{-3}$	$\beta_z(°)$	90
Side_2 (m)	[4, 5]	[4, 5]	[4, 5]	$C_z(kWh/(kg \cdot ℃))$	1/3600	$a_{w,z}$	$18.6 \cdot 10^{-3}$	$\theta(°)$	11.9
Height (m)	[2.5, 3.2]	[2.5, 3.2]	[2.5, 3.2]	$U_{wall,z}(kW/(m^2 \cdot ℃))$	$2.04 \cdot 10^{-3}$	SC_z	0.54	$\theta_z(°)$	39.9
$[T_{min}, T_{max}]_{IDEAL}$ (°C)	[20, 26]	[20, 26]	[20, 26]	$U_{win,z}(kW/(m^2 \cdot ℃))$	$5.6 \cdot 10^{-3}$	p_g	0.2	$R_{se,z}((m^2 \cdot ℃)/kW)$	40
$[T_{min}, T_{max}]_{REG}$ (°C)	[19, 27]	[19, 27]	[19, 27]						

Table 2: Residential Buildings Model Data

MICROGRID 1: BUILDING PARAMETERS			
	B1	B2	B3
Number of Residential Buildings	45	30	60
Total number of thermal zones	135	60	240
MICROGRID 2: BUILDING PARAMETERS			
	B1	B2	B3
Number of Residential Buildings	30	25	10
Total number of thermal zones	90	50	40
MICROGRID 3: BUILDING PARAMETERS			
	B1	B2	B3
Number of Residential Buildings	15	20	25
Total number of thermal zones	45	40	100

Table 3: Count of Residential Buildings per Microgrid

	Building 1	Building 2	Building 3
n_{non_cr}	0.25	0.25	0.25
$n_{shift,min}$	0.70	0.75	0.65
$n_{shift,max}$	1.3	1.25	1.35
$T_{shift,min}$	07:00	07:00	07:00
$T_{shift,max}$	17:00	17:00	17:00

Table 4: Non-Critical Load Parameters

(a) Electrical

	Non-Occupancy Dependent Load (Baseload)
Freezer	100 – 150 (W)
refrigerator	80 – 100 (W)
unknown	1 (W/m^2)
	Occupancy Dependent Load
Occupancy – Area	4 (W/(m^2 $Occupant_{Active}$))
	Light Load
Conversion Efficiency	80% – 100% (Lm/W)

(b) Thermal

	Non-Occupancy Dependent Load
Non – Occupancy – Dependent Appliances – Thermal Conversion Percentage	20% – 30%
	Occupancy Dependent Load
Occupancy – Dependent Appliance – Thermal Conversion Percentage	20% – 30%
Human Body	100 (W/$Occupant_{Indoor}$)
	Light Load
Infared Convertion Percentage	10% – 15%

Table 5: Buildings Load Parameters

MG1: Aggregator (Cluster Of Charging Points)			
Activity Type:	**Home**	**Work**	**Shop-Social**
Number of EVs:	50	150	50
MG2: Aggregator (Cluster Of Charging Points)			
Activity Type:	**Home**	**Work**	**Shop-Social**
Number of EVs:	15	50	35
MG3: Aggregator (Cluster Of Charging Points)			
Activity Type:	**Home**	**Work**	**Shop-Social**
Number of EVs:	10	35	30

Table 6: Forecasting Connected EVs Count to Aggregator Alongside Driver Activity

	PEV type			
	1	**2**	**3**	**4**
Battery Capacity(kWh)	77	45	26.8	66.5
SoC_{max} /SoC_{min} (kWh)	69.3/7.7	40.5/4.5	24.12/2.7	60/6.65
P_{max} /P_{min} (kW)	11/-11	7.2/-7.2	6.6/-6.6	11/-11

Table 7: PEVs Parameters

The probability shape employed to determine the count of permanent occupants for each type of house geometry is outlined in Figure [21] for illustration purposes. In the context of various houses, the functions of individual rooms exhibit diversity, influenced by factors like the house's specific geometry type (number of rooms) and the count of permanent residents. This variability is reflected in Figure [22], which elucidates the potential roles attributed to rooms within a household. These roles are contingent upon the household's unique characteristics and the count of permanent residents it accommodates. As the functions of rooms differ, so do their lighting requirements. This diversity arises from the various activities conducted within these spaces, each aligned with its designated role. Table [8] provides an overview of the lux requirements for each available room type, capturing the distinct lighting needs associated with various activities conducted within them.

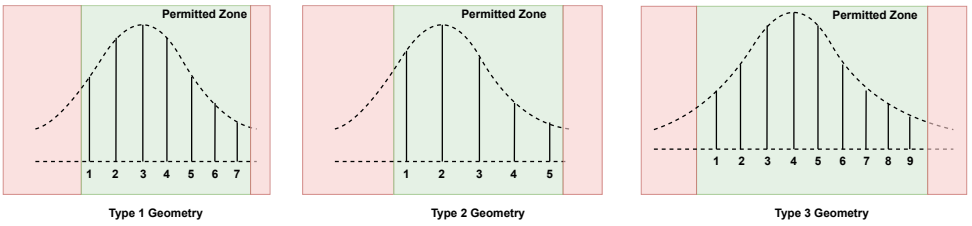

Figure 21: Count of Permanent Occupants for each Type of House

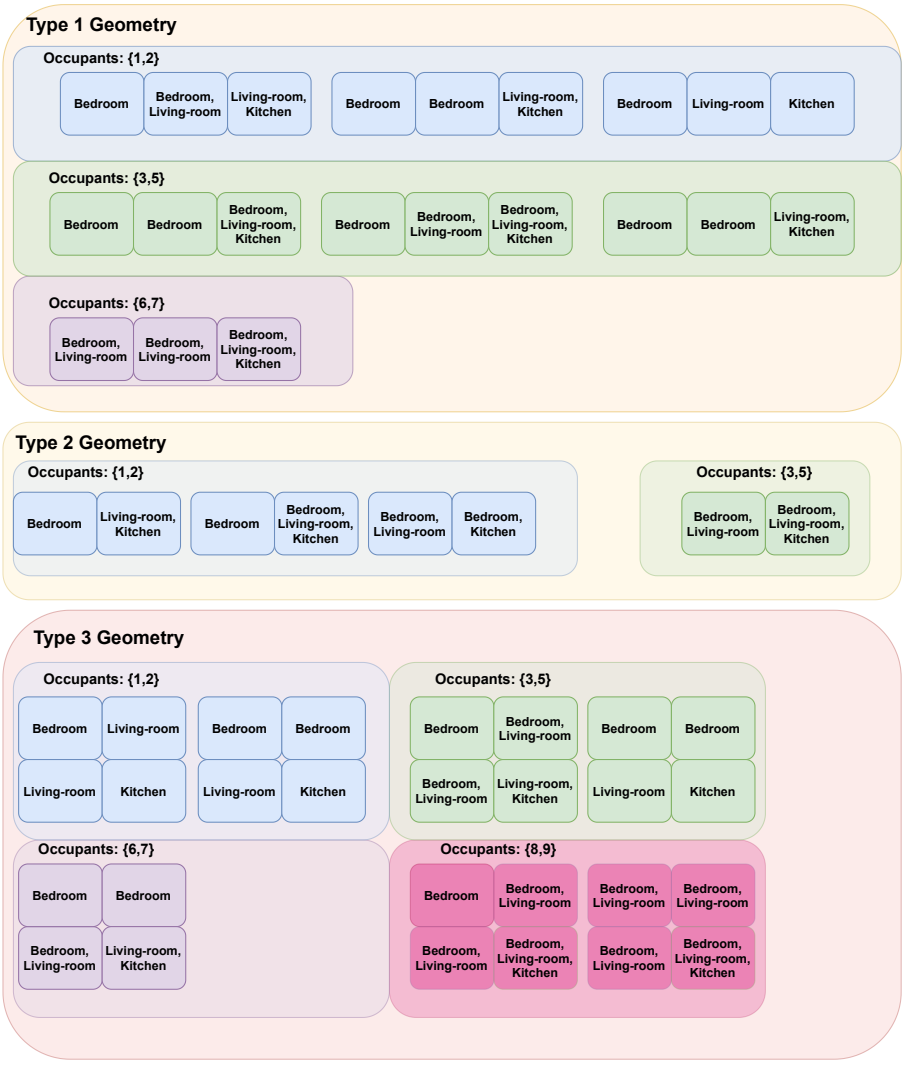

Figure 22: Room Assignments Based on Occupant Count and House type Geometry

Room: Lux Requirements			
	Kitchen	**Livingroom**	**bedroom**
Maximum (lux)	400	100	100
Minimum (lux)	150	150	60

Table 8: Lighting Lux Requirements Based on Room Function [41]

Virtual Skyscraper: Percentage Array for Pmax

20%	17.5%	15%	12.5%	10%	7.5%	5%	2.5%	0%

Virtual Skyscraper: Percentage Array for Pmin

-20%	-17.5%	-15%	-12.5%	-10%	-7.5%	-5%	-2.5%	0%

Virtual Equivalent Battery: Percentage Array for Pmax

30%	27.5%	25%	22.5%	20%	17.5%	15%	12.5%	10%	7.5%	5%	2.5%	0%

Virtual Equivalent Battery: Percentage Array for Pmin

-30%	-27.5%	-25%	-22.5%	-20%	-17.5%	-15%	-12.5%	-10%	-7.5%	-5%	-2.5%	0%

Figure 23: Array of percentages used in maximum-minimum deviation search (Subsection [5.2])

The upcoming thesis is dedicated to the examination of three interconnected Microgrids. These Microgrids are characterized by the topology depicted in Figure [24], where the significant feature is the presence of bidirectional power flow and information exchange between each Microgrid.

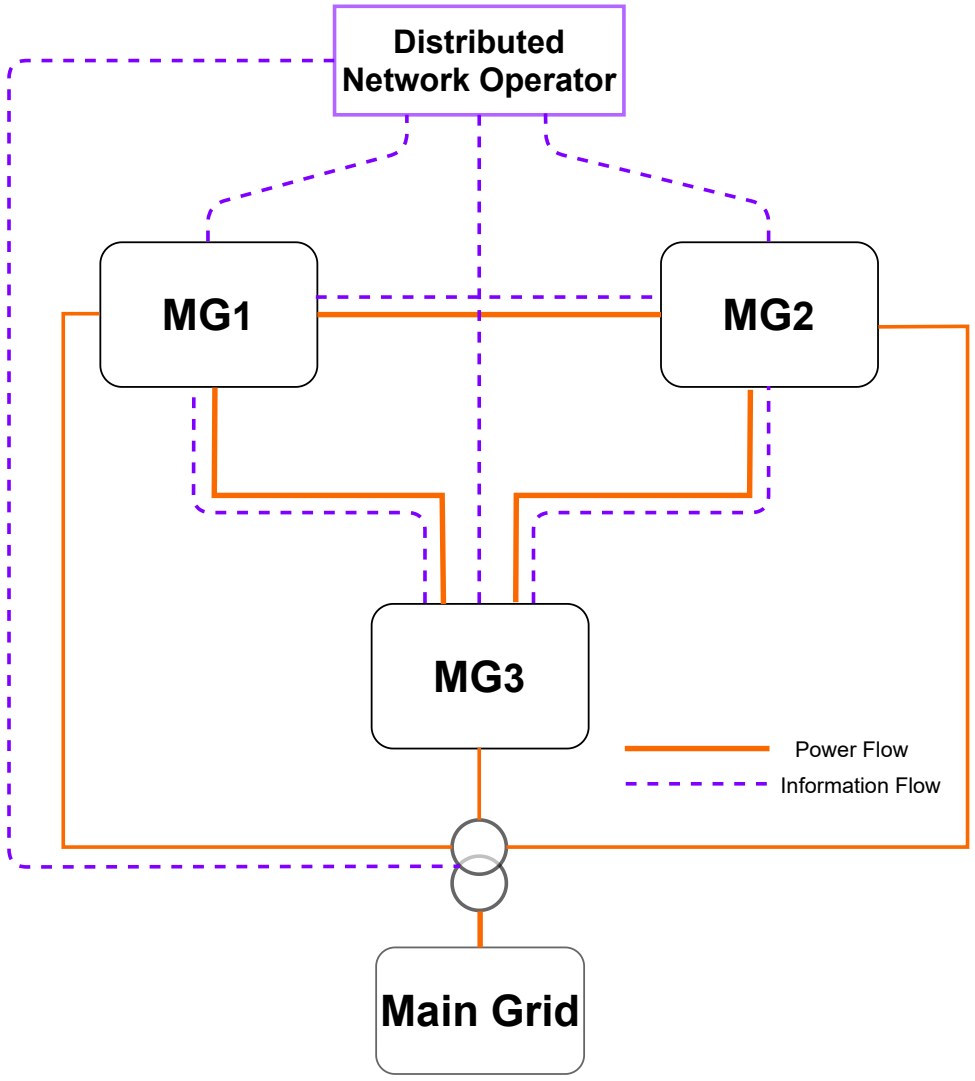

Figure 24: Topology of Interconnected Microgrids

The study operates on the premise that the electricity price forecasting would be handled by the power system operator. These predictions would then be shared with all the MGs. In this scenario, the assumption is that the system operator's forecast is flawless, and there are no disparities between the real-time electricity price and the predicted price. This assumption is grounded in the algorithm's rapid computational speed, which operates within a few minutes, ensuring timely performance following day-ahead market clearance. Notably, the Grid sells power to MGs at different rates than it purchases. Specifically, the Grid sells power to the MGs at a higher price than its buying rate. This market structure is designed to incentivize the adoption of clean energy and encourage MGs to implement energy management techniques. The overarching goal is to offset surplus power, which can subsequently be resold to the grid. As a result, this strategy promotes clean energy use and facilitates peer-to-peer trading among participants. The study used a regular daily temperature dataset from late summer in Greece to represent the outdoor temperature. It's common to see a spike in temperatures around 3:00 PM during summer days.

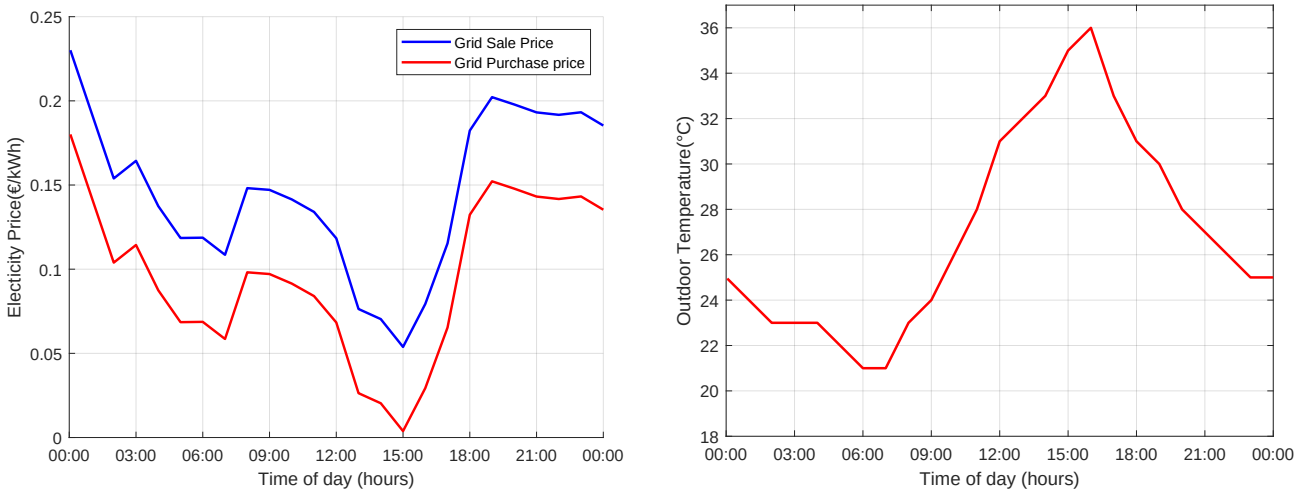

(a) Electricity Price (b) Ambient Temperature

Figure 25: External Data for the Following Day

The occupancy profile holds immense importance as it provides invaluable insights into the day-to-day electrical and thermal activity patterns within households. Figure [26] depicts the count of indoor occupants within each virtual skyscraper across the different MGs. Shifting the focus to Figure [27], it showcases the number of indoor occupants who are actively engaged in activities (excluding those who are sleeping). Moving on to Figure [28], it details the count of indoor occupants currently asleep.

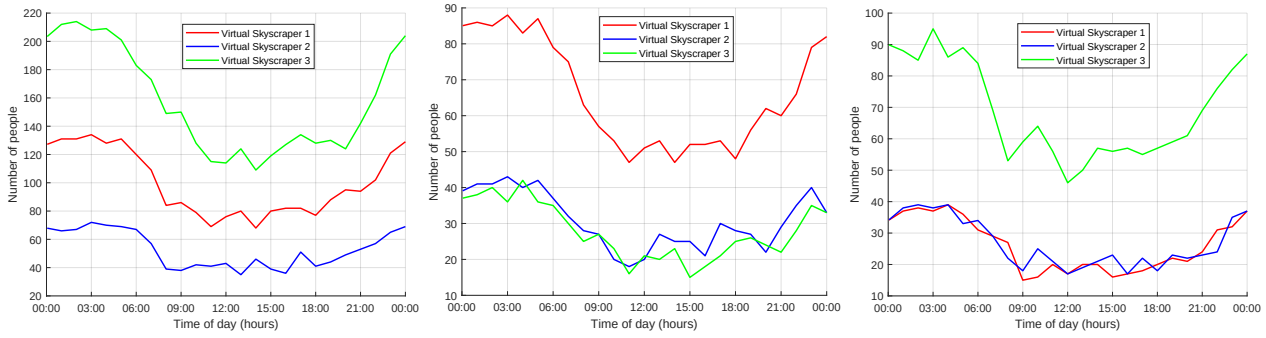

(a) Microgrid 1 (b) Microgrid 2 (c) Microgrid 3

Figure 26: Forecasted Count of Indoor Occupants

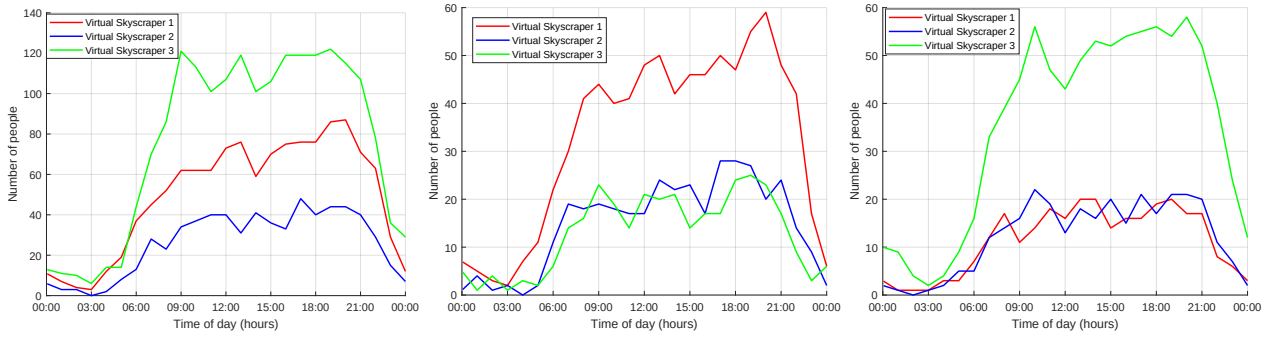

(a) Microgrid 1 (b) Microgrid 2 (c) Microgrid 3

Figure 27: Forecasted Count of Indoor and Active Occupants

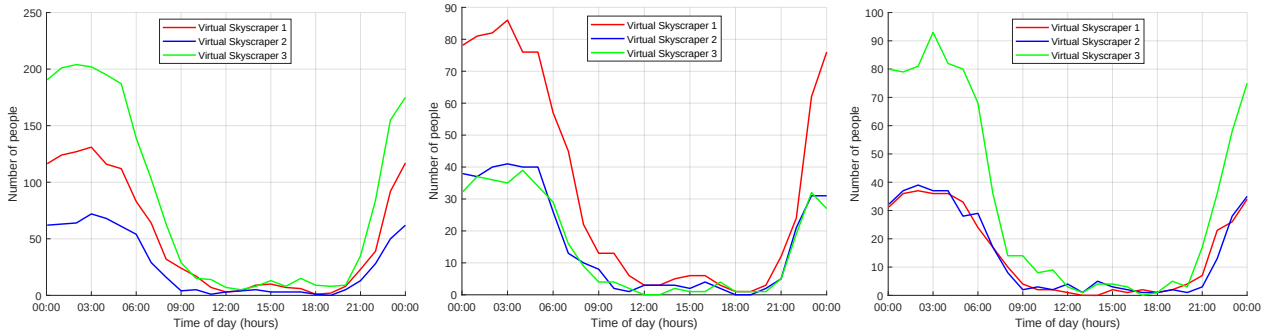

(a) Microgrid 1 (b) Microgrid 2 (c) Microgrid 3

Figure 28: Forecasted Count of Indoor and Sleeping Occupants

The total number of connected EVs within each MG for the upcoming day is illustrated in Figure [29]. The timing of connections (connect time) and the charging periods (dwell time) vary depending on various driver activities, such as being at home, work, or engaging in shopping/social activities. These durations are estimated using corresponding probability density functions (PDFs), as depicted in Figure [30]. The total power generated by the WT park and PV Park for each MG is shown in Figure [31]. Due to their geographic proximity, the MGs share similar characteristics in terms of energy production. Both wind turbines and photovoltaic systems exhibit consistent behavior across these MGs. However, variations arise due to distinct installed capacities, which reflect different penetration rates for each green technology within the various MGs. Consequently, the quantity of electricity generated differs among the MGs due to these varying levels of installed capacity.

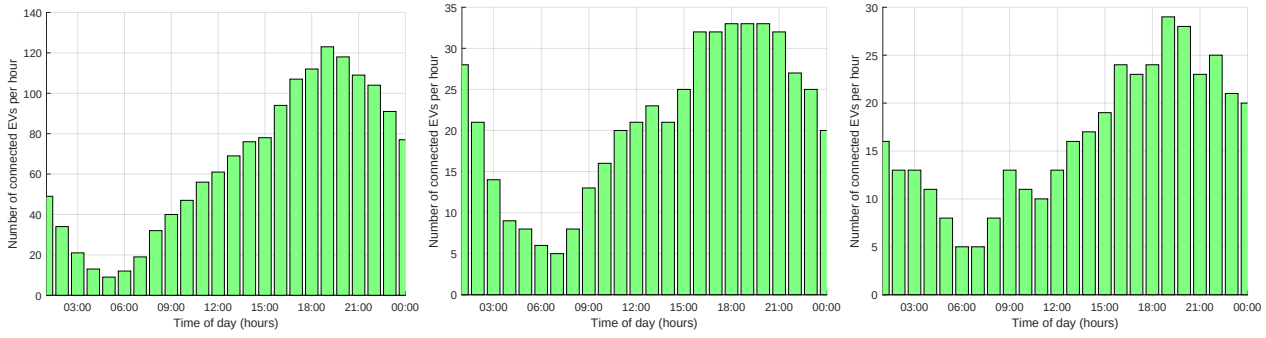

(a) Microgrid 1 (b) Microgrid 2 (c) Microgrid 3

Figure 29: Number of Connected Electric Vehicles

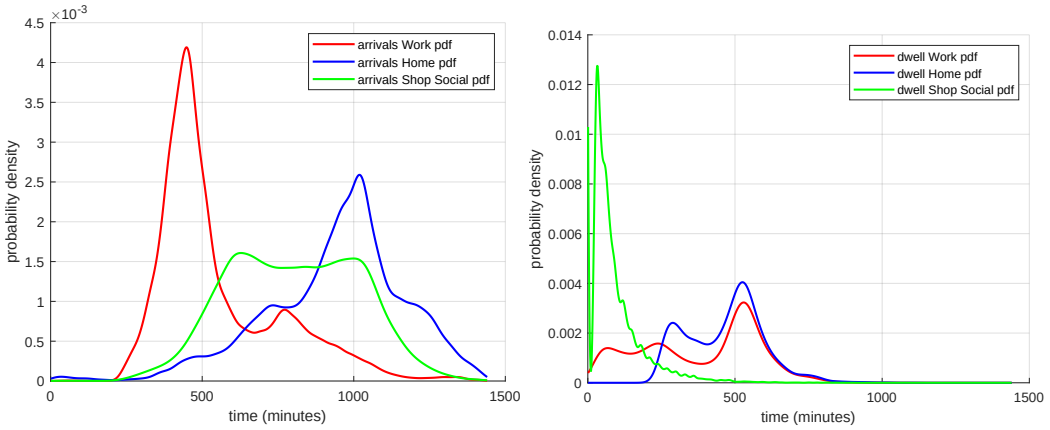

(a) arrival time (b) dwell time

Figure 30: PDFs of Electric Vehicles [3]

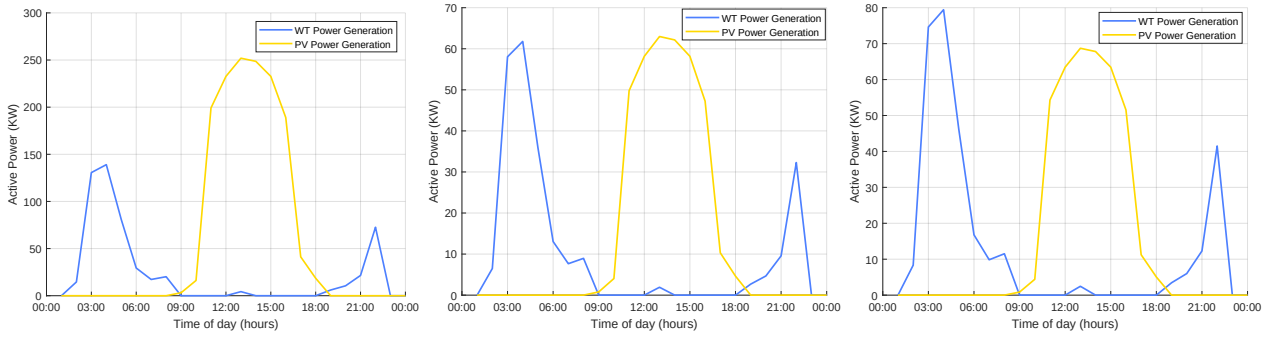

(a) Microgrid 1 (b) Microgrid 2 (c) Microgrid 3

Figure 31: Generation of Power from Renewable Energy Sources

The occupancy profile within each virtual skyscraper significantly influences the electrical and thermal loads of the houses in the MGs. The individual loads constituting the overall thermal and electrical loads are represented indicatively in Figure [32] for first virtual skyscraper of first MG. To understand load sizes, Figure [33] illustrates the load profile of each virtual skyscraper in every MG. Additionally, Figure [34] displays the internal thermal heat gains for each virtual skyscraper within each MG. To give context to the load magnitudes in Figure [35], the average electrical load for each household is estimated by dividing the energy needs of the virtual skyscraper by the number of houses it includes. This helps grasp the electrical load sizing for each house geometry. Furthermore, Figure [36] provides actual electrical load data for specific houses, offering an indicative perspective. Similarly, Figure [37] presents the average thermal load per household for each house geometry. This is calculated by dividing the thermal needs of each virtual skyscraper by the number of houses it comprises, aiding in understanding thermal load dimensioning for each house geometry. Figure [38] provides actual thermal load information for all thermal zones within a random house, serving as an illustrative reference for each house geometry.

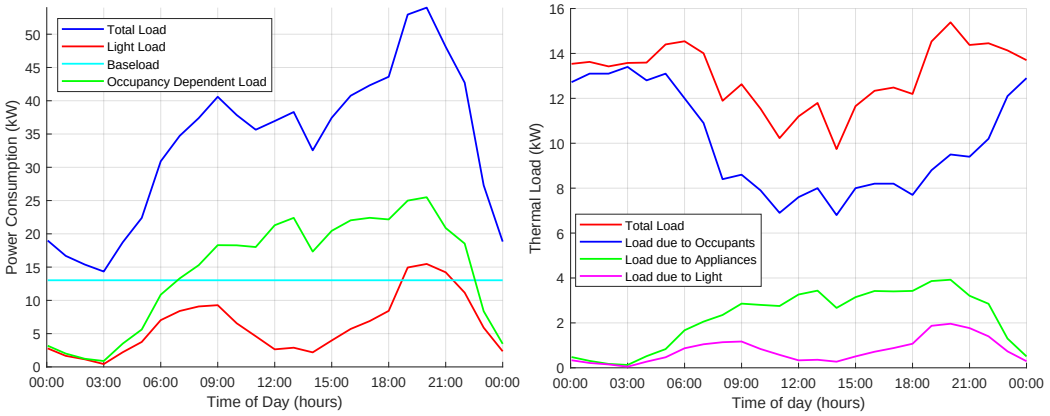

(a) Total Electrical Load (b) Total Thermal Load

Figure 32: Comprehensive Analysis of Total Load Indicative for first VS of First MG

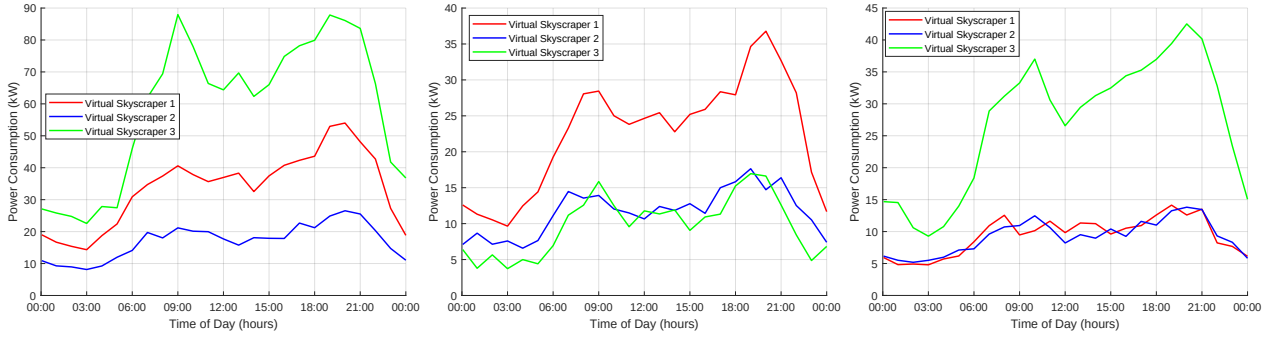

(a) Microgrid 1 (b) Microgrid 2 (c) Microgrid 3

Figure 33: Aggregated Household Electrical Loads

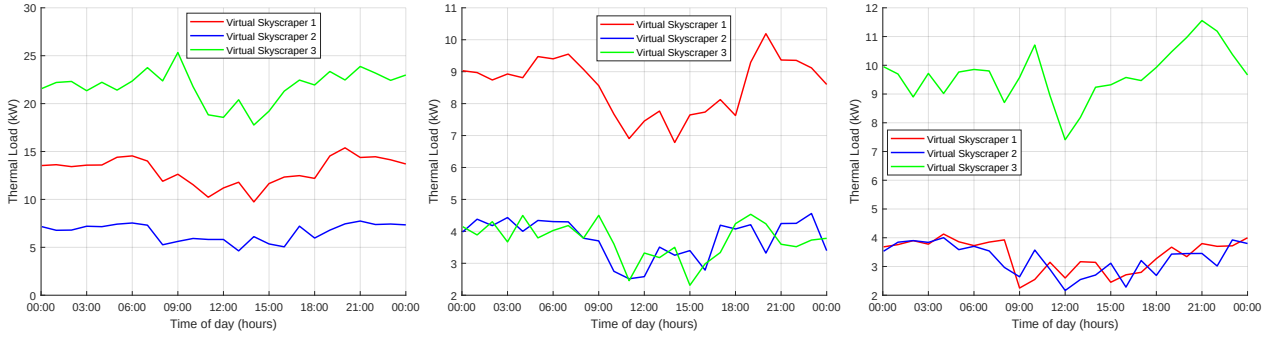

(a) Microgrid 1 (b) Microgrid 2 (c) Microgrid 3

Figure 34: Aggregated Household Thermal Loads

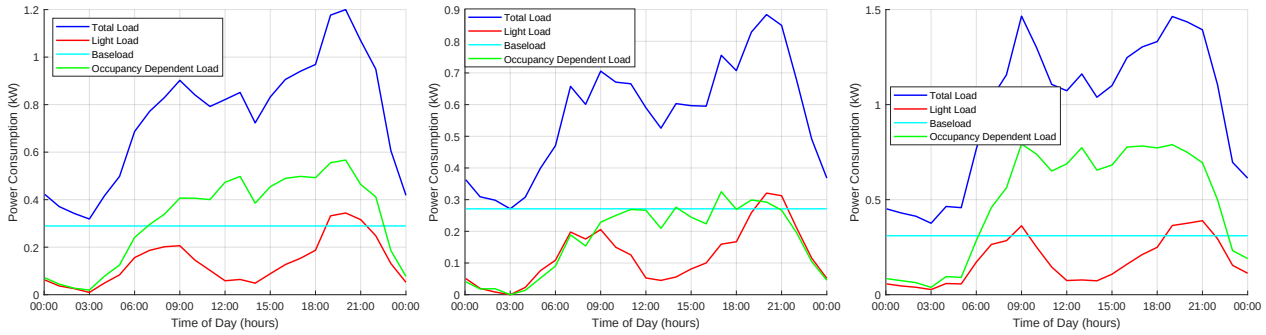

(a) Type 1 Geometry (b) Type 2 Geometry (c) Type 3 Geometry

Figure 35: Average Electrical Load per Individual Household

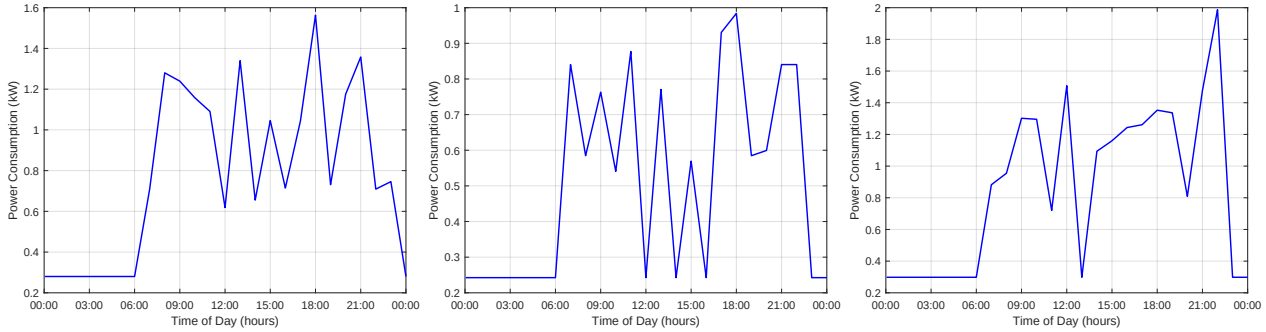

(a) Type 1 Geometry (b) Type 2 Geometry (c) Type 3 Geometry

Figure 36: Indicative Real Electrical Loads for Individual Households

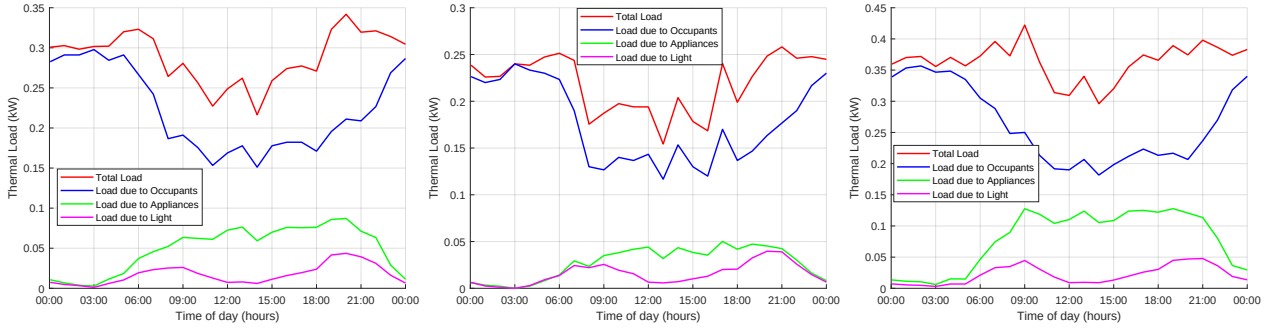

(a) Type 1 Geometry (b) Type 2 Geometry (c) Type 3 Geometry

Figure 37: Average Thermal Load per Individual Household

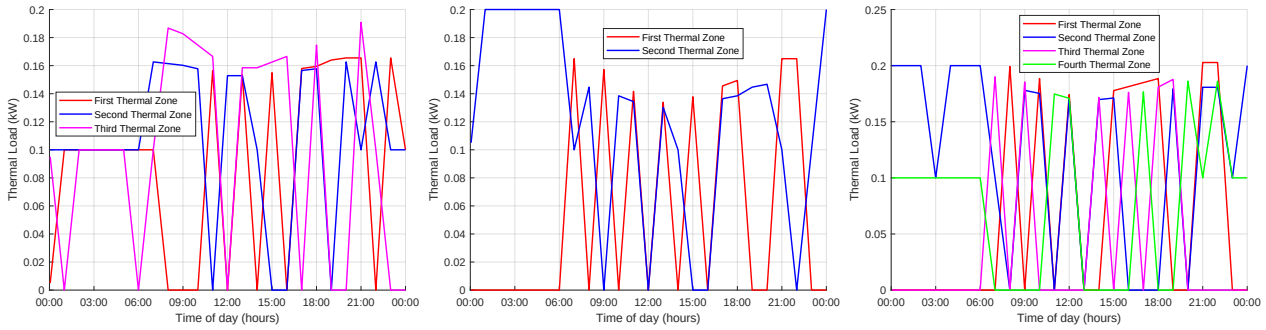

(a) Type 1 Geometry (b) Type 2 Geometry (c) Type 3 Geometry

Figure 38: Indicative Real Thermal Load for Individual Household

The internal temperatures of all thermal zones in each MG's buildings, obtained through the optimization process defined in (4.1), specifically by constraints (4.3) - (4.7) for each MG, along with their upper and lower bounds, are presented in Figure [39]. It was observed that the internal temperatures of all thermal zones within each building were consistently maintained within the comfortable temperature range of 20–26°C, and they exhibited consistent behavior.

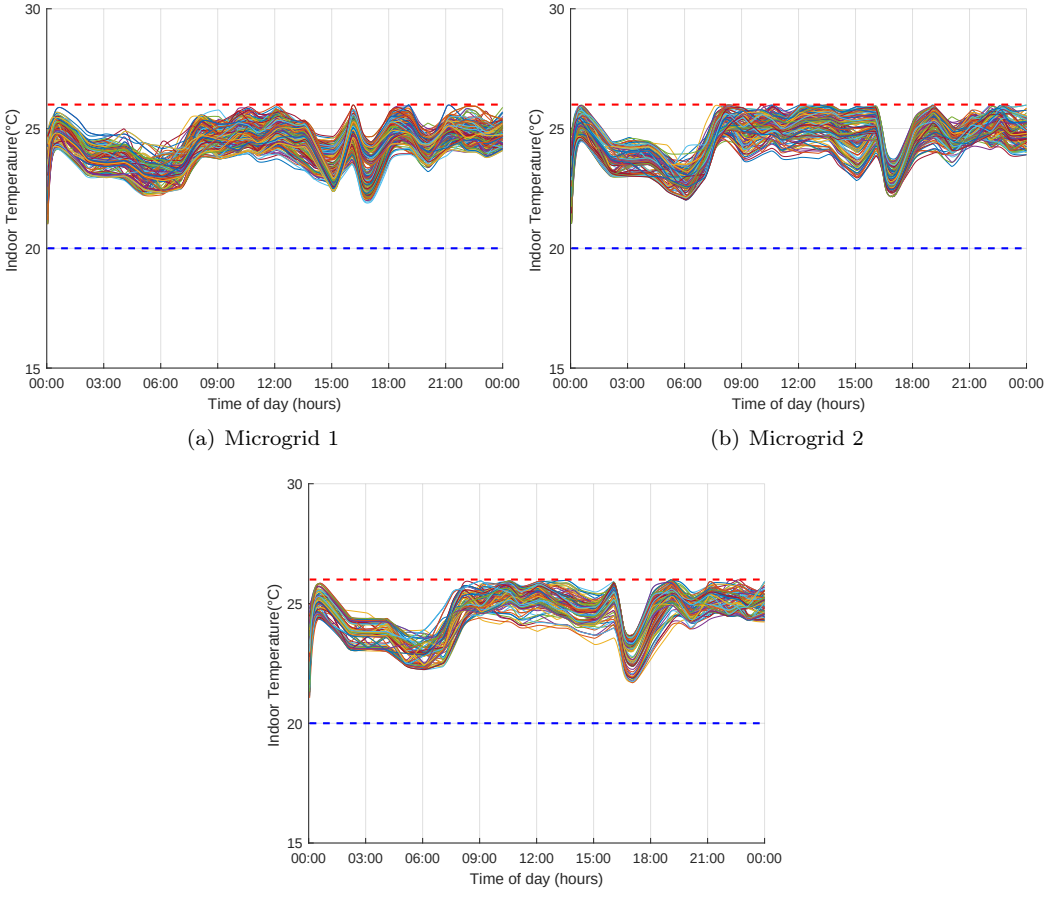

(a) Microgrid 1 (b) Microgrid 2

(c) Microgrid 3

Figure 39: Internal Temperatures of Thermal Zones in All Houses (EMS Section 4)

In Figure [40], the electricity consumption of the HVAC systems within each virtual skyscraper is illustrated for each MG. This consumption is derived from the initial optimization phase in Section [4] prior to Peer to Peer Market Participation. Additionally, Figure [42] demonstrates the aggregated requirement of the entire MG, obtained by cumulatively summing the needs of the virtual skyscrapers constituting each MG. This consumption outcome arises from the effective management of the collective HVAC power of all houses by each MG.

The cooling power for each virtual skyscraper, and thereby the cooling needs of each MG, aligns with the ambient temperature as anticipated. Due to limited storage capacity in each thermal zone within a residential building, driven by its compact dimensions, the system's degrees of freedom are significantly constrained—a fundamental characteristic. Consequently, the power consumption profile should closely track temperature changes to ensure compliance with specific temperature limits for each thermal zone.

As expected, the virtual skyscraper accommodating the largest number of occupants, and consequently having the highest load demands, exhibits the most substantial cooling demand. Furthermore, during periods characterized by elevated electricity prices, the algorithm aims to curtail power usage, as evident from the figures. This is reinforced by the fact that a significant portion of power consumption has been shifted to 15:00, aligning with the lowest observed electricity value.

Figure [41] illustrates the distribution of HVAC power that was intelligently allocated from the virtual skyscraper level to the actual house level, utilizing the smart distribution equations (4.6)-(4.7). It displays HVAC power consumption of indicative houses of each geometry type. This power fluctuates across various house geometries due to their differences in geometry and due to distinct requirements, as depicted in Figure [38].

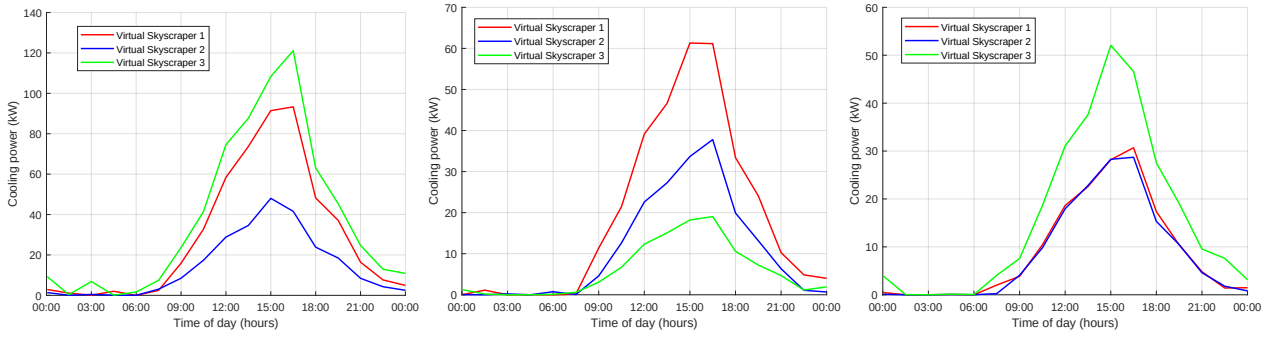

(a) Microgrid 1 (b) Microgrid 2 (c) Microgrid 3

Figure 40: HVAC Power Consumption in Virtual Skyscrapers of each MG

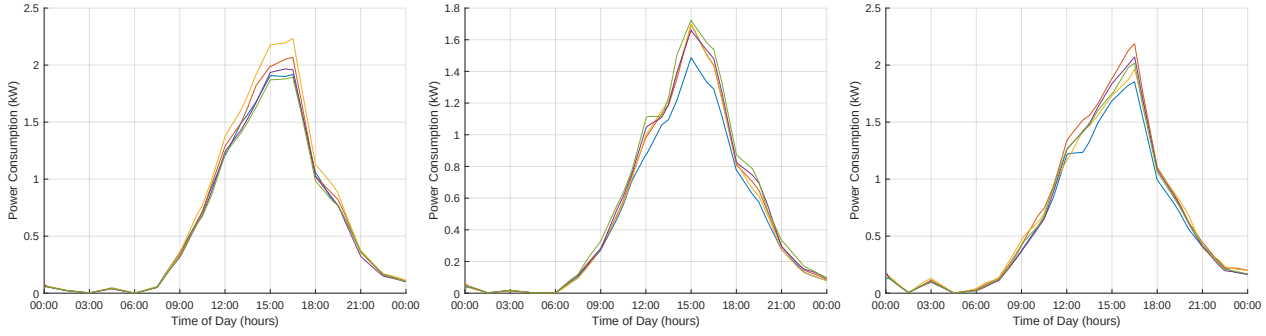

(a) Type 1 Geometry (b) Type 2 Geometry (c) Type 3 Geometry

Figure 41: HVAC Power Consumption of Indicative Houses

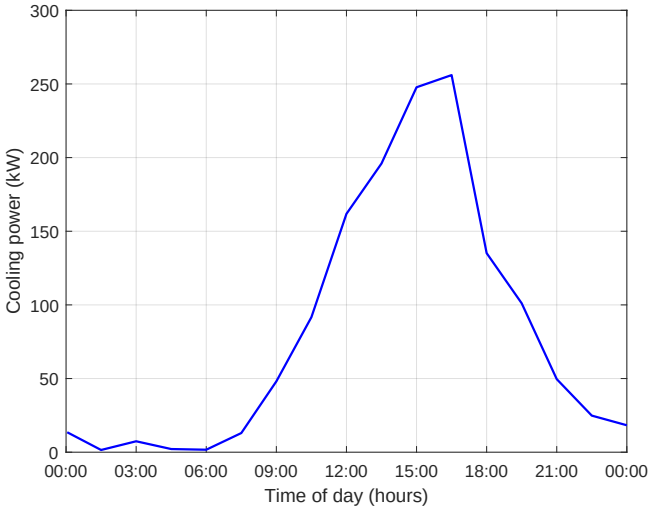

(a) Microgrid 1

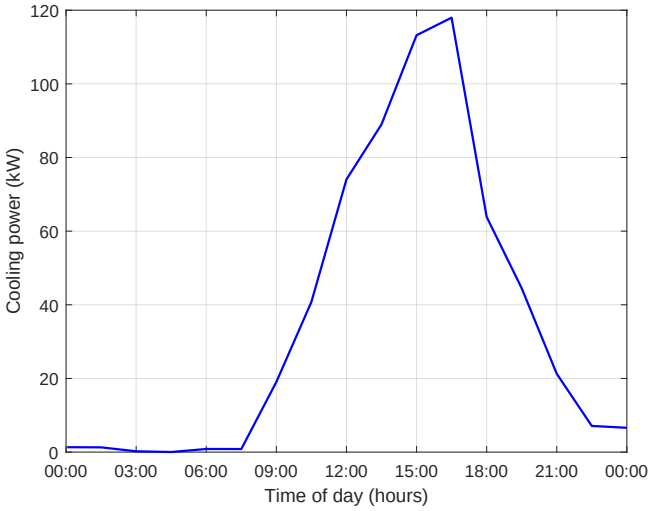

(b) Microgrid 2

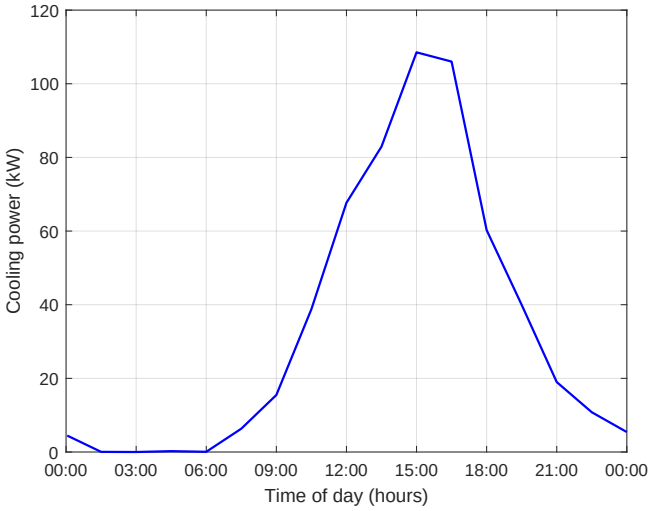

(c) Microgrid 3

Figure 42: Total HVAC Power Consumption in each MG

Figure [43] illustrates the combined non-critical electrical loads of the virtual skyscrapers within each MG, both before and after the execution of the EMS (Section 4). Notably, the non-critical loads are strategically shifted to time slots characterized by lower electricity prices. This adjustment aims to reduce the overall operational cost of each MG while adhering to all operational constraints shown in Table [4]. As shown, a portion of electricity consumption is curtailed during the period of 7:00 - 12:00 and transferred to the period of 12:00-17:00 when the electricity price notably drops. Figure [44] provides a visual representation that shows the indicative display of non-critical loads for each individual skyscraper within the first examined MG, both before and after the optimization phase. These load profiles emerge due to the optimal distribution of electric power demand, harnessing the potential of shiftable loads. The load shifting at the virtual skyscraper level can further be extended to each individual real residential building within the MG.

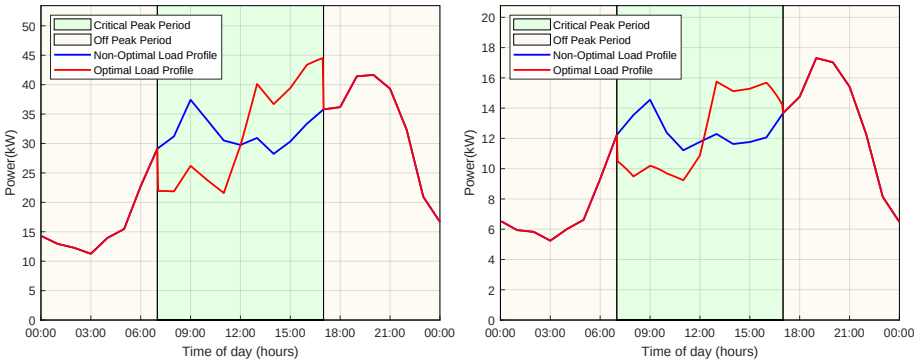

(a) Microgrid 1 (b) Microgrid 2

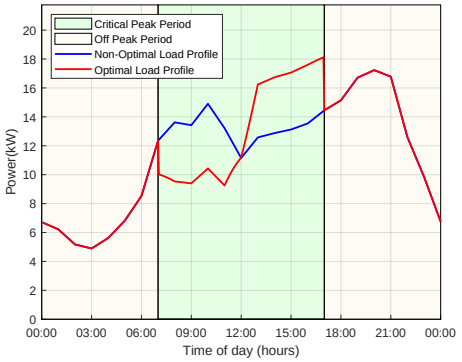

(c) Microgrid 3

Figure 43: Electric Power Consumption of Non-Critical Loads

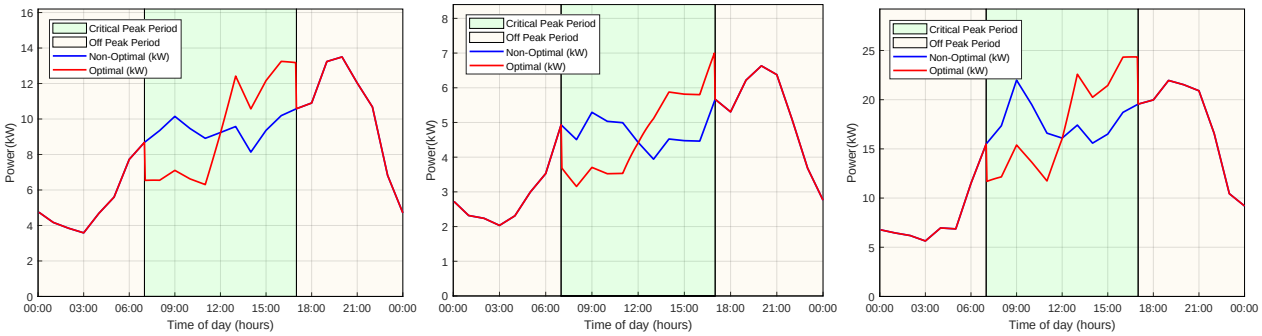

(a) Virtual Skyscraper 1 (b) Virtual Skyscraper 2 (c) Virtual Skyscraper 3

Figure 44: Indicative Electric Power Consumption of Non-Critical Loads in the First Microgrid

The electrical power consumption of HVAC systems and all other loads within each MG are depicted in Figure [45], presented separately to showcase the relationship between the two quantities. Figure [46] displays the combined electrical power consumption for HVAC systems and all other loads of buildings, providing a visualization of the total load within each MG. The total load after each MG implemented optimal operation scheduling is indicated by the red line in the Figure [46].

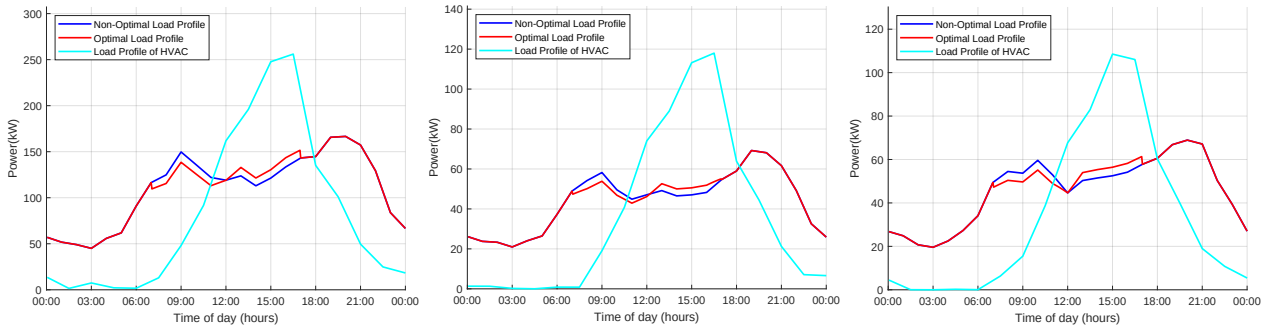

(a) Microgrid 1 (b) Microgrid 2 (c) Microgrid 3

Figure 45: Load Profile of MG

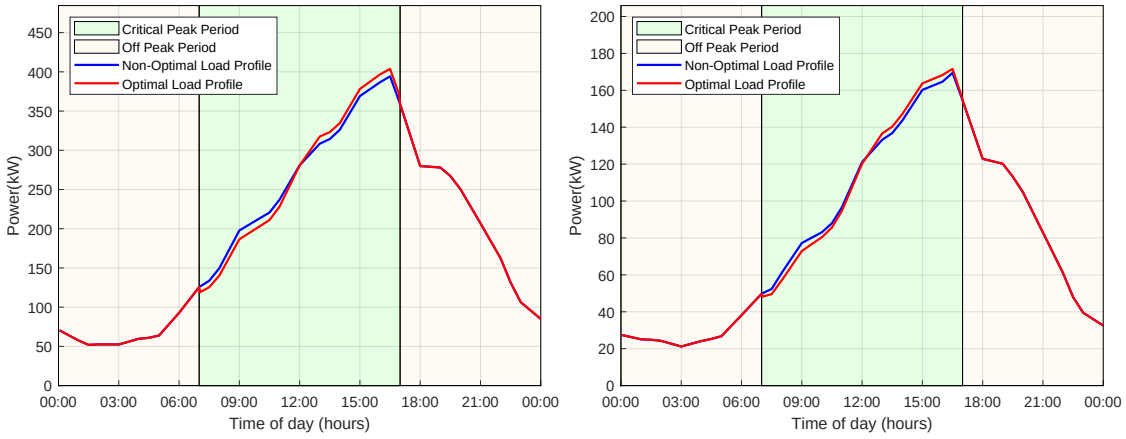

(a) Microgrid 1 (b) Microgrid 2

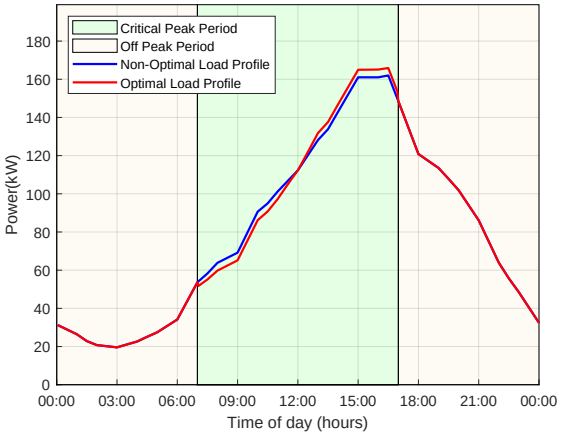

(c) Microgrid 3

Figure 46: Total Load Profile of MG

To provide context for the load magnitudes shown in Figure [47], the average total electrical load for each

household is estimated by dividing the total energy needs of the virtual skyscraper by the number of houses it comprises. This estimation aids in understanding the electrical load dimensions for each house geometry. Moreover, Figure [48] presents actual data on the total electrical load for specific houses, providing an illustrative perspective.

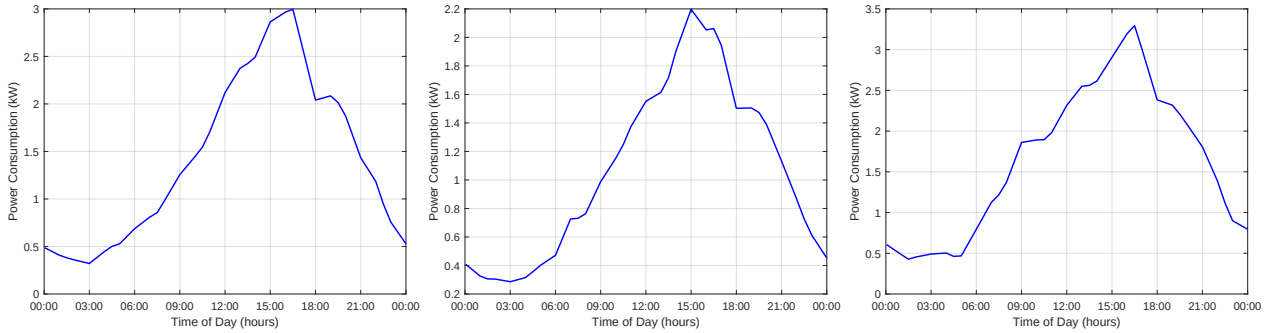

(a) Type 1 Geometry (b) Type 2 Geometry (c) Type 3 Geometry

Figure 47: Average Total Load per Individual Household (Including HVAC)

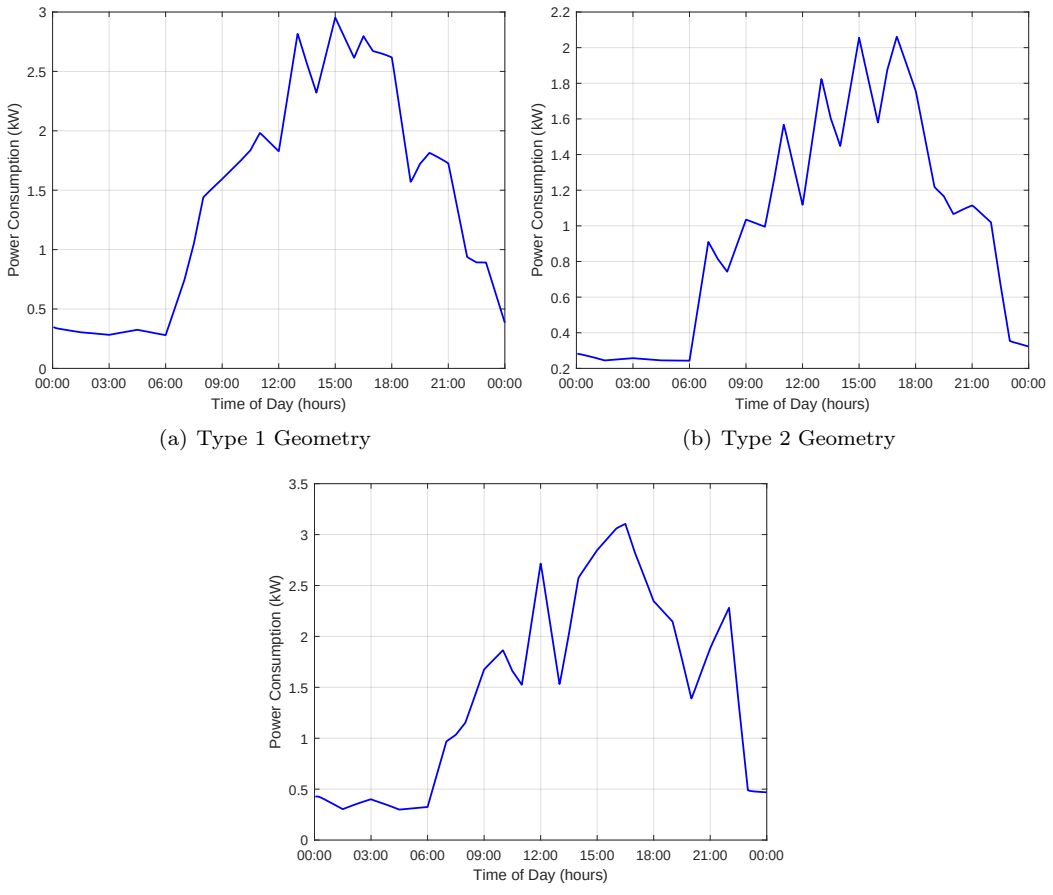

(a) Type 1 Geometry (b) Type 2 Geometry

(c) Type 3 Geometry

Figure 48: Indicative Real Total Load for Individual Households (Including HVAC)

By utilizing the PDFs of Arrival and Dwell times of PEVs in Figure [30], along with the forecasted Number of EVs and the activity of the Driver shown in Table [6], we can calculate the uncontrollable part of the SoC (SoC_{diff}) of the aggregator. This SoC corresponds to the Load of the aggregator that needs to be served to ensure that drivers have sufficient SoC to satisfy their driving needs upon departure. Figure [49] illustrates the SoC that the aggregator 'gains' from EVs, as they have an initial amount of SoC when they plug in. Figure [50] presents the SoC that the aggregator 'loses' from EVs, which is the required level of SoC that drivers need to have at the time of departure. Lastly, Figure [51] depicts the load part of the aggregator, representing the non-controllable part that must be served to meet the drivers' needs, derived with the use of initial and targeted SoC with equation (3.39).

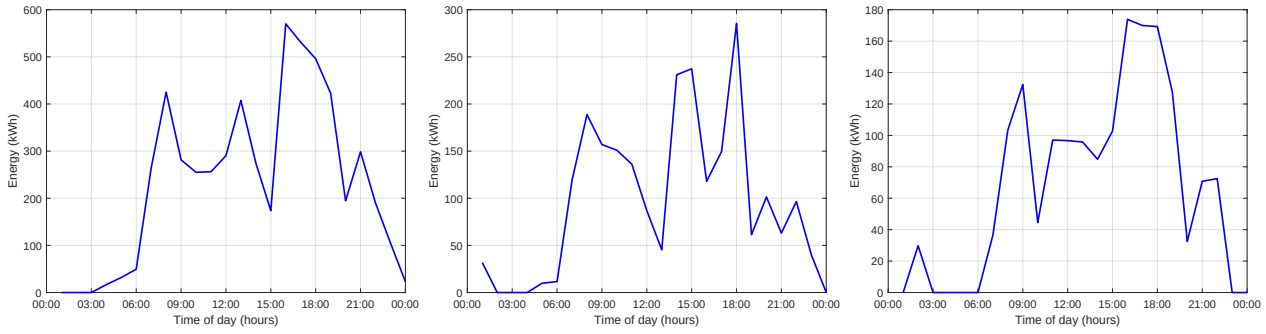

(a) Microgrid 1 (b) Microgrid 2 (c) Microgrid 3

Figure 49: SoC "Gains" of Aggregator From Plug-In Of Individual EVs

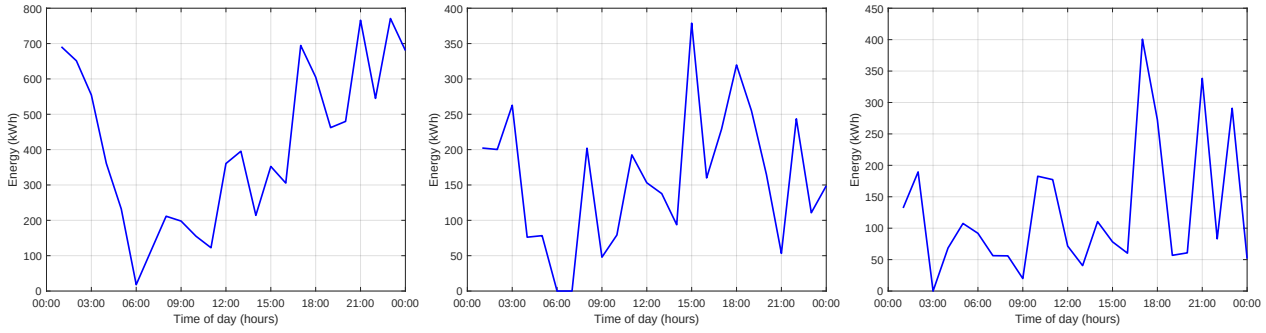

(a) Microgrid 1 (b) Microgrid 2 (c) Microgrid 3

Figure 50: SoC "Losses" of Aggregator From Plug-Out Of Individual EVs

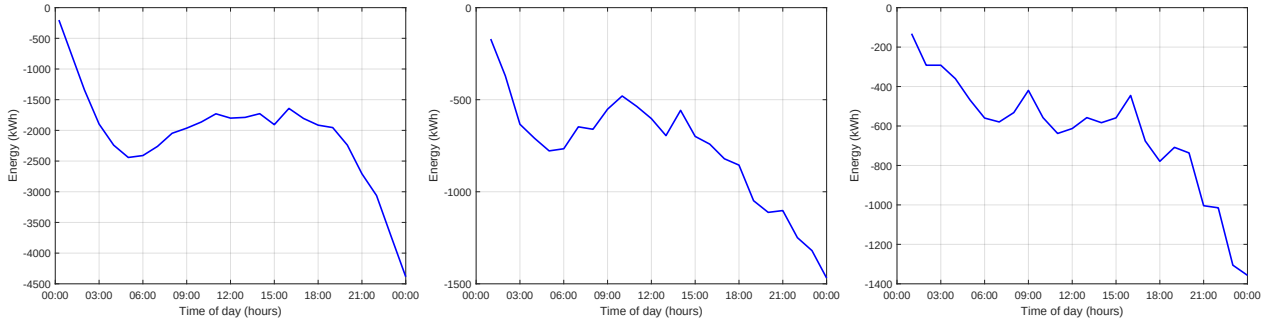

(a) Microgrid 1 (b) Microgrid 2 (c) Microgrid 3

Figure 51: Total Energy that must be Provided to Aggregator (Generation Convention for the Aggregator)

Figure [52] illustrates the total active power exchange between the aggregator (PEV Parking-Lot facility) and the Grid for each MG. This depiction also encompasses the upper and lower technical boundaries, set by the individual EVs it comprises, as formulated in equations (3.33)-(3.34). The generator convention is adopted, using negative values to indicate power absorption from the grid (charging and G2V operation of individual EVs within the virtual battery), and positive values to represent power injection into the grid (discharging and V2G operation of individual EVs within the virtual battery). Figure [53] presents a more detailed view of power exchange and also provides insights into the status of individual EVs that constitute the Virtual Battery (whether in a state of V2G or G2V operation). It's evident that the V2G operation, in which the aggregator injects power back into the grid, remains inactive throughout the observed period due to the absence of significant events, such as a failure in the point of common coupling with the main grid, leading to microgrid islanding.

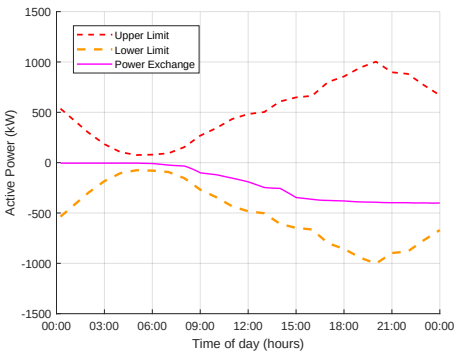

(a) Microgrid 1

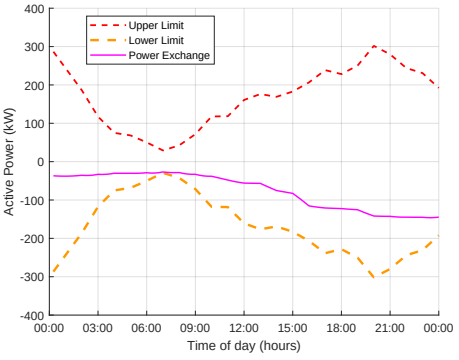

(b) Microgrid 2

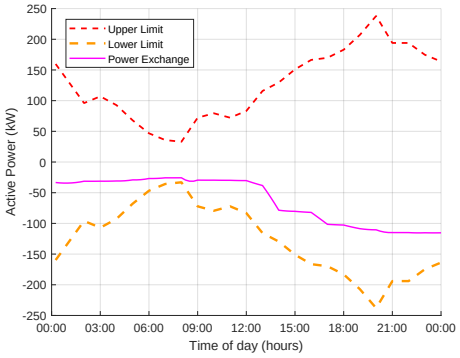

(c) Microgrid 3

Figure 52: Active Power Exchange Between Aggregator and MG, Including Upper and Lower Bounds

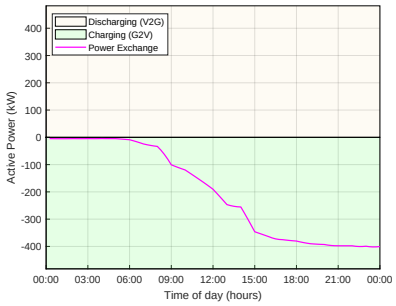

(a) Microgrid 1

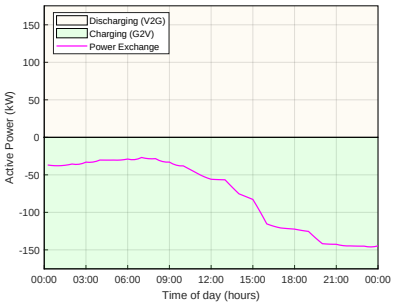

(b) Microgrid 2

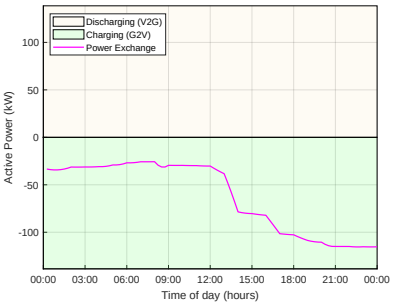

(c) Microgrid 3

Figure 53: Active Power Exchange Between Aggregator and MG, Including Information about the operation Model of Aggregator

Figure [54] portrays the energy stored within each MG's Parking-Lot virtual equivalent battery, along with its upper and lower limits as formulated in equations (3.35)-(3.36). These limits display fluctuations due to the continuous connections and disconnections of EVs and variations in electricity prices. As mentioned in the modeling of the Parking Lot Dynamic Aggregated Battery in Subsection [3.4], the Aggregator assumes a dual role. Given that EVs plug in with low initial SoC and drivers require a high SoC upon departure to meet their driving needs, the Real Aggregator is comprised of not only an energy storage part but also a load part as depicted in Figures [49]-[51]. Therefore, it is imperative to illustrate the energy exchange between the real aggregator (Parking-Lot) and the Microgrid to address the load requirements. This exchange is represented in Figure [55].

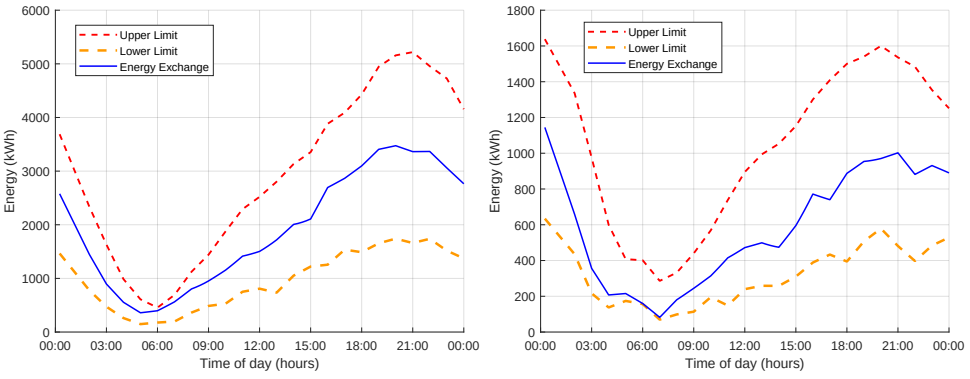

(a) Microgrid 1 (b) Microgrid 2

(c) Microgrid 3

Figure 54: Total Stored Energy within Virtual Equivalent Battery, Alongside Upper and Lower Bounds

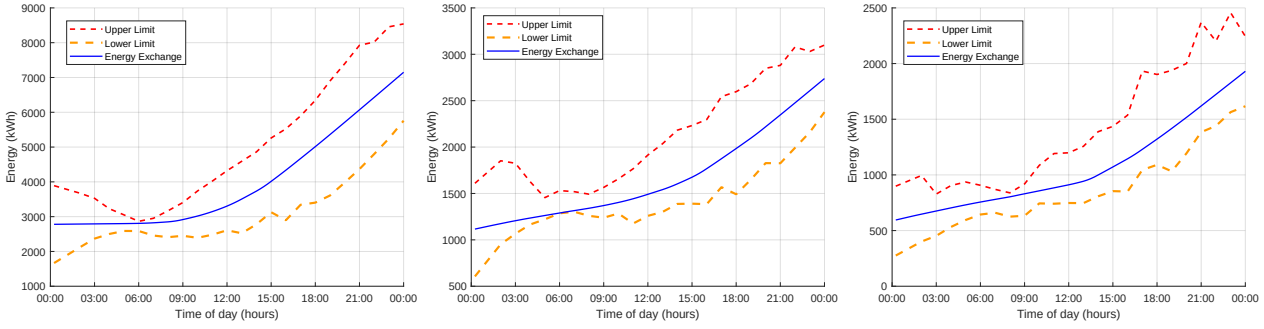

(a) Microgrid 1 (b) Microgrid 2 (c) Microgrid 3

Figure 55: Total Stored Energy within Aggregator, Alongside Upper and Lower Bounds

In the context of power exchange between MG and the main electrical Grid, Load convention has been adopted for the MG. As a result, the power exchange value is considered negative when the MG sells power to the Grid, and conversely, it is positive when the MG purchases power from the Grid. This power exchange arrangement is illustrated in Figure [56] for each MG. It is crucial to differentiate the load convention established between the MG and the main grid from the MG's participation convention in the peer-to-peer electricity market, where a generation convention has been adopted. The fact that a significant portion of the microgrid's power purchases from the main grid takes place at 15:00, coinciding with the period of lowest electricity prices, serves as confirmation of the algorithm's accuracy.

It's important to note that MG1 has a larger installed capacity of PVs compared to the other MGs in proportion to its load. We observe a clear pattern during specific times, typically from 10:00 to 15:00 when PVs generate a substantial amount of power. During this period, MG1 reduces its power draw from the main grid to some extent. Conversely, when PVs cease power generation, MG1 continues to draw power, with a certain degree of flexibility, as the aggregator operates as an energy storage device. This characteristic, where the power drawn from the grid exhibits a concave shape resembling that of a duck, is commonly referred to as the 'duck curve.' The duck curve represents one of the most limiting factors for achieving high penetration rates of PVs. The conventional grid relies on large generators that must closely follow the demand to maintain energy balance. These generators are typically large and operate at a slower pace. When there is a rapid increase in the rate at which power is drawn from the grid, caused by the duck curve resulting from PV penetration, these generators struggle to keep up with the sudden increasing demand, increasing the risk of a blackout.

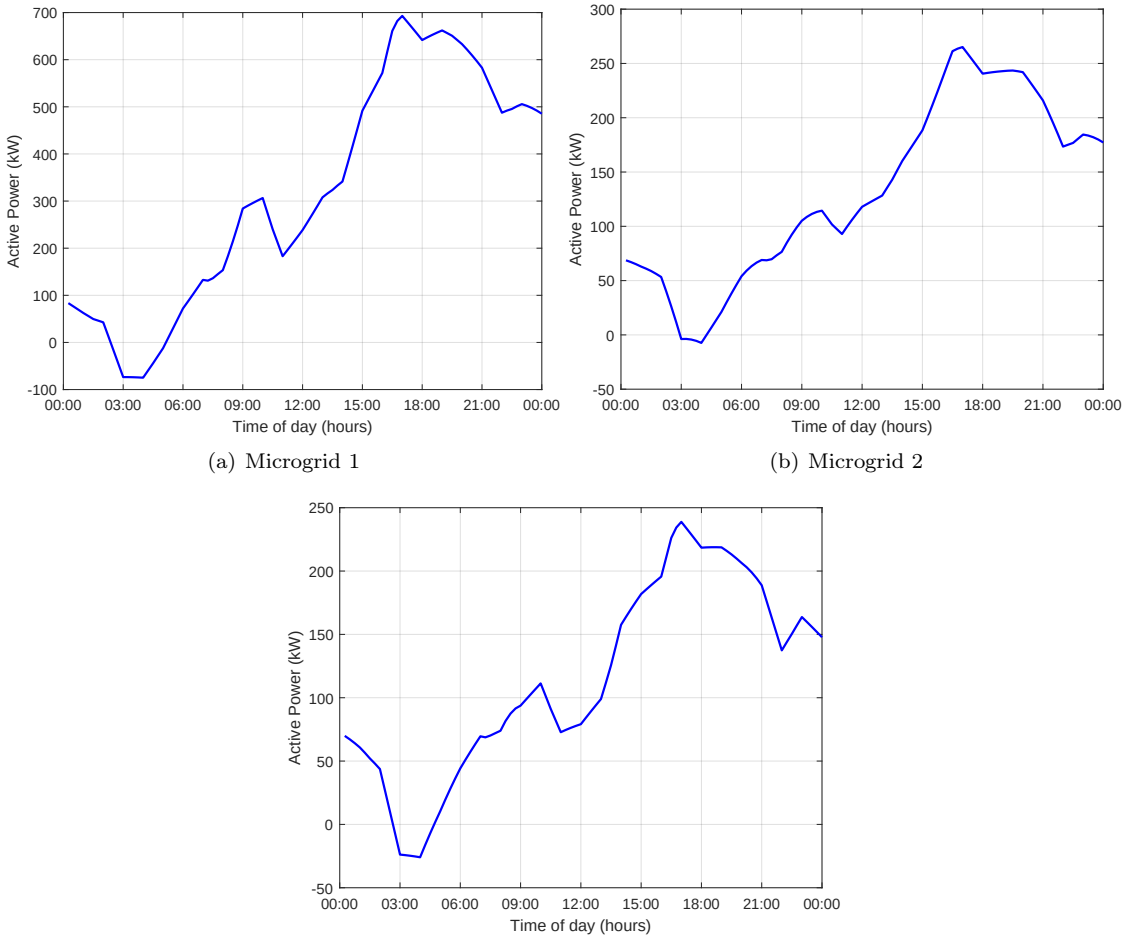

(a) Microgrid 1

(b) Microgrid 2

(c) Microgrid 3

Figure 56: Active Power Exchange between MG and Main Grid (with assigned Load Convention on MG)

At this stage, each MG has optimized its operational schedule for the following 24-hour period (as described in Section [4]). Subsequently, the MGs will engage in a Peer-to-Peer Electricity Market with the aim of maximizing their profit potential, utilizing the algorithm outlined in Section [5]. Market participation will occur at intervals of 1.5 hours, resulting in a total of 16 participation instances over the 24-hour period. To enhance clarity and comprehension, there will be an in-depth analysis of the bargaining outcome of the Non-Cooperative game for a single time instant: 18:00 - 19:30. This analysis involves the three MGs with the topology depicted in Figure [24]. For the sake of enhanced clarity, it's important to note that within each time interval, the three interconnected MGs in the case study engage in participation. However, at most two MGs successfully reach an agreement with each other. As a result, the outcomes of these participations are showcased, focusing only on the two MGs that have successfully sealed a deal. The cost functions of the two MGs are depicted in Figure [57]. The observed discontinuity at the zero power point during role switching (from seller to buyer, or vice versa) is attributed to the dual pricing of the power grid. While this discontinuity is noteworthy, it does not affect the accuracy of the curve. This is because a zero power exchange at that point signifies autonomous operation for the MG. Furthermore, on the right and left sides of the autonomous point of operation, the MG assumes different roles, each with potentially distinct objectives or subject to different constraints. These two operations are distinct events that cannot occur simultaneously, it's either one or the other.

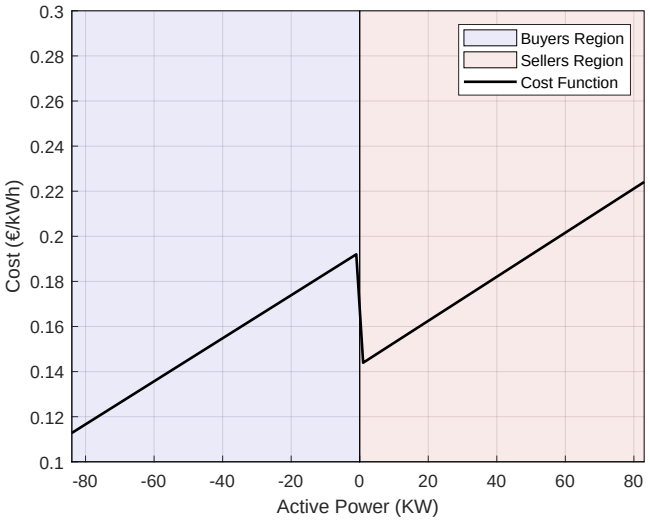

(a) Microgrid 1

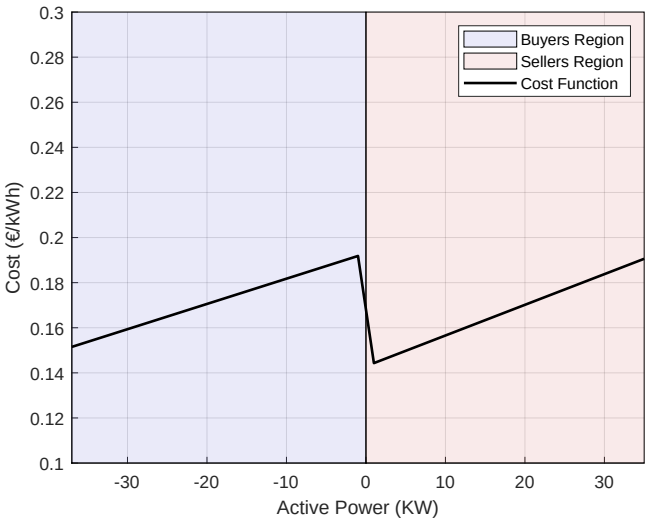

(b) Microgrid 2

Figure 57: Cost Function of Microgrid (both Producer and Consumer Roles) for Time Instant 18:00 - 19:30

The bidding sequence of power values of the two MGs, from the initiation of the game to the point of reaching an agreement, is illustrated in Figure [58]. It is evident that the power balance is maintained, as the quantity of power purchased by MG 1 (10 kWatts) matches the quantity of power sold by MG 2 (-10 kWatts).

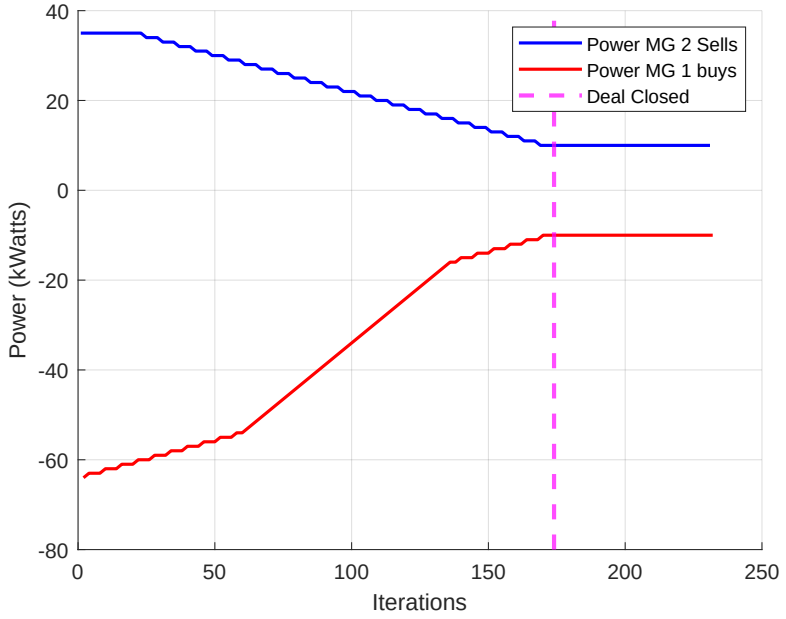

Figure 58: Bidding Sequence of Power Values Between the Two MGs That Successfully Sealed the Deal

Another aspect that reinforces the accuracy of the algorithm is depicted in Figure [59]. It illustrates that in each iteration, the bidding power values by each MG remain within the boundaries of the maximum and minimum allowable power values (dependent on the role of each MG). This adherence to limits aligns with the logic outlined in the flowchart presented in Figure [18]. The flowchart demonstrates that in every iteration where a deal is not established, the power capacity is constrained to facilitate the achievement of power balance.

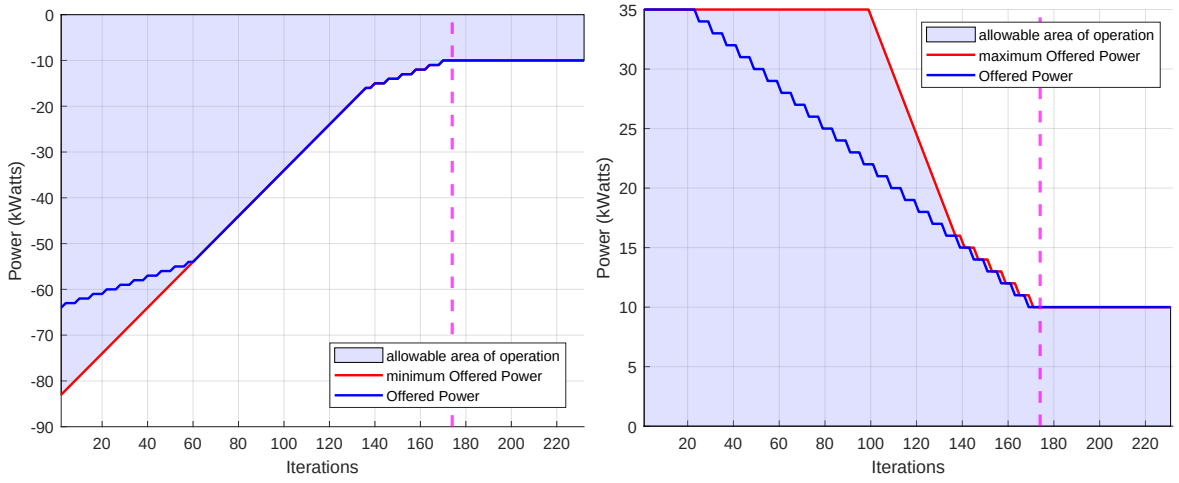

(a) Microgrid 1 in Buyer Role

(b) Microgrid 2 in Seller Role

Figure 59: Bidding Sequence of Power Values Between the Two MGs and the Allowable Area of Operation

The biding sequence of price values by the two MGs, starting from the initiation of the game to the point of agreement, is depicted in Figure [60]. Each MG attempts to maximize its individual benefits, as indicated by the initial prices (in the initial iterations, seller propose very high prices, while buyer propose very low prices). As the algorithm advances and successive negotiations and compromises take place, both MGs gradually converge towards a mutually satisfactory price.

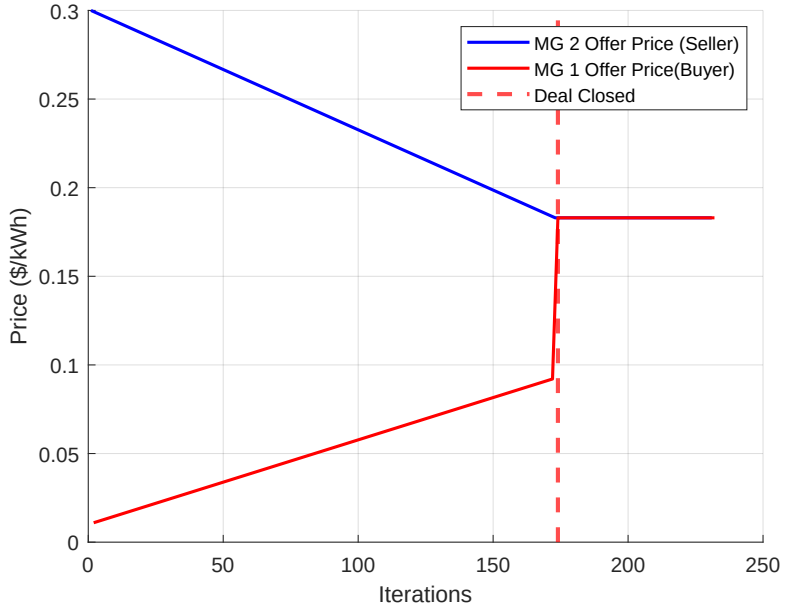

Figure 60: Bidding Sequence of Price Values Between the Two MGs That Successfully Sealed the Deal

Each MG strives to optimize its own benefits, as revealed by the initial prices and the regions of gain (during the initial iterations, sellers propose notably high prices, while buyers suggest significantly lower prices). As the algorithm progresses and negotiations proceed through a series of compromises, both MGs progressively move towards smaller gains. Nevertheless, the gains for both parties remain positive, a fact highlighted by the presence of the blue and orange line within the green region of the gain graph in Figure [61]. It is important to note that while the gains of MG1 are somewhat limited, they still remain positive.

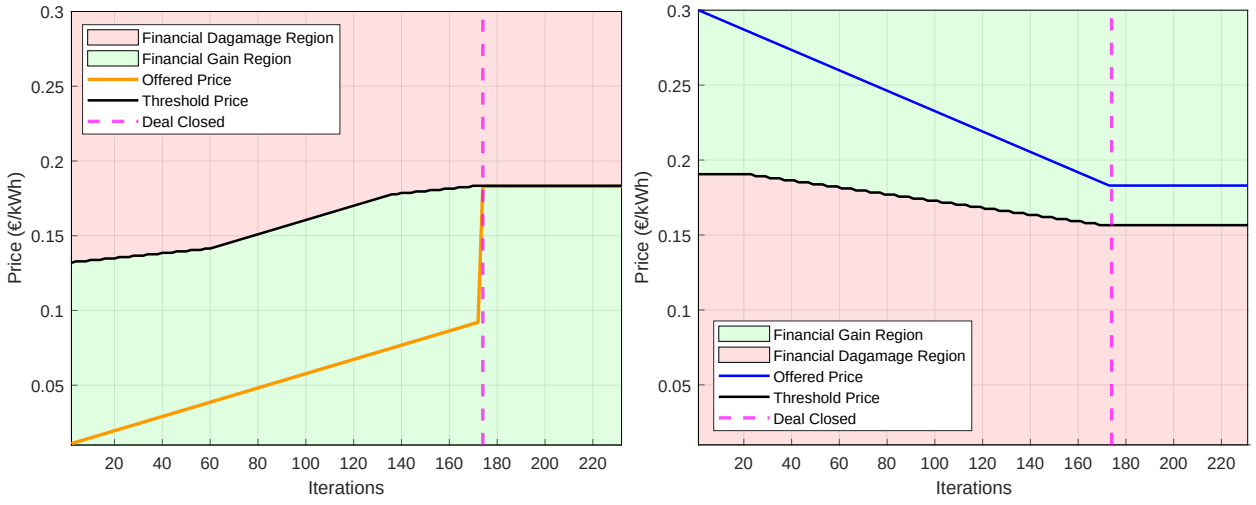

(a) Microgrid 1 in Buyer Role

(b) Microgrid 2 in Seller Role

Figure 61: Bidding Sequence of Price Values Between the Two MGs and the Areas of Gain and Damage

At this stage, a mutually advantageous agreement has been reached between the two MGs, leading to the establishment of a new operational point – a new setpoint for each MG. This new deviation from the optimal point is shown in Figure [58] for each respective MG. Subsequently, this information is communicated back to the Energy Management Systems (EMS) of each individual MG, as depicted in Figure [14].

Following this, as illustrated in Subsection [5.5] , any surplus or deficit power is allocated among the entities within the MG (including the virtual skyscrapers and the aggregator). With the power values for the current time interval now fixed, as dictated by the agreement reached, a new optimal operation scheduling begins at 18:00, aligning with the start of the P2P market, and concludes at 18:00 the following day.

It's important to provide some indicative values of the optimal operation scheduling after the market has closed for the time interval 18:00-19:30. Figure [62] illustrates the temperatures in all the thermal zones of the virtual skyscraper in the first MG, following the optimal operation scheduling that occurred after the P2P Market closed. It also demonstrates the gradual decrease in thermal boundaries over time in a linear manner that is described in Subsection [5.5]. It's clear that all the technical limitations are well managed within the allowable operational area.

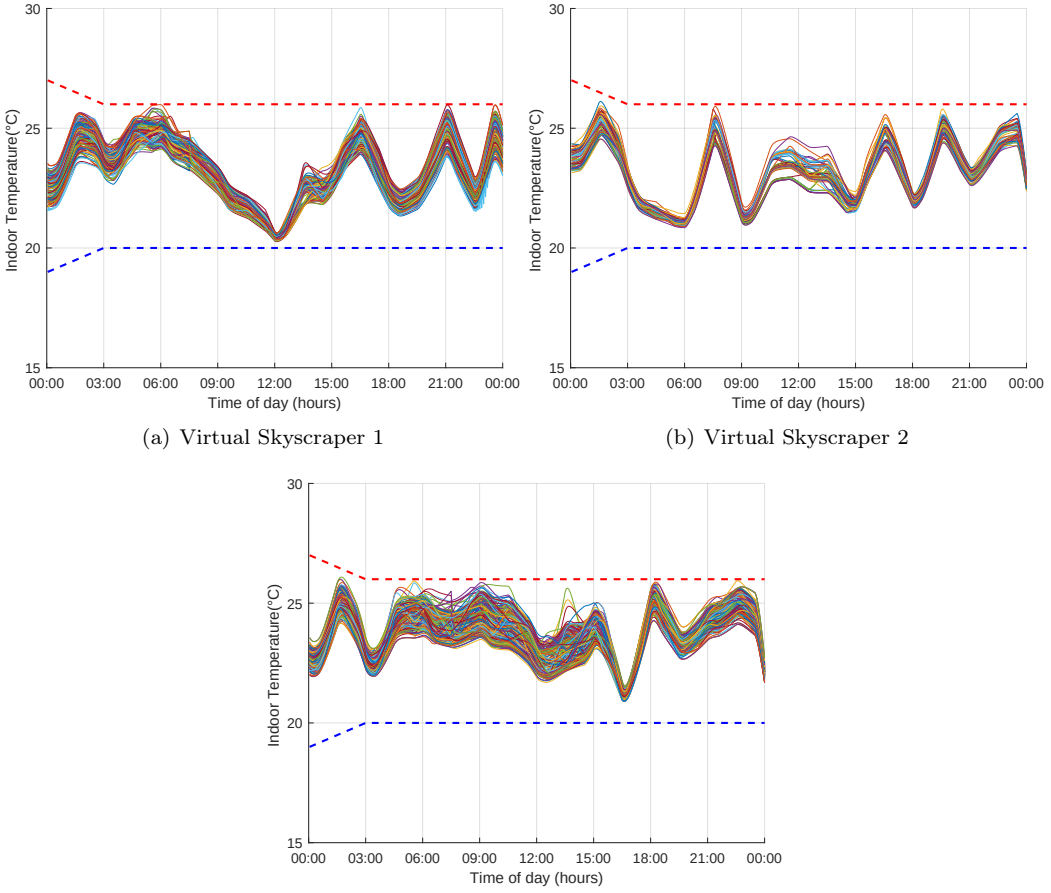

(a) Virtual Skyscraper 1

(b) Virtual Skyscraper 2

(c) Virtual Skyscraper 3

Figure 62: Internal Temperatures of All Thermal Zones in Virtual Skyscrapers of the First Microgrid (Optimal Operation Scheduling: 18:00 - 18:00 Next Day)

After running the simulation for a full day, which includes 16 game sessions with bargaining intervals of 1.5 hours each, the outcomes for all the interconnected MGs are presented in Figure [63].

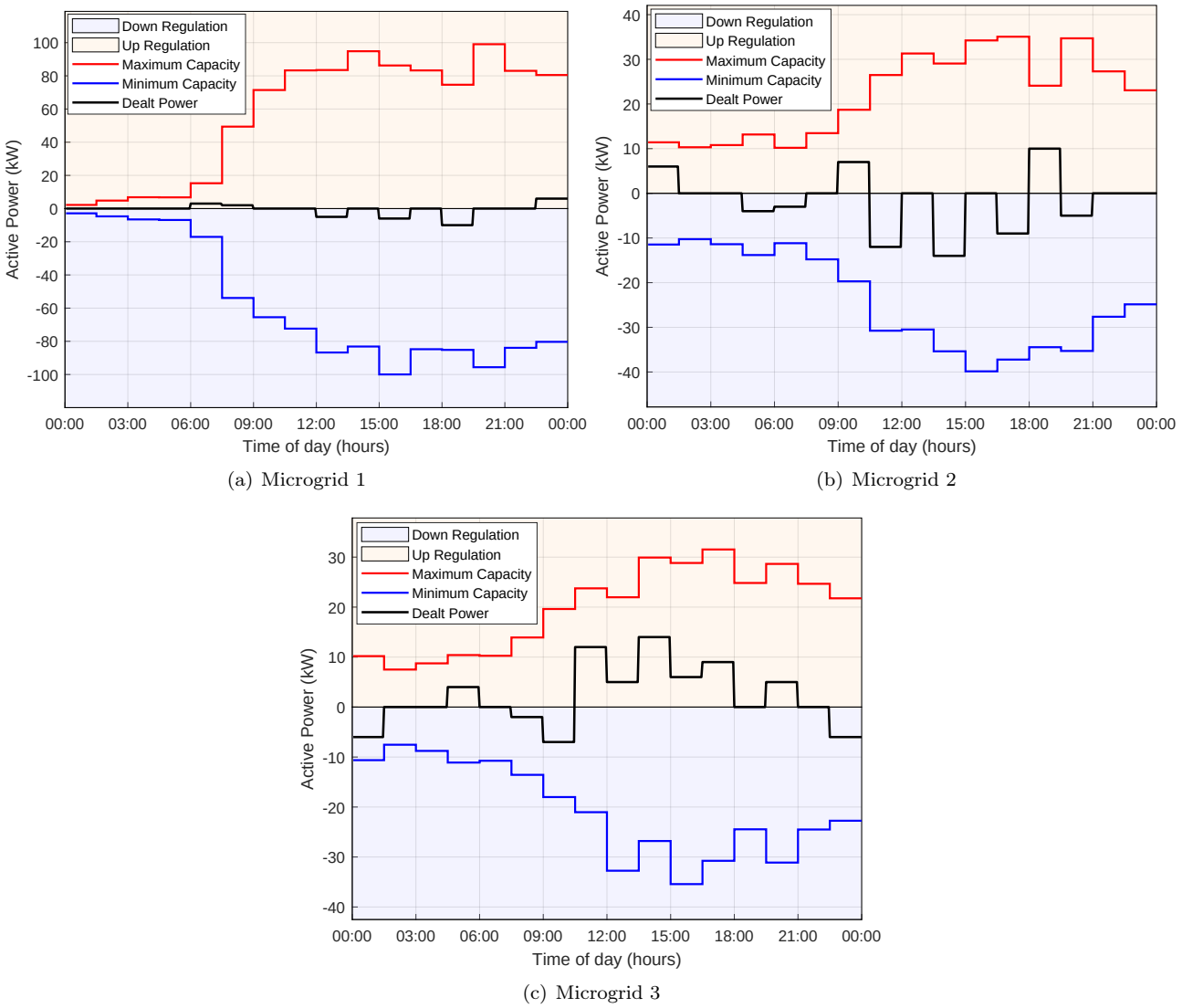

(a) Microgrid 1

(b) Microgrid 2

(c) Microgrid 3

Figure 63: Quantity of Power Exchanged In Peer-to-Peer Electricity Market

As evident from the figure above, the total power exchanged in the P2P market represents a significant percentage of the participation capacities for MG2 and MG3. However, it is not as significant for MG1, primarily due to its larger dimensions. To facilitate a deal in the P2P market, power equilibrium is essential. As a result, the two smaller MGs act as a bottleneck in the amount of power that MG1 can exchange. It's worth noting that another indication of the algorithm's correctness is that during each time interval of the P2P market, two MGs successfully close a deal with power quantities in equilibrium, while the third one does not participate.

To showcase that, after the P2P participation market has concluded for 16 time intervals or else for a 24-hour period, no technical constraints of MGs have been violated, Figure [64] displays the internal temperatures of all houses of the First MG individually, and Figure [65] illustrates the constraints of the aggregator.

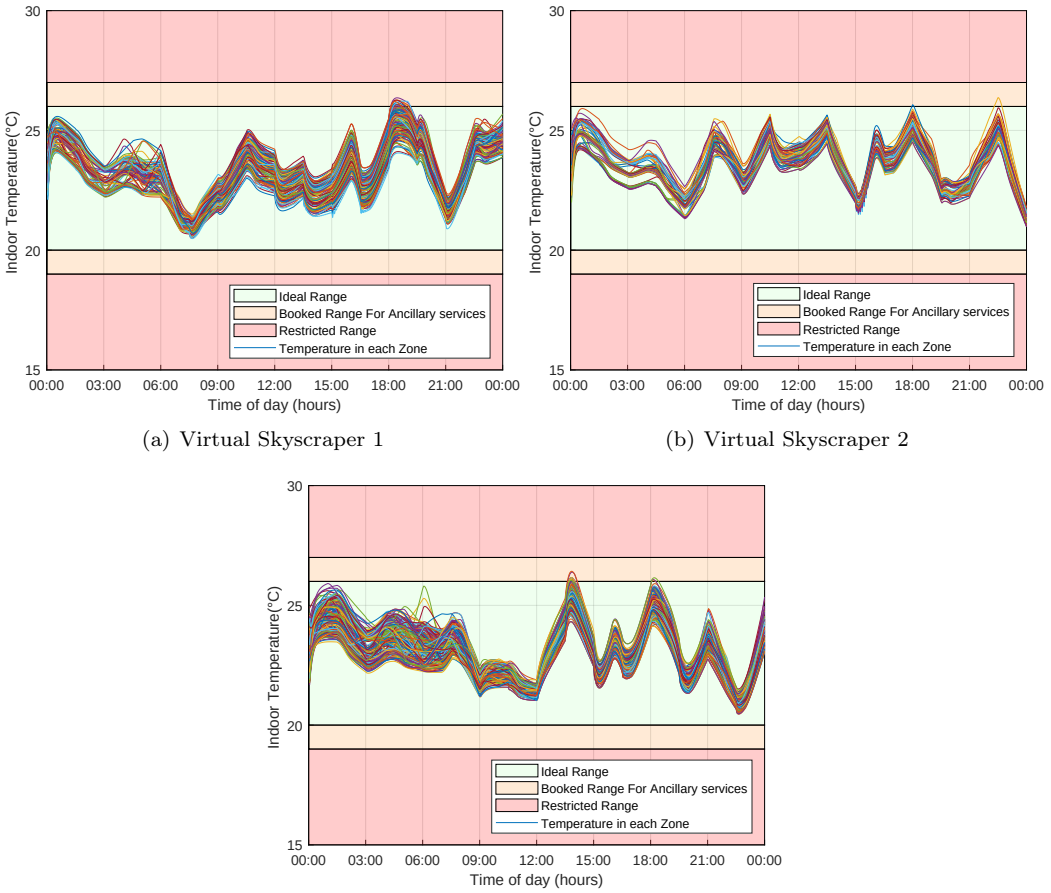

(a) Virtual Skyscraper 1

(b) Virtual Skyscraper 2

(c) Virtual Skyscraper 3

Figure 64: Internal Temperatures of Thermal Zones in all houses of MG1 post 24-hour P2P

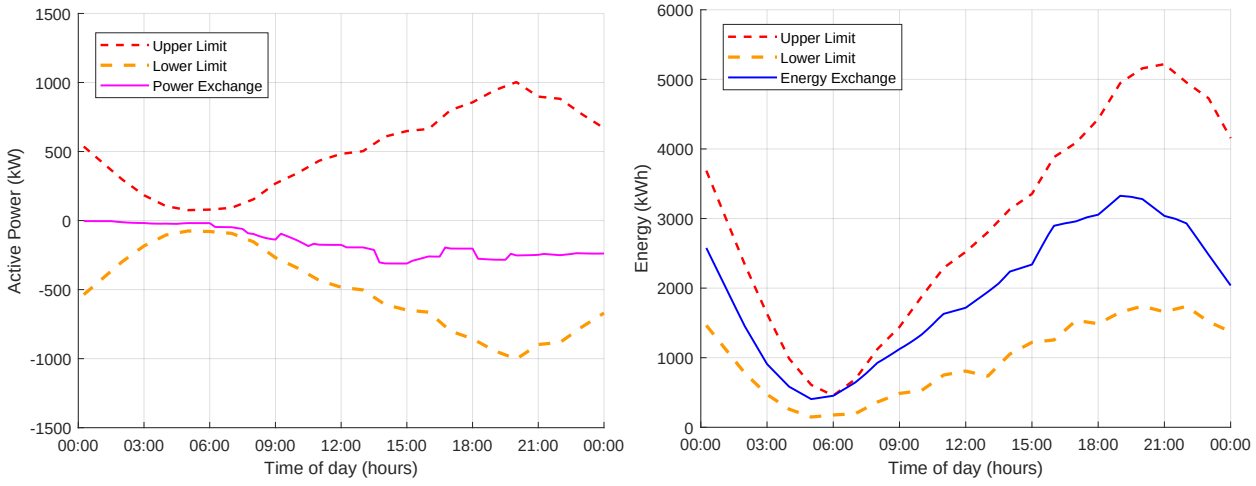

(a) Active Power Exchange Between Aggregator and MG1

(b) Total Stored Energy within Virtual Equivalent Battery

Figure 65: Aggregator Constraints of MG1

7 Conclusion and Future Work

This thesis introduces a novel method for optimizing the coordinated operating schedules of interconnected Microgrids within a Peer-to-Peer Framework. These Microgrids encompass a diverse range of residential buildings, each with distinct geometries, as well as electric vehicle aggregators. The proposed method not only accommodates intricate thermal-electrical power system models but also leverages aggregation techniques to streamline the management of numerous residential buildings, effectively treating them as virtual skyscrapers. Additionally, an aggregator approach is applied to plug-in electric vehicles (PEVs), maintaining high precision while significantly reducing the computational burden. This strategic allocation of thermal and electrical power to actual entities enables real-time operation. The method adeptly handles the complexity presented by building prosumers, employing an innovative strategy to distribute thermal requirements among various building thermal zones. The study capitalizes on the concept of thermal delay, inherent in a building's thermal behavior, to effectively time the provision of thermal energy and achieve desired temperatures. By harnessing the abundant thermal loads as virtual energy reservoirs, alongside the use of aggregators as virtual batteries, the method achieves adept energy management without necessitating additional capital investment in storage units. This innovation leads to efficient operation and cost minimization for both individual Microgrid operations that do not participate in the Peer-to-Peer Market, as well as those that do participate. This is accomplished through a straightforward yet effective decoupling of the two strategies: one focused on Microgrid optimization for its schedule, and the other oriented towards participation in the market. The amalgamation of these strategies results in a comprehensive approach. In summary, this thesis presents a pioneering approach that harmonizes the strategies employed by Microgrids for optimizing their schedules and participating in the market. By integrating these strategies, the study achieves a synergistic effect, enhancing the overall efficiency of Microgrid operations.

List of Symbols

The following list explains the symbols used in this document:

ABBREVIATIONS

DER Distribution Energy Resources

DG Distributed generation

EMS Energy Management System

ESS Energy Storage System

G2V Grid to Vehicle

HVAC Heating, Ventilation and Air Conditioning

IMGs Interconnected Microgrids

MG Microgrid

P2P Peer-to-Peer

PB Parking equivalent Battery

PCC Point Of Common Coupling

PEV Plug-in Electric Vehicle

RES Renewable Energy Sources

SoC State of Charge

V2G Vehicle to Grid

PARAMETERS, CONSTANTS AND VARIABLES

α_w the external wall absorbance coefficient

β_z surface slop

η_{ch} PEVs' charging efficiency coefficient.

η_{disch} PEVs' discharging efficiency coefficient.

$\eta_{non_{cr}}$ Non-critical load percentage referring to the portion of the overall electric load that is attributed to non-critical loads.

$\eta_{shift,max}$ maximum amount of power increase in a time instant while implementing load shifting

$\eta_{shift,min}$ minimum amount of power decrease in a time instant while implementing load shifting

η_{shift} optimal load shifting coefficient

$\dot{Q}_{ex,wall,z}$ external walls heat exchange (kW)

$\dot{Q}_{in,wall,z}$ internal walls heat exchange (kW)

$\dot{Q}_{in,z}$ internal heat gains (kW)

$\dot{Q}_{sg,z}$ solar radiation through the windows (kW)

$\dot{Q}_{sw,z}$ heat gain of external walls' solar radiation (kW)

$\dot{Q}_{win,z}$ heat transfer across the windows (kW)

τ_{win} window glass transmission coefficient

θ incidence angle

θ_z zenith angle

C_z specific heat capacity of air $(J/(kg \cdot Celcius))$

F_{wall} wall surface area (m^2)

F_{win} window surface area (m^2)

I total radiation on horizontal surface

I_b beam radiation on horizontal surface

I_d diffuse radiation on horizontal surface

$I_{T,z}$ total solar radiation

$P^*_{non_{cr}}$ Power consumption of non critical loads after Load shifting.

$P_{el,b}$ Power consumption of bth building

$P_{el_{load,z}}$ power consumption of zth thermal zone of building

p_g ground reflectance

$P_{non_{cr}}$ Power consumption of non critical loads before Load shifting.

p_z density of air of the zth thermal zone

$Q_{HVAC,b}$ Buildings's power production for cooling (kW).

$Q_{HVAC,z}$ thermal zone's power production for cooling (kW)

R_b geometric factor which is defined as the ratio of beam radiation on a tilted surface to that on a horizontal surface

R_{se} heat resistance of the external surface

SC the shading coefficient of the windows

$T_{in,nz}$ indoor temperature of the neighbor thermal zone (Celsius)

$T_{in,z}$ thermal zone's temperature (Celsius)

T_{out} outdoor temperature (Celsius)

$Tshift_0$ starting point of the optimization horizon for the controllable loads

$Tshift_f$ stoping point of the optimization horizon for the controllable loads

U_{wall} factor of the heat exchange of the external wall $(W/(m^2 \cdot Celsius))$

U_{win} factor of the heat exchange of the external window $(W/(m^2 \cdot Celsius))$

V_z volume of the air of the zth thermal zone

COP coefficient of HVAC performance.

EP_{buy} Electricity Price that Grids buys Power from MGs

EP_{sell} Electricity Price that Grids sells Power from MGs

$P_{HVAC,total,b}$ Building Power Consumption (kW).

$P_{HVAC,total,max,b}$ Building Power Consumption (kW).

$P_{HVAC,total,max,b}$ maximum Building Power Consumption (kW).

$P_{HVAC,total,z}$ Thermal zone Power Consumption.

P_{max} maximum Charging Power of PEV.

P_{MG} Power exchange between Microgrid and Grid (Microgrid has Load Convention).

P_{min} minimum Charging Power of PEV.

P_{opt} Optimal Power exchange between Aggregator and Grid (Aggregator has Load Convention).

$P_{PB,\,max}$ maximum Charging Power of Equivalent Battery

$P_{PB,\,min}$ minimum Discharging Power of Equivalent Battery

P_{PV} Photovoltaic power production (kW).

P_{WT} Wind Turbines power production (kW).

SoC_0 Initial energy level of PEV at the start of charging (kWh).

SoC_{high} maximum dynamic bound of stored energy (kWh) of PEV

SoC_{low} minimum stored energy (kWh) of PEV

SoC_{max} maximum allowable limit for SoC.

SoC_{min} minimum allowable limit for SoC

$SoC_{PB,\,0}$ Initial energy level of Equivalent Battery at the start of charging (kWh).

$SoC_{PB,\,max}$ maximum dynamic bound of stored energy (kWh) of Equivalent Battery

$SoC_{PB,\,min}$ minimum dynamic bound of stored energy (kWh) of Equivalent Battery

$SoC_{PB,\,target}$ Target energy level of Equivalent Battery at the end of charging (kWh).

$SoC_{PB}T_0$ The initial State of Charge of the equivalent battery at the beginning of the optimization horizon.

$SoC_{PB}T_f$ The concluding State of Charge of the equivalent battery at the end of the optimization horizon.

SoC_{target} Target energy level of PEV at the end of charging (kWh).

T_0 Time point indicating the start of the optimization period.

t_0 time point at which the EV is connected (plugged)

T_f Time point indicating the end of the optimization period.

t_f time point at which the EV is disconnected (unplugged)

t_{H1} time point when EV reach SoC_{max} after charging with maximum power, assuming this action began when the EVs arrived (t_0).

t_{H2} time point when EV begins discharging at the maximum power from SoC_{max} and reaches SoC_{target} just in time.

t_{L1} time point when EV reach SoC_{min} after discharging with maximum power, assuming this action began when the EVs arrived (t_0).

t_{L2} time point when EV begins charging at the maximum power from SoC_{min} and reaches SoC_{target} just in time.

$T_{max,z}$ Thermal zone's temperature Upper Bound.

$T_{min,z}$ Thermal zone's temperature Lower Bound.

SETS AND INDICES

$\jmath$ internal walls set

ε external walls set

N_z thermal zones total number

b building's number index

N neighboring thermal zones set

x xth internal wall index

y yth external wall/window index

z zth thermal zone index

References

[1] Abdullah Dik, Siddig Omer, and Rabah Boukhanouf. Electric vehicles: V2g for rapid, safe, and green ev penetration. *Energies*, 15(3):803, 2022.

[2] Laura Canale, Anna Rita Di Fazio, Mario Russo, Andrea Frattolillo, and Marco Dell'Isola. An overview on functional integration of hybrid renewable energy systems in multi-energy buildings. *Energies*, 14(4):1078, 2021.

[3] Summary of travel trends 2009 national household travel survey. Available Online:https://nhts.ornl.gov/2009/pub/stt.pdf.

[4] Features and benefits about microgrids. Available Online:https://www.districtenergy.org/microgrids/about-microgrids97/features.

[5] E.S.N. Raju P and Trapti Jain. Chapter 2 - distributed energy resources and control. In Rajeev Kumar Chauhan and Kalpana Chauhan, editors, *Distributed Energy Resources in Microgrids*, pages 33–56. Academic Press, 2019.

[6] Yimy E García Vera, Rodolfo Dufo-López, and José L Bernal-Agustín. Energy management in microgrids with renewable energy sources: A literature review. *Applied Sciences*, 9(18):3854, 2019.

[7] James Momoh. *Renewable Energy and Storage*, pages 140–159. 2012.

[8] Lithium-ion batteries. Available Online:https://www.cei.washington.edu/research/energy-storage/lithium-ion-battery/.

[9] Lead acid batteries. Available Online: https://www.pveducation.org/pvcdrom/batteries/lead-acid-batteries.

[10] Flow batteries. Available Online:https://flowbatteryforum.com/what-is-a-flow-battery/.

[11] Hydrogen fuel cells. Available Online:https://www.energy.gov/eere/fuelcells/fuel-cells.

[12] High-power ultracapacitor energy storage solutions based on breakthrough graphene material. Available Online:https://www.skeletontech.com/ultracapacitor-technology.

[13] Willett Kempton and Jasna Tomić. Vehicle-to-grid power fundamentals: Calculating capacity and net revenue. *Journal of power sources*, 144(1):268–279, 2005.

[14] Snigdha Sharma, Amrish K Panwar, and MM Tripathi. Storage technologies for electric vehicles. *Journal of traffic and transportation engineering (english edition)*, 7(3):340–361, 2020.

[15] J Carlos Gómez and Medhat M Morcos. Impact of ev battery chargers on the power quality of distribution systems. *IEEE transactions on power delivery*, 18(3):975–981, 2003.

[16] Why the future of driving is electric. Available Online:https://evolveetfs.com/2018/11/why-the-future-of-driving-is-electric/.

[17] Advantages of electric cars – top benefits of evs. Available Online:https://www.energysage.com/electric-vehicles/advantages-of-evs/.

[18] Dirk Uwe Sauer, Martin Kleimaier, and Wolfgang Glaunsinger. Relevance of energy storage in future distribution networks with high penetration of renewable energy sources. In *CIRED 2009-20th International Conference and Exhibition on Electricity Distribution-Part 1*, pages 1–4. IET, 2009.

[19] Francis Mwasilu, Jackson John Justo, Eun-Kyung Kim, Ton Duc Do, and Jin-Woo Jung. Electric vehicles and smart grid interaction: A review on vehicle to grid and renewable energy sources integration. *Renewable and sustainable energy reviews*, 34:501–516, 2014.

[20] W Shireen and S Patel. Plug-in hybrid electric vehicles in the smart grid environment. In *IEEE PES T&D 2010*, pages 1–4. IEEE, 2010.

[21] Henrik Lund and Willett Kempton. Integration of renewable energy into the transport and electricity sectors through v2g. *Energy policy*, 36(9):3578–3587, 2008.

[22] Antonio Colmenar-Santos, Antonio-Miguel Muñoz-Gómez, Enrique Rosales-Asensio, and África López-Rey. Electric vehicle charging strategy to support renewable energy sources in europe 2050 low-carbon scenario. *Energy*, 183:61–74, 2019.

[23] David Dallinger and Martin Wietschel. Grid integration of intermittent renewable energy sources using price-responsive plug-in electric vehicles. *Renewable and Sustainable Energy Reviews*, 16(5):3370–3382, 2012.

[24] Willett Kempton and Jasna Tomić. Vehicle-to-grid power implementation: From stabilizing the grid to supporting large-scale renewable energy. *Journal of power sources*, 144(1):280–294, 2005.

[25] Abdellatif Elmouatamid, Radouane Ouladsine, Mohamed Bakhouya, Najib El Kamoun, Mohammed Khaidar, and Khalid Zine-Dine. Review of control and energy management approaches in micro-grid systems. *Energies*, 14(1):168, 2020.

[26] F Bandeiras, E Pinheiro, M Gomes, P Coelho, and J Fernandes. Review of the cooperation and operation of microgrid clusters. *Renewable and Sustainable Energy Reviews*, 133:110311, 2020.

[27] Electricity markets in the eu. Available Online:https://fsr.eui.eu/electricity-markets-in-the-eu/.

[28] Epex spot and ecc reduce lead-time on austrian, french and swiss intraday markets. Available Online:https://www.epexspot.com/en/news/epex-spot-and-ecc-reduce-lead-time-austrian-french-and-swiss-intraday-markets.

[29] Udi Helman, Harry Singh, and Paul Sotkiewicz. Chapter 19 - rtos, regional electricity markets, and climate policy. In Fereidoon P. Sioshansi, editor, *Generating Electricity in a Carbon-Constrained World*, pages 527–563. Academic Press, Boston, 2010.

[30] Nicoló Mazzi and Pierre Pinson. 10 - wind power in electricity markets and the value of forecasting. In George Kariniotakis, editor, *Renewable Energy Forecasting*, Woodhead Publishing Series in Energy, pages 259–278. Woodhead Publishing, 2017.

[31] International renewable energy agency. peer-to-peer electricity trading. Available Online:https://www.irena.org/.

[32] Xiaolong Jin, Jianzhong Wu, Yunfei Mu, Mingshen Wang, Xiandong Xu, and Hongjie Jia. Hierarchical microgrid energy management in an office building. *Applied Energy*, 208:480–494, 2017.

[33] Dimitra G Kyriakou and Fotios D Kanellos. Optimal operation of microgrids comprising large building prosumers and plug-in electric vehicles integrated into active distribution networks. *Energies*, 15(17):6182, 2022.

[34] Dimitra G Kyriakou and Fotios D Kanellos. Sustainable operation of active distribution networks. *Applied Sciences*, 13(5):3115, 2023.

[35] George K Farinis and Fotios D Kanellos. Integrated energy management system for microgrids of building prosumers. *Electric Power Systems Research*, 198:107357, 2021.

[36] European health information gateway. average number of people per room in occupied housing unit. Available Online:https://gateway.euro.who.int/en/indicators/hfa_469-4350-average-number-of-people-per-room-in-occupied-housing-unit/.

[37] American time use survey percent of the population engaging in selected activities by time of day, 12 am to 11 am, average for the combined years 2013-17. Available Online:https://www.bls.gov/tus/tables/a3-1317.htm.

[38] American time use survey activity lexicon 2021. Available Online:https://www.bls.gov/tus/lexicons/lexiconwex2021.pdf.

[39] Fotios D Kanellos. Optimal scheduling and real-time operation of distribution networks with high penetration of plug-in electric vehicles. *IEEE Systems Journal*, 15(3):3938–3947, 2020.

[40] Fotios D Kanellos, Kostas Kalaitzakis, Ioannis Psarras, and Yannis Katsigiannis. Efficient and robust power and energy management for large clusters of plug-in electric vehicles and distribution networks. *IET Energy Systems Integration*, 4(3):393–408, 2022.

[41] Recommended lighting levels for residential and office spaces. Available Online:https://vtacblog.com/recommended-lighting-levels-for-residential-and-office-spaces.